



Die Bedeutung von microRNAs für die Funktion von Endothelzellen

Dissertation zur Erlangung
des Doktorgrades der Naturwissenschaften

Vorgelegt beim Fachbereich Biowissenschaften
der Goethe Universität Frankfurt am Main

Von
Angelika Bonauer
aus Hilden im Rheinland

Frankfurt 2008



The role of microRNAs for endothelial cell function

Dissertation zur Erlangung
des Doktorgrades der Naturwissenschaften

Vorgelegt beim Fachbereich Biowissenschaften
der Goethe Universität Frankfurt am Main

Von
Angelika Bonauer
aus Hilden im Rheinland

Frankfurt 2008

Vom Fachbereich Biowissenschaften der
Goethe Universität als Dissertation angenommen

Dekan: Professor Dr. Volker Müller

1. Gutachter: Professor Dr. Beatrix Süß
2. Gutachter: Professor Dr. Stefanie Dimmeler

Datum der Disputation:

Danksagung

An dieser Stelle möchte ich allen danken, die mir mein Studium und die Beendigung der Promotion ermöglichten.

Mein besonderer Dank gilt Frau Prof. Dr. Stefanie Dimmeler und Herrn Prof. Dr. Andreas Zeiher für die Überlassung dieses interessanten, neuen Themas und den ausgezeichneten Arbeitsbedingungen.

Die Begeisterung von Frau Prof. Dimmeler für dieses Thema und ihr unermüdlicher Enthusiasmus haben maßgeblich zum Gelingen dieser Arbeit beigetragen. Mit stets neuen Herausforderungen hat sie viele Fortschritte, nicht nur im Rahmen des Promotionsprozesses, angeregt und ermöglicht.

Dörte Scharner, Ariane Fischer, Dr. Alessia Orlandi und Guillaume Carmona danke ich für ihre Freundschaft und Unterstützung in sämtlichen Lebenslagen und Phasen dieser Arbeit und für die vielen nützlichen wissenschaftlichen Diskussionen.

Natalja Reinfeld danke ich für die intensive, praktische Unterstützung im letzten Jahr meiner Promotion und für ihre stets sehr gute und zuverlässige Arbeit, die maßgeblich zum Gelingen des Projektes beigetragen hat.

Desweiteren danke ich meinen gegenwärtigen und ehemaligen Laborkollegen Natalja Reinfeld, Andrea Knau, Nicole Konecny, Carmen Döbele, Henrik Fox, David Kaluza, Reinier Boon und Florian Diehl für das entspannte, freundschaftliche und stets motivierende Arbeitsklima im Labor.

Ich danke dem „Task Force Team“ bestehend aus Ariane Fischer, Marion Muhly-Reinholz und Tino Röxe für die gute Zusammenarbeit und ihren 150%igen Einsatz im Rahmen von sämtlichen, mehr oder weniger langen Revisionen.

Der gesamten Molekularen Kardiologie danke ich für die sehr schönen letzten 3 Jahre, das sehr angenehme Arbeitsklima und dafür, die Arbeitsgruppe nicht nur als Ansammlung von Mitarbeitern zu verstehen.

Meiner Familie danke ich für ihre Unterstützung und den privaten Rückhalt, den sie mir während meiner gesamten Ausbildung geleistet haben.

Vor allem aber danke ich meinem Schatz Christoph dafür, daß er in allen Situationen und Lebenslagen an mich geglaubt und mich unterstützt hat und dadurch maßgeblich zu meiner emotionalen und wissenschaftlichen Entwicklung beigetragen hat. Ohne ihn wäre ich vermutlich nicht dort angekommen, wo ich hier und heute stehe.

Contents

1	INTRODUCTION	1
1.1	The circulatory system.....	1
1.2	Vasculogenesis, angiogenesis and arteriogenesis.....	1
1.2.1	Organization of the vascular system.....	3
1.2.2	The endothelium.....	4
1.2.3	Angiogenesis and disease.....	5
1.3	MicroRNAs.....	8
1.3.1	The diverse role of non-coding RNAs.....	8
1.3.2	MicroRNA history.....	9
1.3.3	Biogenesis.....	10
1.3.4	Target prediction and regulation.....	11
1.3.5	Regulation of microRNA activity.....	14
1.3.6	Role of Dicer and Drosha in endothelial cells.....	15
1.3.7	Specific microRNAs involved in angiogenesis.....	16
1.3.8	Role of microRNAs in diseases.....	18
1.3.9	miR-17-92 cluster.....	19
1.4	Aim of the study.....	22
2	MATERIAL AND METHODS	23
2.1	Cell culture of HUVEC.....	23
2.2	Cell culture of HEK293.....	23
2.3	Growth media.....	24
2.4	Transfection of oligonucleotides.....	24
2.5	Transfection of pre-miRNA.....	25
2.6	RNA isolation.....	26
2.7	RT-PCR and real time PCR.....	26
2.8	Stem loop RT and quantitative PCR of miRNAs.....	27
2.9	MicroRNA expression analysis.....	28
2.10	MicroRNA array analysis.....	29

2.11	Protein isolation.....	29
2.12	SDS polyacrylamide gel electrophoresis (SDS-PAGE)	30
2.13	Western blot analysis	30
2.14	Immunocytochemistry for protein detection	30
2.15	Immunofluorencence	32
2.16	Stimulation with VEGF.....	32
2.17	Stimulation with zVAD	32
2.18	Tube forming assay	32
2.19	Spheroid-based angiogenesis assay.....	33
2.20	MTT viability assay	33
2.21	Cell-matrix adhesion.....	33
2.22	Migration assay	34
2.23	Cytokine and receptor array	34
2.24	Flow cytometry analysis	35
2.25	Proliferation assay.....	35
2.26	Annexin V staining of cardiomyocytes.....	35
2.27	Luciferase cloning and transfection	35
2.28	Plasmid preparation	36
2.29	<i>In vivo</i> Matrigel plug assay with transfected HUVEC.....	36
2.30	Antagomirs	37
2.31	<i>In vivo</i> matrigel experiments.....	37
2.32	Murine ischemic hind limb model	38
2.33	Induction of myocardial infarction and functional evaluation.....	38
2.34	Detection of miRNA and mRNA expression	39
2.35	<i>In situ</i> hybridization.....	40
2.36	TUNEL staining	40
2.37	Affimetrix mRNA profiling	40
2.38	Statistical analysis	41

3	RESULTS	42
3.1	Expression and localization of Dicer and Drosha in endothelial cells	42
3.2	Role of Dicer and Drosha for sprouting, tube formation and migration of endothelial cells.....	44
3.3	Dicer is required for <i>in vivo</i> angiogenesis.....	47
3.4	microRNAs enriched in endothelial cells	48
3.5	Dicer and Drosha regulate the expression of miRNAs in endothelial cells	50
3.6	Dicer and Drosha silencing induces the upregulation of thrombospondin-1 expression	53
3.7	Effect of Dicer and Drosha silencing on cytokine expression and AKT signaling	55
3.8	Regulation of <i>in vitro</i> angiogenesis by highly expressed miRNAs	58
3.9	miR-92a impairs <i>in vitro</i> and <i>in vivo</i> angiogenesis.....	59
3.10	Inhibition of miR-92a enhances angiogenesis and neovascularization <i>in vitro</i> and <i>in vivo</i>	63
3.11	MiR-92a is regulated by ischemic injury	67
3.12	Antagomir-92a improves functional recovery after hind limb ischemia	69
3.13	Antagomir-92a improves functional recovery after acute myocardial infarction	71
3.14	Genes regulated by miR-92a.....	77
3.15	Integrin $\alpha 5$ is a direct target of miR-92a	79
4	DISCUSSION	85
4.1	MicroRNAs are crucial regulators of endothelial cell biology	85
4.1.1	Role of Dicer and Drosha in endothelial cells.....	85
4.1.2	Let-7f and miR-27b are regulated by Dicer and Drosha.....	88
4.2	Regulation and function of miR-92a	89
4.2.1	The miR-17-92 cluster is highly expressed in EC.....	89
4.2.2	miR-92a inhibits angiogenesis <i>in vitro</i> and <i>in vivo</i>	90
4.2.3	MiR-92a is upregulated under ischemic conditions and is efficiently suppressed by antagomir-92a treatment <i>in vivo</i>	91

4.2.4	Inhibition of miR-92a promotes angiogenesis and functional recovery after ischemia <i>in vivo</i>	93
4.2.5	MiR-92a effects the expression of a variety of pro-angiogenic genes	95
5	CONCLUSION	99
6	ZUSAMMENFASSUNG	101
7	ABBREVIATIONS.....	103
8	BIBLIOGRAPHY	105

1 Introduction

1.1 The circulatory system

In our body, there are two major circulatory systems, the blood vascular system and the lymphatic vascular system. Their most important function is to carry fluids (blood and lymph fluids) and both systems mainly consist of vessels that are lined by a cell type called endothelial cells. The blood vascular system is a closed circular system that delivers oxygen and nutrients as well as signaling molecules to the body tissue and removes tissue waste. The lymphatic system is an open end linear system which begins at the peripheral tissues or various organs and ends to its connection to the vein. The lymphatic vessels deliver tissue fluids, cells and macromolecules to the blood vascular system for recirculation.

1.2 Vasculogenesis, angiogenesis and arteriogenesis

During embryonic development the first step of blood vessel formation is characterized by vasculogenesis. Vasculogenesis refers to the *in situ* differentiation of the hemangioblast, a common progenitor of endothelial and hematopoietic cells into the angioblast, which migrates and gives rise to the formation of a primitive network, the vascular plexus (Carmeliet, 2000). Most important factors involved in vasculogenesis are vascular endothelial growth factor (VEGF), its receptors VEGFR1 and VEGFR2 as well as basic fibroblast growth factor (bFGF), which influence angioblast differentiation, and molecules mediating cell-matrix interactions such as Integrin subunit $\alpha 5$ and its ligand fibronectin (Carmeliet, 2000). Additionally, during the angioblast stage the transcription factor gridlock (Zhong et al., 2000) and subsequently members of the ephrin family mediate the fate of endothelial cells to become integrated either in arteries or veins (Gale and Yancopoulos, 1999). While the term “vasculogenesis” originally described only the embryonic de novo blood vessel formation from angioblasts, it meanwhile refers also to the formation of blood vessels in the adult by endothelial progenitor cells or other adult stem cells

(Carmeliet, 2000). During angiogenesis, the vascular plexus expands and remodels. Several important key processes are involved in angiogenesis. VEGF as well as ANG2 increase the vascular permeability, therefore releasing the path for proliferating endothelial cells to migrate. The establishment of blood flow requires the formation of a vascular lumen. There is increasing evidence that lumen formation is driven by intracellular and intercellular fusion of endothelial vacuoles (Kamei et al., 2006). Angiogenesis is completed by the recruitment of perivascular cells, which stabilize nascent vessels by inhibiting proliferation and migration of endothelial cells.

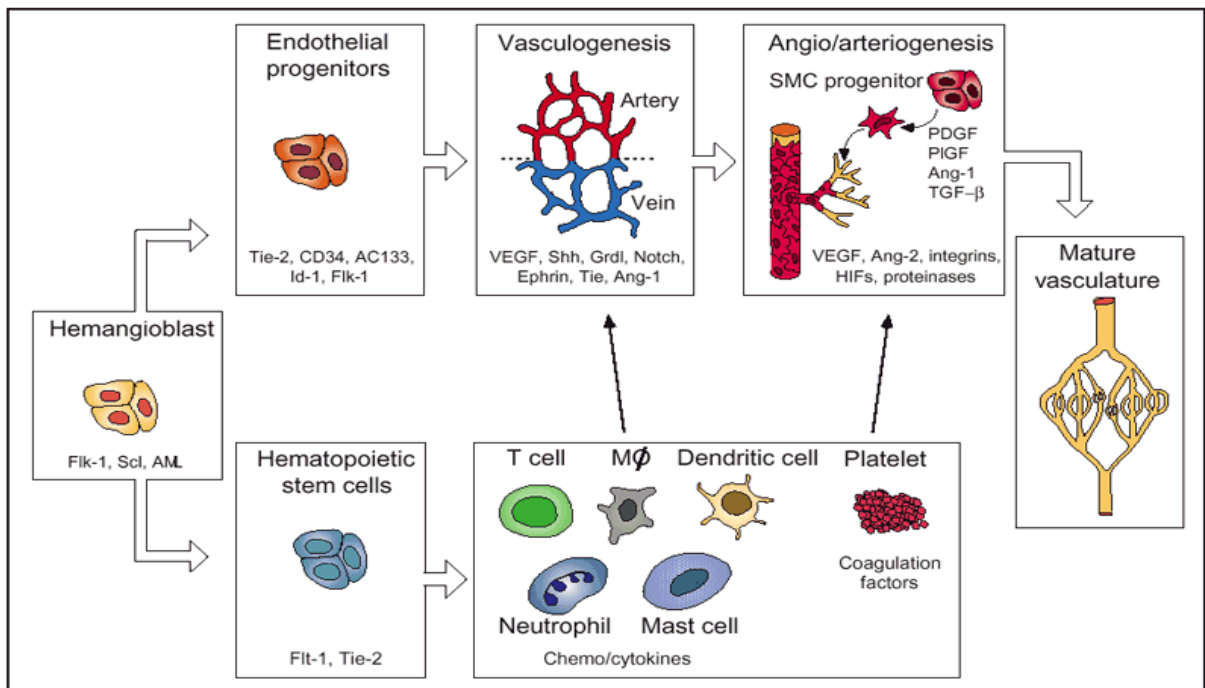


Figure 1.1 Formation of a vascular network

Endothelial progenitors differentiate to arterial and venous EC, which assemble in a primitive capillary plexus. Vessels then sprout and become stabilized by SMCs, differentiating from their progenitors. HSCs contribute to angiogenesis directly and indirectly, by differentiating to leukocytes or platelets. A partial list of molecules is indicated. (Carmeliet, 2003)

Subsequent arteriogenesis is characterized by the outgrowth of collateral arteries in response to increased luminal shear stress leading to the enlargement of small pre-existing anastomoses towards large conductance arteries and covering of the vessels with a muscular coat (Silvestre et al., 2008).

Angiogenesis and vasculogenesis are physiological processes during development, play essential roles in the recovery of blood flow in ischemic tissues and are fundamental steps in tumor growth. Enhancement of angiogenesis and neovascularization has been identified as potential therapeutic strategy, for example in patients suffering from critical ischemia. In tumor angiogenesis, inhibition of these processes leads to repression of tumor growth.

1.2.1 Organization of the vascular system

The vascular system consists of arteries, veins, arterioles and venules as well as capillaries. The innermost layer of all vessels is made up from a monolayer of endothelial cells (EC), the EC tube. Large and small vessels mainly differ in the composition of the surrounding stabilizing cells. Whereas capillaries consist of the EC tube surrounded by a sparse layer of pericytes embedded in the EC basement membrane, arterioles and venules have an increased coverage of mural cells. Larger vessels consist of three specialized layers: an intima composed of endothelial cells, a media of smooth muscle cells (SMC) and an adventitia of fibroblasts, together with matrix and elastic laminae (Fig. 1.2).

The advential layer has its own blood supply, known as vasa vasorum that extends in part into the media (Jain, 2003). Endothelial-derived factors control SMCs and elastic laminae, which in turn contribute to the vessel tone and mediate the control of vessel diameter and blood flow.

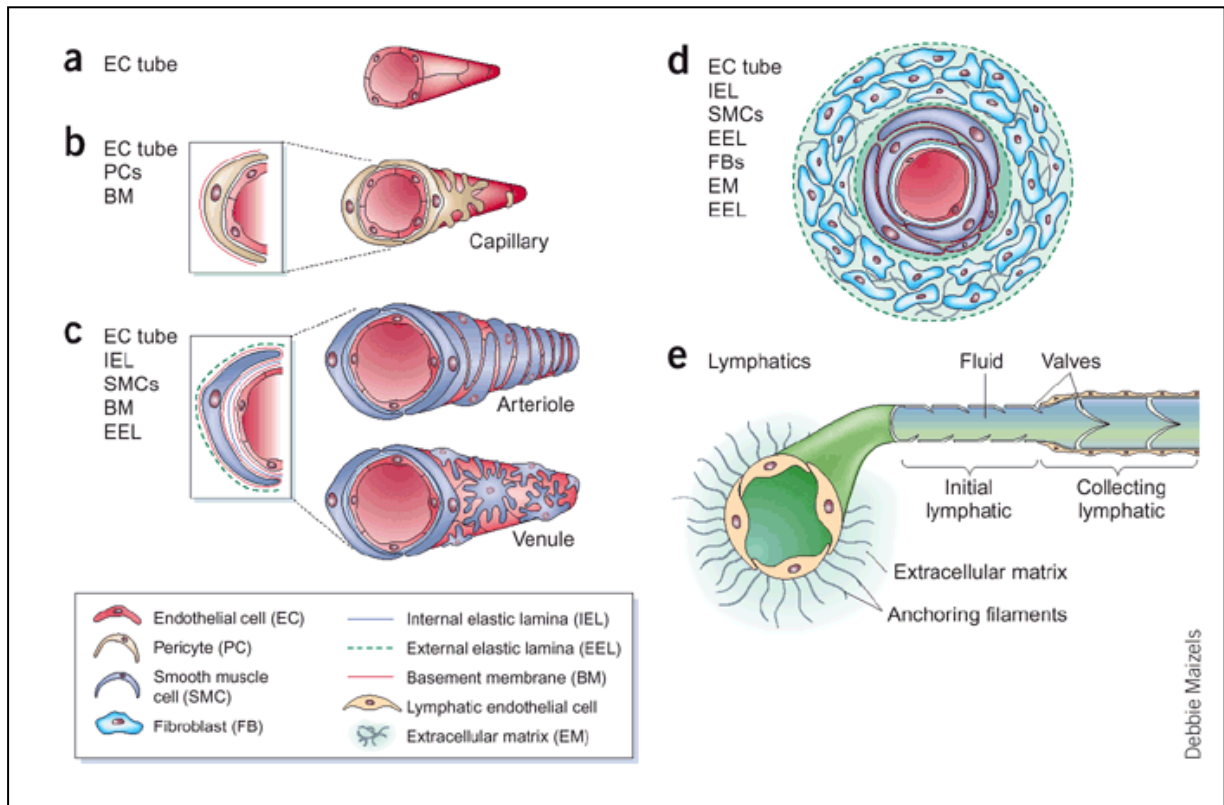


Figure 1.2 Wall composition of nascent versus mature vessels

A) Nascent vessels consist of a tube of EC. **B)** Capillaries consist of the EC tube surrounded by a sparse layer of pericytes and the EC basement membrane. **C)** Arterioles and venules have an increased coverage of mural cells compared to capillaries. **D)** The walls of larger vessels consist of three specialized layers: an intima composed of endothelial cells, a media of SMCs and an adventitia of fibroblasts, together with matrix and elastic laminae. **E)** Lymphatic capillaries lack pericytes, but larger (collecting) lymphatic vessels are invested in a basement membrane. (Jain, 2003)

1.2.2 The endothelium

The endothelium is essential for the normal function of the cardiovascular, cerebrovascular, renovascular, and pulmonary vascular systems. The vascular endothelium is not merely a lining for blood cells and plasma, it is rather a metabolic active organ and plays crucial roles in regulating vascular permeability, macromolecular transport, vascular tone, inflammation, coagulation, and vascular wall structure (Sato, 2001).

Vascular permeability, the capacity of blood vessel walls to allow the passage of small molecules (ions, water, and nutrients) or even whole cells to the interstitial space is regulated by endothelial cell-cell contacts. During inflammation, for example, white blood cells interact with endothelial cells via cell adhesion molecules (CAMs) and specific receptors, thereby promoting adhesion of leukocytes to the activated endothelium, transmigration and penetration in areas of infection or tissue damage (Patarroyo and Makgoba, 1989). Furthermore, endothelial cells react to mechanical forces generated by blood flow under pressure by releasing vasoactive substances. Under physiological conditions, endothelial cells continuously release nitric oxide (NO) leading to vasorelaxation by relaxing surrounding smooth muscle cells (Ignarro et al., 1987). On the other hand, activated endothelium can secrete also vasoconstrictors like endothelin-1 (ET-1) that affect differentiation and growth of smooth muscle cells (Hirata et al., 1988; Komuro et al., 1988; Yanagisawa et al., 1988). Normally, endothelial cells exhibit anticoagulant and antithrombotic properties by secreting antiplatelet substances such as PGI₂ and NO. However, after vessel injury thrombin is generated at the site of endothelial denudation causing a series of coagulation responses (Sato, 2001). Additionally, endothelial cells contribute to the formation of new vessels. Usually, endothelial cells are quiescent, but still have the ability to proliferate and migrate. Angiogenesis, the formation of new capillaries from pre-existing vessels mediated by endothelial cells is a fundamental process during development and is crucial for recovery after ischemia.

Since the vascular endothelium is sensitive to various stimuli including cytokines, oxidized low density lipoprotein (LDL), hypoxia and mechanical stress it is directly involved in the development and progression of a variety of severe diseases like heart diseases, stroke, venous thrombosis, diabetes and tumor growth. With this respect, the endothelium represents a biological determinant that could be modulated to prevent disease development and progression.

1.2.3 Angiogenesis and disease

As already mentioned in paragraph 1.1.1, angiogenesis, the outgrowth of new capillaries from pre-existing vessels, is a major player during development. Over the

past decades, however, angiogenesis has been spotlighted on account of its contribution in the progression and initiation of severe diseases such as coronary artery disease (CAD), cancer, ocular, joint and skin disorders or, on the other hand, the possibility to improve functional recovery after ischemic disorders. One of the most important endothelial mitogens is vascular endothelial growth factor (VEGF), which includes a family of three different growth factors involved in vascular and lymphangiogenesis. VEGF mRNA is substantially upregulated in most human tumors (Ferrara and Davis-Smyth, 1997). Although tumor cells represent the main source of VEGF, tumor-associated stroma is also an important site of VEGF production (Fukumura et al., 1998). Furthermore, there are high plasma levels of VEGF in tumor patients in comparison to healthy controls, which are associated with a poor outcome before chemotherapy (Salven et al., 1998).

Pro-angiogenic factors	Examples
Chemokines / Cytokines	VEGF, bFGF, SDF1, IL-8, TGF- β , PDGF-BB
Adhesion molecules	Integrins, CAMs, VE-Cadherin
Signaling molecules	RAP1, PI3K, AKT, ANG 2
Transcription factors	FOXO, ETS1, SIRT1, HIF-1 α , SP1
Receptors	TIE2, VEGFR-1, VEGFR-2

Table 1.1 Pro-angiogenic factors

VEGF: Vascular endothelial growth factor; bFGF: basic fibroblast growth factor; SDF 1: Stromal cell-derived factor-1; IL-8: Interleukin-8; TGF- β : Transforming growth factor- β ; PDGF-BB: Platelet-derived growth factor-BB; CAMs: Cell adhesion molecules; RAP1: RAS associated protein 1; PI3K: Phosphoinositide 3-Kinase; AKT: Protein Kinase B; ANG2: Angiopoietin 2; FOXO: Forkhead box transcription factor class O ; ETS1: V-ets erythroblastosis virus E26 oncogene homolog 1; SIRT1: Silent mating type information regulation 2 homolog 1; HIF-1 α : Hypoxia inducible factor 1 α ; SP1: Transcription factor; TIE2: Protein tyrosine kinase; VEGFR-1: VEGF receptor 1; VEGFR-2: VEGF receptor 2.

First studies showed that several tumor cell lines can be substantially growth-

inhibited by treatment with antibodies against VEGF indicating the involvement of VEGF in tumorigenesis (Kim et al., 1993). Since this first studies, intensive effort has been undertaken to develop therapeutic strategies to inhibit angiogenesis by using VEGF antagonists or antibodies targeting the VEGF receptors (Carmeliet, 2005).

Furthermore, NO, a gaseous molecule continuously released by endothelial cells under physiological conditions, exert pro- and anti-tumorigenic effects. The decision, if NO promotes or inhibits tumor progression is dependent on several factors, like the activity and localization of the different NO Synthase (NOS) isoforms, concentration and duration of NO exposure, and the cellular sensitivity to NO (Fukumura et al., 2006). Thereby, NO triggers multiple signaling pathways through S-nitrosylation and/or cGMP leading either to tumor cell proliferation, migration, invasion and increased resistance to apoptosis or tumor cell apoptosis and necrosis (Fukumura et al., 2006).

In contrast, stimulation of blood vessel formation in tissue deficient of normal blood flow, so-called therapeutic angiogenesis, is a promising intervention for patients suffering from severe diseases such as coronary artery disease. However, none of the techniques that have been used in VEGF therapy trials, including protein, plasmid, and adenoviral-based therapies, had any significant impact on the amount of VEGF in circulating blood or in ischemic tissues (Simons, 2005). This might be on the one hand attributed to a suboptimal delivery strategy, on the other hand growth factor delivery alone might not be sufficient to stimulate the formation of functional vessels. Therefore, novel strategies, involving transplantation of bone-marrow-derived cells or delivery of molecules stimulating the growth of proximal collateral vessels may be required for the future.

Additional strategies have been developed to target mural cells, hematopoietic cells and neoplastic cells. This therapeutical intervention might be also useful for treatment of diseases like diabetic retinopathy or age-related macular degeneration (AMD).

1.3 MicroRNAs

1.3.1 The diverse role of non-coding RNAs

Only less than 1.5% of the human genome encodes protein-coding sequences, whereas the vast majority of the human transcriptional output (~ 98 %) is non-coding RNA. The work of the recent years suggests a complex role of these non-coding RNAs (ncRNAs) on various levels of gene regulation using a wide range of mechanisms (Fig. 1.3) (Amaral et al., 2008). Starting with the chromatin architecture, Piwi-interacting RNAs (piRNAs) contribute to the formation of euchromatin (Yin and Lin, 2007), while small interfering RNAs (siRNAs) are linked to the formation of heterochromatin (Buhler and Moazed, 2007). Although there is some evidence for the involvement of ncRNAs in epigenetic control, it is so far poorly understood. HOTAIR, a 2.2 kilobase ncRNA residing in the HOXC locus, represses transcription *in trans* across 40 kilobases of the HOXD locus.

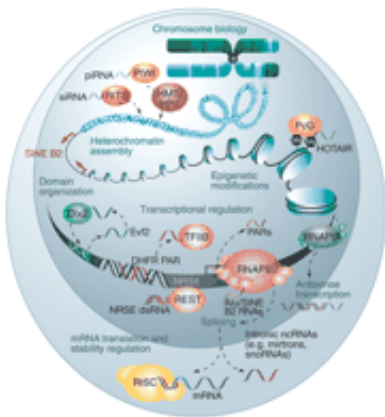


Figure 1.3 The world of non-coding RNAs

Recent examples of the various levels of regulation of eukaryotic gene expression and cell biology by ncRNAs. dsRNA, double-stranded RNA; HMT, histone methyltransferases; HP1, heterochromatin protein 1; PARs, promoter-associated RNAs; PcG, Polycomb group proteins; RISC, RNA-induced silencing complex; RITS, RNA-induced initiation of transcriptional gene silencing; siRNA, small interfering RNA; TFIIIB, transcription factor IIB; and UCE, ultraconserved element (Amaral, 2008)

HOTAIR interacts with Polycomb Repressive Complex 2 (PRC2) and is required for PRC2 occupancy and histone H3 lysine-27 trimethylation of the HOXD locus (Rinn et al., 2007) known primarily as a negative transcriptional regulator. This interaction results in the NRSF/REST complex no longer binding to HDACs, MeCP2, and MBD1, thereby switching cofactors from repressors to activators (Kuwabara et al., 2004). Additionally, promoter-directed sequence-specific RNAs, e.g. microRNAs (Place et al., 2008), have been shown to induce or repress transcription. Moreover, a wide class of ncRNAs, microRNAs, are able to regulate gene expression on the

posttranscriptional level by binding the target mRNA, thereby leading to translational repression or mRNA degradation.

1.3.2 MicroRNA history

The proper regulation of gene expression plays a crucial role in nearly all biological processes. Until now the epigenetic control by histone and DNA modification as well as transcription factors, which suppress or promote gene expression on the transcriptional level, are the best studied mechanisms involved in gene regulation.

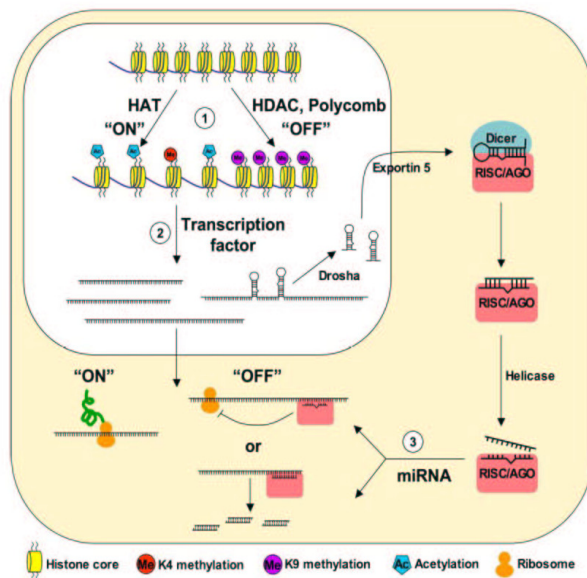


Figure 1.4 Global regulatory network

Gene expression is regulated on the epigenetic level by histone and DNA modifications (1) or on the transcriptional level by transcription factors (2). Recent studies described a third mechanism in which microRNAs inhibit gene expression by binding to the 3' UTR of the target mRNA (3). (Cheng, 2005)

However, in 1993, Victor Ambros and colleagues first discovered that *lin-4*, a gene known to control timing of *C. elegans* larval development, does not code for a protein, but instead produces a pair of small RNAs. This RNA was shown to be approximately 22 nt in length, and has antisense complementarity to multiple sites in the 3' UTR of the *lin-14* gene. First studies proposed a model in which *lin-4* RNAs pair to the *lin-14* 3' UTR leading to the specific translational repression of *lin-14* gene thereby triggering the transition from cell divisions of the first larval stage to the second (Lee et al., 1993; Wightman et al., 1991; Wightman et al., 1993). The shorter *lin-4* RNA is now recognized as the founding member of an abundant class of tiny regulatory RNAs called microRNAs (miRNAs) (Lagos-Quintana et al., 2001; Lau et al., 2001; Lee and Ambros, 2001) representing a new regulatory mechanism to post-

transcriptionally regulate translational repression or degradation of the target mRNA (Bartel, 2004) (Fig. 1.4). So far about 500 human miRNAs have been discovered and there is increasing evidence that miRNAs are involved in various biological processes such as cardiogenesis, skeletal muscle proliferation and differentiation, brain morphogenesis, oncogenesis and hematopoietic lineage differentiation while their dysregulation contributes to a variety of human diseases (Chen et al., 2004; Chen et al., 2006; Esquela-Kerscher and Slack, 2006; Giraldez et al., 2005; Zhao et al., 2007; Zhao et al., 2005). However, microRNAs are not only key regulators in animals but also in plants. These miRNAs regulate plant tissue differentiation, development and growth, control auxin signal transduction and are involved in plant response to a variety of abiotic and biotic environmental stresses (Wang and Li, 2007).

1.3.3 Biogenesis

MicroRNAs are generated in a two-step processing pathway mediated by two major enzymes, Dicer and Drosha, which belong to the class of RNase III endonucleases. Drosha is part of a multiprotein complex, the microprocessor, which mediates the nuclear processing of the primary miRNAs (pri-miRNA) into stem-loop precursors of approximately 60-70 nucleotides (pre-miRNA) (Lee et al., 2003). The treatment of HeLa cells with RNA interference against Drosha results in the strong accumulation of pri-miRNA and the reduction of pre-miRNA and mature miRNA (Lee et al., 2003). Exportin-5 mediates the nuclear export of correctly processed miRNA precursors in a RAN-GTP dependent manner (Lund et al., 2004). In the cytoplasm, the pre-miRNA is cleaved by Dicer into the mature 22 nucleotide miRNA (Bartel, 2004). Dicer was originally recognized for its role in generating small interfering RNAs (siRNA) (Bernstein et al., 2001) and was later shown to be also involved in miRNA maturation (Grishok et al., 2001). The mature miRNA incorporates as single-stranded RNA into a ribonucleoprotein complex, known as the RNA-induced silencing complex (RISC) (Hammond et al., 2001).

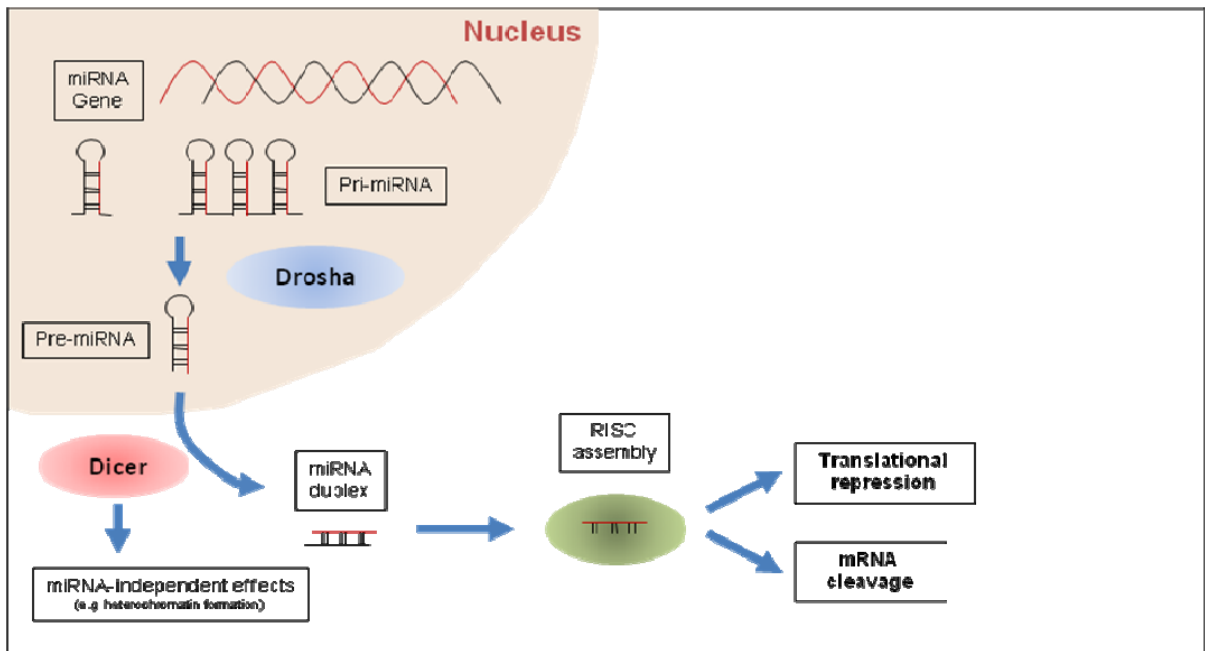


Figure 1.5 microRNA biogenesis

miRNAs are transcribed by Pol II into the primary miRNA (pri-miRNA), which is processed by the RNase III endonuclease Drosha into a 60-70 nucleotide stem loop intermediate (pre-miRNA). The pre-miRNA is transported to the cytoplasm by Exportin-5 and its cofactor RAN-GTP, where it is cleaved by Dicer into the mature miRNA. The incorporation of the mature miRNA into the RISC complex directs the miRNA to the target mRNA and leads to translational repression or mRNA degradation.

This complex directs the miRNA to the target mRNA, which leads either to translational repression or degradation of the target mRNA (Bartel, 2004) (Fig. 1.5).

1.3.4 Target prediction and regulation

A central goal for understanding microRNA function is to understand how they recognize their target message and how the binding of the microRNA to the target site in the 3'UTR leads to downregulation. Conserved Watson-Crick pairing to the 5' end of the microRNA enables prediction of targets. However, in contrast to small-interfering RNA (siRNA), which binds complementary to the target mRNA, thereby leading to mRNA degradation, miRNA has rarely perfect complementarity to the target mRNA. Several different algorithms, either based on the complementarity or thermodynamic-based algorithmy accessible on various online databases (e.g.

TargetScan, PicTar, miRanda, Diana-microT) have been developed to overcome the problem of false-positive predictions. In the following, the algorithm used for target prediction with the TargetScan database will be introduced in greater detail (Grimson et al., 2007). Complementary microRNA binding sites, so called seed sequences, in the 3'UTR of target mRNA are classified in three different groups: 7mer-A1, 7mer-m8 and 8mer (Fig. 1.6). The 7mer-A1 refers to the binding of the miRNA nucleotides 2-7 to the target mRNA augmented by an A at target position 1. Another 7mer is the 7mer-m8 with a direct match of miRNA nucleotides 2-8. The 8mer is a combination of the 7mer-A1 and 7mer-m8 with a direct match at position 2-8 and an additional A at target position 1. However, only a minority of single target sites induces the degradation of the target mRNA (19% 7mer-A1, 25% 7mer-m8 and 43% 8mer) suggesting that multiple target sites are associated with higher mRNA stability.

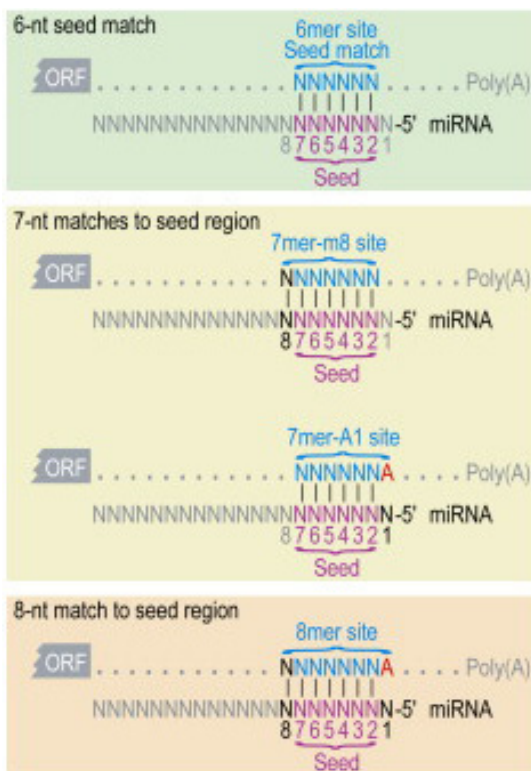


Figure 1.6 Downregulation of messages with 6-8mer sites

Canonical miRNA complementary sites. The 6mer is the perfect 6 nt match to the miRNA seed (miRNA nucleotides 2–7). The best 7mer site, referred to here as the 7mer-m8 site, contains the seed match augmented by a match to miRNA nucleotide 8. Also effective is another 7mer, the 7mer-A1 site, which contains the seed match augmented by an A at target position 1. The 8mer site comprises the seed match flanked by both the match at position 8 and the A at position 1. (Grimson, 2007)

Indeed, multiple target sites show a multiplicative effect meaning that the repression for a gene with two different target sites matches the result anticipated by multiplying the repression from two single sites. However, the repression tends to be even stronger when the two independent target sites are closely spaced within 100 nucleotides. An additional requirement for sufficient downregulation is Watson-Crick pairing close to the 3`end of the microRNA between nucleotides 12-17. Apart from

sequence specificity of the target site its localization in the 3'UTR is also an important factor. Effective target sites preferentially reside within a local AU-rich context, which might be associated with weaker secondary structure in the vicinity of the site and thus increased accessibility to the seed site. Further on, effective sites are favorable located close to both ends of the 3'UTR, whereas binding sites less than 15 nucleotides from the stop codon are less effective, probably because of the local interference of the microRNA with adjacent ribosomes bound to the open reading frame of the mRNA. Beside the previously described characteristics of miRNA mRNA binding, the secondary structure and therefore the accessibility of the mRNA has been also shown to play a crucial role in target prediction (Zhao et al., 2005). Using mFold, Zhao et al. analysed the binding sites of all identified targets and found, that all binding sites are located in unstable regions with low free energy (ΔG) suggesting a locally linear miRNA-binding site.

Published studies indicate that miRNAs bound to the target mRNA repress protein expression in four distinct ways (Eulalio et al., 2008) (Fig. 1.7): The postinitiation mechanisms describes a model in which microRNAs repress translation of target mRNAs by blocking translation elongation or by promoting premature dissociation of ribosomes (ribosome drop-off). The cotranslational protein degradation model proposes that translation is not inhibited, but rather the nascent polypeptide chain is degraded cotranslationally. The putative protease is unknown. On the other hand microRNAs interfere with a very early step of translation, prior to elongation (initiation mechanisms). This model suggests a key role of Argonaut proteins, which either compete with eIF4E for binding to the cap structure, recruit eIF6, which prevents the large ribosomal subunit from joining the small subunit or prevent the formation of the closed loop mRNA configuration by an ill-defined mechanism that includes deadenylation.

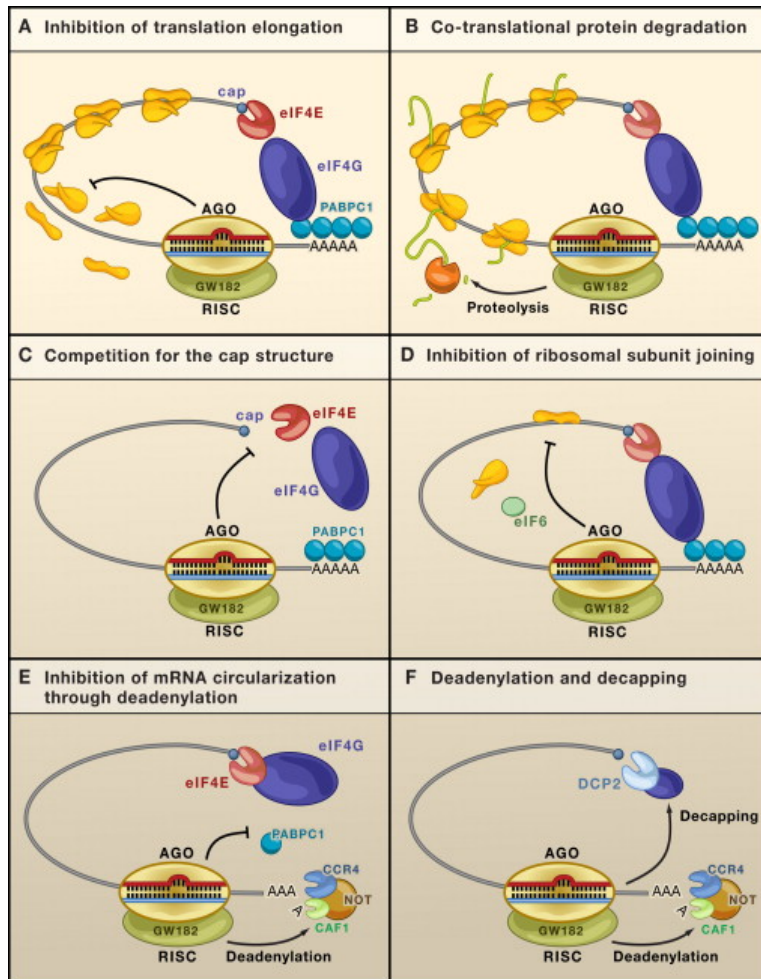


Figure 1.7 Mechanisms of miRNA-mediated gene silencing

A) Postinitiation mechanisms.
B) Cotranslational protein degradation. **C–E)** Initiation mechanisms. **F)** MicroRNA-mediated mRNA decay. (Eulalio, 2007)

Beside the translational repression microRNAs mediate mRNA decay by triggering deadenylation and subsequent decapping of the mRNA target. Proteins required for this process include components of the major deadenylase complex (CAF1, CCR4, and the NOT complex), the decapping enzyme DCP2, and several decapping activators.

1.3.5 Regulation of microRNA activity

Considering the fact that microRNAs are involved in a wide variety of physiological processes, it is not surprising that the biogenesis and activity of microRNAs is a tightly regulated process. Recent studies indicate that a large subset of microRNAs is associated with CpG islands indicating that these genes represent candidate targets for DNA methylation (Weber et al., 2007). Treatment of cells with a combination of inhibitors of DNA methylation and histone deacetylation activates the expression of

particular microRNAs that may act as tumor suppressors (Saito et al., 2006). Moreover, it was demonstrated that various microRNA genes are affected by epigenetic inactivation due to aberrant hypermethylation and that this is an early and frequent event in breast cancer development (Lehmann et al., 2008). However, microRNA regulation is not only restricted to the level of epigenetic control, but also takes place during microRNA biogenesis. Thus it has been shown that Lin28, a developmentally regulated RNA-binding protein, selectively inhibits the processing of pri-let-7 by sufficiently blocking the microprocessor-mediated cleavage in embryonic stem cells (Viswanathan et al., 2008). In contrast, receptor-regulated SMAD proteins (R-SMAD) are capable to stimulate processing of the pri-miR-21 by binding the microprocessor complex in human vascular smooth muscle cells (Davis et al., 2008). Furthermore, several microRNAs are modified by RNA editing, leading either to changes in RNA stability or target selection (Kawahara et al., 2007; Knight and Bass, 2002). Finally, microRNA activity is regulated on the level of microRNA to target mRNA binding. RNA-binding proteins associate with the target sequence in the 3'UTR of mRNAs, thereby preventing the binding of the specific microRNA (Bhattacharyya et al., 2006; Davis et al., 2008)

1.3.6 Role of Dicer and Drosha in endothelial cells

Dicer, which mediates the cytoplasmatic cleavage of the precursor miRNA into the mature miRNAs has been shown to be implicated in several physiological processes such as heart function (Chen et al., 2008), chondrocyte proliferation and differentiation (Kobayashi et al., 2008), neuronal survival (Schaefer et al., 2007), immune regulation (Cobb et al., 2006), brain morphogenesis (Giraldez et al., 2005), skin morphogenesis (Yi et al., 2006) as well as angiogenesis (Suarez et al., 2007; Yang et al., 2005) . Dicer is constitutively expressed in endothelial cells and its expression is not altered in response to stimuli, such as VEGF (Suarez et al., 2007). Previous publications have described a crucial role of the miRNA-regulating enzyme Dicer in angiogenesis *in vitro* and *in vivo*. Thus, Dicer^{ex1/2} mutant mice display angiogenic defects in embryos and yolk sacs, while vasculogenesis and initial steps of angiogenesis proceed normally (Yang et al., 2005). Consistently, in zebrafish, the blood circulation is disrupted in dicer mutants (Giraldez et al., 2005). Deletion of

Dicer in endothelial cells impairs the development of capillary-like structures and exhibits an anti-proliferative effect (Suarez et al., 2007). The migration of Dicer-deficient endothelial cells on collagen matrix could be shown to be not affected (Suarez et al., 2007).

Furthermore, Dicer knockdown causes profound dysregulation of angiogenesis-related genes *in vitro* and *in vivo*. Despite the requirement of Dicer for vascularization, crucial regulators of angiogenesis, for instance vascular endothelial growth factor (VEGF) and its receptors FLT1 and KDR, have been shown to be upregulated by depletion of Dicer (Suarez et al., 2007; Yang et al., 2005). Furthermore, protein levels of the angiopoietin receptor TIE1, expressed in vascular endothelium during angiogenesis, are decreased in Dicer^{ex1/2} embryos (Yang et al., 2005), whereas its expression is strongly enhanced in Dicer-depleted cultured endothelial cells (Suarez et al., 2007). This phenomenon might be explained by the complex mixture of miRNAs being spatiotemporally expressed during development compared to isolated endothelial cells in culture.

In contrast to Dicer, the involvement of Drosha in angiogenic processes was unknown at the beginning of this project.

1.3.7 Specific microRNAs involved in angiogenesis

The majority of miRNAs are expressed in many cell types with variations in the expression levels, whereas about one-third of microRNAs show substantially tissue-specificity. When this study was initiated, the expression profile of miRNAs in EC was still unknown. Meanwhile, we and others profiled microRNA expression in EC in order to identify miRNAs involved in the control of EC biology (Poliseno et al., 2006; Suarez et al., 2007).

Analyzing the two published expression patterns reveals that eight miRNAs are highly expressed in human umbilical cord endothelial cells: let-7b, miR-16, miR-21, miR-23a, miR-29, miR-100, miR-221, and miR-222 (Poliseno et al., 2006; Suarez et al., 2007). Among the highly expressed miRNAs, only a few have been functionally characterized so far.

First studies addressed the role of highly expressed miR-221 and miR-222 in endothelial cells. Transfection of endothelial cells with miR-221 and miR-222 inhibits *in vitro* angiogenesis by blocking tube formation and migration and reduced wound healing of endothelial cells *in vitro* (Poliseno et al., 2006). MiR-221 and miR-222 decrease protein levels of c-kit, the receptor for stem cell factor, whereas mRNA levels were not affected indicating that miR-221/222 target c-kit expression by blocking protein translation (Poliseno et al., 2006). In addition, miR-221 and miR-222 overexpression has been shown to indirectly reduce the expression of the endothelial nitric oxide synthase (eNOS) in the context of Dicer silencing (Suarez et al., 2007). Given that eNOS contributes to endothelial cell functions, its reduction by miR-221/222 may have caused the functional impairment such as inhibited tube formation, migration and wound healing observed in miR-221/222 transfected endothelial cells. Since miR-221 and miR-222 target at least two important regulators of pro-angiogenic endothelial cell function, c-kit and eNOS, it might be an attractive tool to block angiogenesis. In addition, miRNAs 221 and 222 also inhibit cell proliferation and reduce c-kit expression in hematopoietic progenitor cells (Felli et al., 2005), which can contribute to vessel growth. Whether inhibition of miR-221/222 might be useful to enhance therapeutic angiogenesis *in vivo* (e.g. in ischemic tissues) remains to be elucidated. Moreover, in order to use miRNAs as therapeutic tools the complete spectrum of miRNA targets in different tissues needs to be specified in detail. Indeed, miR-221 and miR-222 exhibit opposing effects on proliferation of cancer cells in contrast to endothelial cells. While high expression of miR-221/222 blocked angiogenesis in endothelial cells these miRNAs promoted proliferation in cancer cells by targeting the cell cycle inhibitor p27 (le Sage et al., 2007) suggesting a cell type specific regulation of proliferation. MiR-130a downregulates the anti-angiogenic homeobox proteins GAX (growth arrest homeobox) and HoxA5, and functionally antagonized the inhibitory effects of GAX on endothelial cell proliferation, migration and tube formation and the inhibitory effects of HOX A5 on tube formation *in vitro* (Chen and Gorski, 2008). MiR-126 inhibited the expression of vascular cell adhesion molecule 1 (VCAM-1), which mediates leukocyte adherence to endothelial cells. Thus, decreasing miR-126 in endothelial cells increases TNF- α -stimulated VCAM-1 expression and enhances leukocyte adherence to endothelial cells (Harris et al., 2008).

Two other miRNAs, which might be involved in angiogenesis, are miR-15b and miR-16. Although the direct effect of miR-15b and miR-16 in endothelial cells has not been elucidated, both miRNAs are downregulated by hypoxia in a carcinoma cell line (Hua et al., 2006). MiR-15b and miR-16 control the expression of VEGF, a key pro-angiogenic factor particularly involved in tumor angiogenesis (Hua et al., 2006). These data indicate that hypoxia-induced reduction of these miRNAs contributes to an increase in VEGF levels. Interestingly, miR-15b and miR-16 induce apoptosis of leukemic cells by targeting the anti-apoptotic protein BCL2, block cell cycle progression and are frequently downregulated in chronic lymphocytic leukemia (Cimmino et al., 2005; Linsley et al., 2007). Therefore, one may speculate that miR-15b/miR-16 overexpression might be an attractive anti-tumor strategy by targeting tumor cell survival and proliferation and by blocking VEGF-mediated angiogenesis.

1.3.8 Role of microRNAs in diseases

Whereas several years ago microRNAs were supposed to be fine tuners, just modulating different processes, emerging evidence suggest a key role of microRNAs in nearly all physiological and pathophysiological processes. About one- third of the microRNAs show substantially tissue specificity, while the others vary in their expression levels but are not particularly cell or tissue-specific. The involvement of microRNAs was shown for stem cell biology, meiotic spindle formation and chromosome organization, skeletal muscle proliferation and differentiation as well as cardiac function, hematopoiesis and immunity and the nervous system. Hence it is not surprising that microRNAs came under close investigation in a variety of diseases.

Several microRNAs have been identified as crucial players in the development of heart failure. MiR-195 is consistently overexpressed in human and rodent hypertrophic hearts leading to dilated cardiomyopathy and heart failure, probably by targeting multiple prosurvival genes (van Rooij et al., 2006). MiR-208 is required for stress-dependent cardiac hypertrophy and fibrosis by blocking THRAP1 expression and therefore β -MHC upregulation (van Rooij et al., 2007). MiR-1 has a crucial function in cardiac development and contractility by targeting the transcription factor

HAND2 and IRX5 as well as the potassium channel KCND2 (Zhao et al., 2007; Zhao et al., 2005). MiR-133 is downregulated in human heart disease as well as three models of cardiac hypertrophy (Care et al., 2007). These data suggest a role of miR-133 in the inhibition of remodeling processes and hypertrophy.

In addition, there is evidence for the participation of microRNAs in neuronal diseases like Alzheimer and Parkinson's disease. MiR-133b is specifically expressed in midbrain dopaminergic neurons and is deficient in midbrain tissue from patients suffering from Parkinson's disease. MiR-133b regulates the maturation and function of midbrain dopaminergic neurons including PITX3 for fine tuning of dopaminergic behaviors like locomotion (Kim et al., 2007). Loss of miR-29a/b-1 in the brain contributes to increased BACE1 and A β levels, which in turn has been shown to be associated with sporadic Alzheimer disease (Hebert et al., 2008). Furthermore, the implication of several microRNAs was shown for infectious diseases (Cullen, 2006).

Most studies of the last decade, however, focused on the contribution of microRNAs to the initiation and progression of cancer. MicroRNAs involved in cancer are divided in two groups: microRNAs located in portions of chromosomes deleted in cancers function as tumor suppressors and microRNAs located on genomic regions amplified in cancer and function as oncogenes, so-called oncomirs. Members of the let-7 family targeting the Ras oncogenes and the miR-15a-miR-16-1 cluster targeting the anti-apoptotic gene BCL2 seems to act as tumor suppressors. On the other hand miR-21 and members of the miR-17-92 cluster are highly overexpressed in many solid tumor types and have been shown to act as oncogenes.

1.3.9 miR-17-92 cluster

The miR-17-92 cluster is a polycistronic miRNA gene encoding the miRNAs, miR-17-5p, miR-17-3p, miR-18a, miR-19a, miR-20a, miR-19b and miR-92-a-1 (Venturini et al., 2007) grouped on chromosome 13. The sequences of the mature miRNAs as well as their organization are highly conserved between all vertebrates.

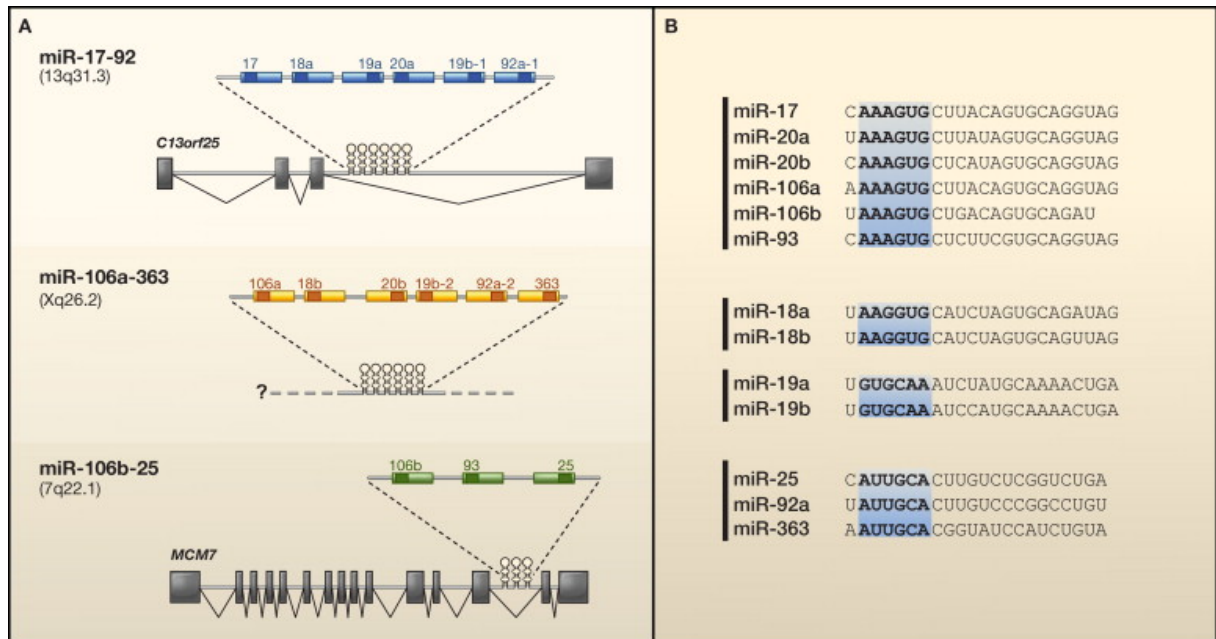


Figure 1.8 Genomic organization of three homologues microRNA cluster

A) The genomic organization and primary transcript structures of the human miR-17-92, miR-106a-363, and miR-106b-25 clusters. The miR-106a-363 primary transcript has not been characterized. **B)** Based on their seed sequences—which are the regions considered most important for target selection (nucleotides 2–7; shown in blue)—the miRNAs of these clusters can be grouped into four families: the miR-17 family (miR-17, miR-20a/b, miR-106a/b, and miR-93); the miR-18 family (miR-18a/b); the miR-19 family (miR-19a/b); and the miR-25 family (miR-25, miR-92a, and miR-363). (Mendell, 2008)

The miR-17-92 cluster has two paralogues in mammals: the miR-106a-363 cluster on the X-chromosome encoding miR-106a, miR-18b, miR-20b, miR-19b-2, miR-92-a-2 and miR-363 and the miR-106b-25 cluster on chromosome 7 encoding miR-106b, miR-93 and miR-25 (Fig. 1.8). While miR-17-92 and miR-106b-25 clusters are abundantly expressed across many tissues, the miR-106a-363 cluster is in most cases undetectable or expressed at very low levels. Consistently, a deletion of the miR-106a-363 cluster or the miR-106b-25 cluster has no obvious phenotypic consequences, whereas deletion of miR-17-92 cluster leads to death shortly after birth. The phenotype is often characterized by lung hypoplasia and a ventricular septal defect. Whereas little is known so far about the miR-106a-363 and miR-106b-25 clusters, the functional impact of the whole miR-17-92 cluster as well as several mature microRNAs expressed from the cluster are analyzed in more detail.

It was shown, that miR-17-92 is highly expressed in embryonic stem cells, with expression levels decreasing during embryonic development in mice (Thomson et al., 2004). These results support the idea that high levels of miR-17-92 promote the proliferation of progenitor cells and inhibit their differentiation. Additionally, a significant upregulation could be observed in Myc-induced tumors and miR-17-92 has been shown to specifically target anti-angiogenic proteins (Dews et al., 2006). Specific evaluation of the targets revealed that miR-18 suppresses connective tissue growth factor (CTGF) expression, whereas miR-19 targets the potent angiogenesis-inhibitor thrombospondin-1 (TSP1) (Dews et al., 2006). MiR-20 and miR-92 do not affect the expression levels of the thrombospondin type 1 repeats-containing proteins. Transgenic overexpression of miR-17-92 in lungs displayed an abnormal lethal phenotype with numerous proliferative epithelial cells that retain high levels of SOX9 and inhibited differentiation of proximal epithelial cells (Lu et al., 2007b). Transgenic mice overexpressing miR-17-92 in lymphocytes developed lymphoproliferative disease and autoimmunity and died prematurely, probably by suppressed expression of the tumor suppressor PTEN and the proapoptotic protein Bim (Xiao et al., 2008). Consistently, ablation of the miR-17-92 cluster led to increased levels of Bim and inhibited B-cell development at the pro-B to pre-B transition (Ventura et al., 2008).

So far, there is only sparse information about the transcriptional regulation of the miR-17-92 cluster. C-myc, a factor frequently hyperactive in cancer cells was reported to transactivate the miR-17-92 cluster. Moreover, members of the E2F family of transcription factors, which are critically involved in cell cycle and apoptosis, are regulated by the miR-17-92 cluster, but in turn can directly activate the expression of these microRNAs as a positive feedback.

1.4 Aim of the study

MicroRNAs are small non-coding RNAs regulating gene expression on the posttranscriptional level by binding to the target mRNA thereby promoting translational repression or mRNA decay. The research of the last decade demonstrates that microRNAs are involved in nearly all physiological and pathophysiological processes, e.g. differentiation, oncogenesis and cardiogenesis by regulating whole networks of genes. However, at the beginning of this study nothing was known about the specific role of microRNAs in endothelial cells as well as in endothelial cell dependent processes like angiogenesis and neovascularization. Hence, following aspects were specifically studied:

1. Dicer and Drosha are the major microRNA-processing enzymes. Using siRNA targeting Dicer and Drosha, we planned to analyse the general role of microRNAs in endothelial cell biology.
2. We aimed to determine the microRNA expression profile in EC in order to identify specific microRNAs, which are involved in EC biology. Based on the identification of the highly expressed microRNA, miR-92a, we proposed to study the role of miR-92a in angiogenesis and neovascularization *in vitro* and *in vivo* in more detail.

2 Material and Methods

2.1 Cell culture of HUVEC

Pooled human umbilical vein endothelial cells (HUVEC) were purchased from Cambrex and cultured in endothelial basal medium (EBM; Cambrex) supplemented with hydrocortisone, bovine brain extract, epidermal growth factor, antibiotics and 10% fetal calf serum (FCS; Gibco) at 37°C, 5% CO₂ air humidity until the third passage. For passaging, cells were washed with 10 ml phosphate buffer saline and detached with 3 ml Trypsin/EDTA. After removal of Trypsin, cells were resuspended in 10 ml medium and seeded in new T-75 cell culture flasks. For experiments, cells were seeded in 6 cm culture dishes for at least 24-48 hours to the indicated confluency.

Cells	Description
HUVEC	Human umbilical vein endothelial cells (Lonza)
HMVEC	Human microvasculare endothelial cells (Lonza)
HEK293	Human embryonal kidney epithelial cells (transformed cell line)
HCM	Human cardiac myocytes
HAoSMC	Human aortic smooth muscle cells (PromoCell)
HAoAF	Human aortic adventitial fibroblasts (PromoCell)
CD34+	Cells expressing CD34 on the cell surface isolated from peripheral blood

Table 2.1 Cell types

2.2 Cell culture of HEK293

HEK293 were cultivated in DMEM 4500 including supplements (table 2.2) at 37°C, 5% CO₂ air humidity. For passaging, cells were washed with 10 ml PBS and detached with 3 ml Trypsin/EDTA. After removal of Trypsin, cells were resuspended in 10 ml medium

and seeded in new T-75 cell culture flasks. For transfection, cells were seeded in 24-well plates for 24 hours.

2.3 Growth media

Growth media used for cultivation of human cells are listed below.

Cells	Medium	Supplements
HUVEC	Endothelial basal medium (EBM), Cambrex	10% fetal calf serum (FCS), Boehringer Mannheim, hEGF (10 µg/ml), hydrocortisone (1 µg/ml), Bovine brain extract (3 µg/ml), Gentamycin sulfate (50 µg/ml), Amphotericin-B (50 mg/ml), Cambrex
HMVEC	Endothelial basal medium-2 (EBM-2), Cambrex	10% FCS, Boehringer Mannheim, EGM [®] -MV Bullet Kit, Cambrex
HEK293	DMEM 4500 Glucose with Glutamax, Gibco	25% FCS, 2.5% NEAA Gibco
EPC	Endothelial basal medium (EBM), Cambrex	20% fetal calf serum (FCS), Boehringer Mannheim, hEGF (10 µg/ml), hydrocortisone (1 µg/ml), Bovine brain extract (3 µg/ml), Gentamycin sulfate (50 µg/ml), Amphotericin-B (50 mg/ml), Cambrex
HCM	Myocyte growth medium, PromoCell	Supplement mix/Myocyte growth medium, PromoCell
HAoSMC	Smooth muscle cell growth medium 2, PromoCell	Supplement Mix/ Smooth muscle cell growth medium 2, PromoCell
HAoAF	Fibroblast growth medium 2, PromoCell	Supplement Mix/ Fibroblast growth medium 2, PromoCell

Table 2.2 Growth media

2.4 Transfection of oligonucleotides

For the suppression of expression of specific genes or microRNAs, HUVEC were transfected with siRNA (small interfering RNA) or 2`O-methyl antisense oligoribonucleotides (Table 2.3). Therefore, cells seeded in 6 cm dishes (3.1×10^5 cells/well) were grown to 60-70% confluence and transfected either with 60 nM siRNA or 50 nM 2`O-methyl antisense oligoribonucleotides using GeneTrans II[®]

(MoBiTec) according to the manufacturer's protocol. Control sequences, which do not bind endogenous mRNAs or miRNAs were used.

2.5 Transfection of pre-miRNA

For overexpression of miRNAs, HUVEC were seeded in 6 cm dishes (3.5×10^5 cells/well) and grown to 50% confluence. 10nM of the precursor or control pre-miR (Ambion) were transfected with Lipofectamine RNAiMAX (Invitrogen) according to the manufacturer's protocol.

siRNA	Sequence	Company
Dicer I	UGCUUGAAGCAGCUCUGGA	Eurogentec
Dicer II	UUUGUUGCGAGGCUGAUUC	Eurogentec
Drosha I	AACGAGUAGGCUUCGUGACUU	Eurogentec
Drosha II	AAGGACCAAGUAUUCAGCAAG	Eurogentec
Integrin $\alpha 5$	UCCUUA AUGGCUCAGACAU	Qiagen
scrambled	UCAAGAAGCCAAGGAUAAU	Eurogentec
2`O-methyl oligoribonucleotides	Sequence	Company
GFP	AAGGCAAGCUGACCCUGAAGUU	VBC Biotech
92a	CAGGCCGGGACAAGUGCAAUA	VBC Biotech
let-7f	AACUAUACAAUCUACUACCUCA	VBC Biotech
27b	GCAGAACUUAGCCACUGUGAA	VBC Biotech
151	CCUCAAGGAGCUUCACUCUAGU	VBC Biotech
191	AGCUGCUUUUGGGAUUCCGUUG	VBC Biotech
214	CUGCCUGUCUGUGCCUGCUGU	VBC Biotech
222	GAGACCCAGUAGCCAGAUGUAGCU	VBC Biotech

Table 2.3 Oligonucleotides used for transfection

2.6 RNA isolation

RNA for quantification of gene expression from human cells was isolated using the RNeasy kit (Qiagen). Trizol (Sigma) was used for quantification of microRNAs and RNA isolation from animal tissue. Cells or tissue were lysed in a defined volume of Trizol, mixed with chloroform and centrifuged. The upper clear phase contained the RNA, which was precipitated with isopropanol and washed with 75% ethanol. The pellet was resuspended in a defined volume of H₂O.

2.7 RT-PCR and real time PCR

In order to analyse the expression of specific genes, 1 µg of RNA was reverse transcribed into cDNA and subjected either to semiquantitative end-point PCR or quantitative real time PCR (Table 2.4). As loading control GAPDH was used. The semiquantitative analysis of the PCR was performed densitometrically after running an agarose gel using Scion Image software (Scion Corporation). Quantitative real time PCR was performed using the LightCycler[®] SYBR Green^{plus} I Kit (Roche), LightCycler 1.2 and LightCycler 3 software. To assess the differential miRNA expression in HUVEC transfected with 2'-O-methyl antisense oligoribonucleotides or pre-miRNAs, we isolated total RNA using Trizol 24 h after transfection.

PCR	sense (5' → 3')	antisense (5 → 3')
Human Dicer	CAAGTGTCAGCTGTCAGAACTC	CAATCCACCACAATCTCACA TG
Human Drosha	CACCTGTTCTAGCAGCTCAGAC	CTCCTCCCACTGAAGCATAT TG
Mouse Integrin α5	CATTTCCGAGTCTGGGCCAA	TGGAGGCTTGAGCTGAGCT T
GAPDH	TCACCATCTTCCAGGAGCGAGAT C	GAGACCACCTGGTGCTCAG TG TAG

Cloning	sense (5' → 3')	antisense (5' → 3')
Integrin α 5 seed 4x	AGCTTTTTATTGCACTTGCAACAG AGTTTATTTATTGCACTTGCAACA GAGTTTATTTATTGCACTTGCAAC AGAGTTTATTTATTGCACTTGCAA CAGAGTTTAA	CTAGTTAAACTCTGTTGCAA GTGCAATAAATAAACTCTGT TGCAAGTGCAATAAATAAAC TCTGTTGCAAGTGCAATAAA TAAACTCTGTTGCAAGTGCA ATAAAA
Integrin α 5 seed mm 4x	AGCTTTTTATTACGCTTACAAAAG AGTTTATTTATTACGCTTACAAA GAGTTTATTTATTACGCTTACAAA AGAGTTTATTTATTACGCTTACAA AAGAGTTTAA	CTAGTTAAACTCTTTTGTA GCGTAATAAATAAACTCTTT TGTAAGCGTAATAAATAAAC TCTTTTGTAAGCGTAATAAA TAAACTCTTTTGTAAGCGTA ATAAAA 3

Table 2.4 Primer for PCR and cloning

RT-PCR was performed using the *mirVana*[™] qRT-PCR miRNA Detection Kit (Ambion) and primer sets for specific miRNAs or U6 as loading control (Ambion) (one cycle: 3 min at 95°C, 20 cycles: 15 seconds at 95°C, 30 seconds at 60°C).

2.8 Stem loop RT and quantitative PCR of miRNAs

Total RNA was isolated using Trizol. 100 ng RNA was reverse transcribed into cDNA in a pulsed RT reaction using specific stem-loop Primer containing the binding site of probe #21 (Universal Probe Library, Roche) as described by Wu et al., 2007. Subsequent real-time PCR using UPL probe #21 (Roche) and specific primer was performed on LightCycler 1.2 (Roche). Primer sequences used are listed in table 2.5. (Varkonyi-Gasic et al., 2007).

2.9 MicroRNA expression analysis

Total RNA from HUVEC was isolated using TRIZOL. The expression of 360 mature human miRNAs in HUVEC was profiled using real-time PCR (DNAvision, Belgium). Gene expression data were normalized to RNU48. The relative expression was determined for 23 of the 360 miRNAs using the formula $2^{-\Delta Ct}$.

MicroRNA	Stem loop primer	
miR-92a	GTTGGCTCTGGTGCAGGGTCCG AGGTATTCGCACCAGAGCCAACC AGGCC	
miR-92b	GTTGGCTCTGGTGCAGGGTCCG AGGTATTCGCACCAGAGCCAACG GAGG	
miR-93	GTTGGCTCTGGTGCAGGGTCCG AGGTATTCGCACCAGAGCCAACC TACCT	
miR-18a	GTTGGCTCTGGTGCAGGGTCCG AGGTATTCGCACCAGAGCCAACC TATCT	
miR-19a	GTTGGCTCTGGTGCAGGGTCCG AGGTATTCGCACCAGAGCCAAC CAGTT	
miR-24	GTTGGCTCTGGTGCAGGGTCCG AGGTATTCGCACCAGAGCCAACC TGTT	
U48	GTTGGCTCTGGTGCAGGGTCCGAG GTATTCGCACCAGAGCCAACGGTCA G	

Real time PCR	sense (5' → 3')	antisense (5' → 3')
miR-92a	CGGCGGTATTGCACTTGTCCC	GTGCAGGGTCCGAGGT
miR-92b	CGGCGGTATTGCACTCGTCCCG	GTGCAGGGTCCGAGGT
miR-93	CGCCCAAAGTGCTGTTTCGTGC	GTGCAGGGTCCGAGGT
miR-18a	CGCCTAAGGTGCATCTAGTGC	GTGCAGGGTCCGAGGT
miR-19a	GCCGCCTGTGCAAATCTATGCAA	GTGCAGGGTCCGAGGT
miR-24	CGGCGTGGCTCAGTTCAGCAG	GTGCAGGGTCCGAGGT
U48	GAGTGATGATGACCCCAGGTAA	GTGCAGGGTCCGAGGT

Table 2.5 Primer for qRT-PCR

2.10 MicroRNA array analysis

Total RNA from HUVEC was isolated using Trizol (Invitrogen) according to the manufacturer's protocol. MicroRNA expression profiling of 344 microRNAs was performed by microRNA profiling service (Exiqon) using miRCURY LNA arrays.

2.11 Protein isolation

Cells were washed with cold phosphate buffer, pelletized and resuspended in 150 µl RIPA buffer (Sigma) containing protease inhibitor cocktail (Roche) and 1mM PMSF. After 20 min incubation on ice the protein lysate was separated from the insoluble debris by centrifugation (20.000 x g, 15 min, 4°C). Protein concentration was determined by mixing 2 µl protein lysate or 2 µl lysis buffer as control with 798 µl H₂O and 200 µl Bradford reagent (Biorad). Absorption was measured in the photometer at $\lambda = 595$ nm. Concentration was measured using a bovine serum albumine (BSA) standard curve.

2.12 SDS polyacrylamide gel electrophoresis (SDS-PAGE)

Protein lysates were mixed with 4x sample buffer (250 mM Tris/HCl pH 6.8, 8% SDS, 40% glycerine, 0.04% bromine phenol blue, 200 mM DTT) and boiled 5 min at 100°C. The separation of the proteins occurred by discontinuous SDS-PAGE, whereas proteins were first focussed by the stacking gel (1 M Tris/HCl pH 6.8, 0.4% SDS) and separated by size in the separating gel (1.5 M Tris/HCl pH 8.8, 0.4% SDS) using the Mini Protean II gel electrophoresis system (Biorad). Proteins in the stacking gel were run at 80 V, in the separating gel at 120 V. The running buffer consisted of 0.25 M Tris, 0.96 M glycine and 1% SDS.

2.13 Western blot analysis

Proteins separated by SDS-PAGE were blotted onto PVDF or Nitrocellulose membranes and immobilized. The PVDF membrane was activated by incubation for 1 min in methanol. Gel, membranes and Whatman papers were equilibrated in transfer buffer (0.05 M Tris, 0.038 M glycine, 0.1% SDS, 20% methanol) and placed bubble free within two scotch pads. An electric current (20 W for 1.5 – 2 hours, 4°C) was used to transfer proteins from the gel onto the PVDF or nitrocellulose membrane. Proteins were detected by immunocytochemistry (Table 2.6).

2.14 Immunocytochemistry for protein detection

Depending on the antibodies used for detection, the membrane was blocked for 1.5 hours at room temperature in TBS/Tween (50 mM Tris/HCl pH 8, 150 mM NaCl, 2.5 mM KCl, 0.1% Tween-20) containing either 5% milk powder (Töpfer, Dietmannsried) or 3% bovine serum albumin (Merck). Subsequently, the membrane was incubated with a specific antibody over night at 4°C (Table 2.6). After washing 3x with TBS/Tween, the membrane was incubated for 1 hour at room temperature with the adequate secondary antibody coupled with horseradish peroxidase. After 3x washing the membrane with TBS/Tween, specific proteins were detected by chemiluminescence using ECL reagent (Amersham).

Western blot	Company	Dilution	Blocking	Secondary antibody
anti-Dicer	Abcam	1/500	3% BSA	anti-mouse-HRP
anti-Drosha	Upstate	1/1000	5% Milk	anti-rabbit-HRP
anti-TOPO I	Santa Cruz	1/250	5% Milk	anti-rabbit-HRP
anti-HSP70	Upstate	1/500	5% Milk	anti-rabbit-HRP
anti-TSP	Lab Vision	1/250	3% BSA	anti-mouse-HRP
anti-Integrin α 5	Chemicon	1/500	3% BSA	anti-rabbit-HRP
anti-SIRT1	Upstate	1/1000	5% Milk	anti-rabbit-HRP
anti-eNOS	BD	1/2500	3% BSA	anti-mouse-HRP
anti-MKK4	Cell Signaling	1/1000	5% Milk	anti-rabbit-HRP
Anti-AKT	Cell Signaling	1/1000	3% BSA	anti-mouse-HRP
Anti-P-AKT	Cell Signaling	1/1000	5% Milk	anti-rabbit-HRP
anti-Tubulin	Dianova	1/1500	3% BSA	anti-mouse-HRP
Immunostaining	Company	Dilution	Blocking	Secondary antibody
anti-Dicer	Abcam	1/50	2% BSA	anti-mouse-544
anti-Drosha	Upstate	1/50	10% FCS	anti-rabbit-546
anti-Phospho-H3-488	Cell Signaling	1/10	0.2% BSA	/
SYTOX Blue	Invitrogen	1/1000	/	/
Phalloidin-633	Invitrogen	1/300	/	/
anti-SMA-Cy3	Sigma	1/300	1% BSA	/
anti-CD31-PE	BD	1/100	1% BSA	/
Lectin (biotinylated)	Vector	1/50	1% BSA	SAV Alexa 555 or 488
Lectin-FITC	Sigma	0.2 mg in 200 μ l <i>i.v.</i>	/	/
Anti-CD49e	BD	1/25	2% Donkey serum	Anti-rat Alexa 594
FACS	Company	Dilution	Blocking	Secondary antibody
anti-CD49e-FITC	Immunotech	1/10	1% BSA	/

Table 2.6 Antibodies for Western Blot and Immunostaining

2.15 Immunofluorescence

For detection of intracellular proteins, HUVEC were grown on a cover slip for 24 hours. Cells were washed with phosphate buffer and fixed in 4% paraformaldehyde (PFA) for 15 min at room temperature and permeabilized with 0.25% Triton X-100. After blocking in 2% BSA for 30 min at room temperature, cover slips were incubated over night a

t 4°C with the primary antibody. After washing 3x with phosphate buffer, cover slips were incubated for 1 hour at room temperature with the adequate secondary antibody.

Cover slips were washed again incubated stepwise with antibodies for staining of cytoskeleton, nucleus and proliferation status. Proteins were detected by confocal microscopy.

2.16 Stimulation with VEGF

For stimulation with vascular endothelial growth factor (VEGF), HUVEC were grown until 70% confluence. 1 hour before stimulation medium was replaced by EBM containing 5% BSA. 20 ng/ml or 50 ng/ml human VEGF were added to the medium and RNA was isolated after 24 h and 48 h as described above.

2.17 Stimulation with zVAD

In order to inhibit apoptosis of HUVEC, cells were transfected and incubated over night with zVAD (100µM) or the solvent DMSO. The next day, cells were subjected to a spheroid assay as described above.

2.18 Tube forming assay

The vascular tube forming assay is a method to analyse the angiogenic potential of transfected cells *in vitro*. 48 h after transfection HUVEC (7×10^4) were cultured in a 12-well plate (Greiner) coated with 200 µl Matrigel Basement Membrane Matrix (BD

Biosciences). After several hours cells spontaneously form capillary-like structures. Tube length was quantified after 24 hours by measuring the cumulative tube length in five random microscopic fields with a computer-assisted microscope using the program KS300 3.0 (Zeiss).

2.19 Spheroid-based angiogenesis assay

The 3-D spheroid assay is another assay to investigate the angiogenic potential of endothelial cells. Endothelial cells are cultured over night in a viscous medium in 96-well U-bottom shaped wells to allow the formation of spheroids. After collecting, the spheroids are embedded in a collagen-methocel gel, which polymerizes in a 24-well plate (Diehl et al., 2006; Korff and Augustin, 1998). Depending on the experimental outline 30 ng/ml bFGF were added to stimulate angiogenesis. Spheroids were quantified by measuring the cumulative length of the sprouts that had grown out of each spheroid using a digital imaging software (Axioplan, Zeiss) analyzing 10 spheroids per experimental group and experiment.

2.20 MTT viability assay

Assessment of cell viability was performed using the [3-(4,5-dimethylthiazol-2-yl)-2,5-diphenyl-2H-tetrazolium bromide] MTT assay. 48 h after transfection 0.5 mg/ml MTT was added to each well and cells were incubated for 4 h at 37 °C. Cells were washed with PBS and lysed 30 min at room temperature with lysis buffer (40 nM HCl in isopropanol). Absorbance was photometrically measured at 550 nm.

2.21 Cell-matrix adhesion

Ninety-six-well plates were coated over night at 4 °C with 1 µg/mL soluble recombinant human collagen I (Roche, Mannheim, Germany) or 2.5 µg/mL human fibronectin (Roche, Mannheim, Germany) in PBS and then blocked for one hour at room temperature with 3 % (w/v) heat-inactivated (2 h, 56 °C) human serum albumin

(HSA). 48 h after transfection, HUVEC were stained with 2',7'-bis-(2-carboxyethyl)-5-(and-6)-carboxyfluorescein acetoxymethyl ester (BCECF-AM) or CellTracker Green (Molecular Probes, Eugene, Oregon) and after detachment with trypsin were resuspended in EBM with 0.05 % HSA. Then, cells were seeded at 50000 cells/well in 100 μ L in the coated wells for 15, 30 and 45 min at 37 °C. After washing of non-adhering cells with warm EBM, adherent cells were quantified in triplicates with a fluorescence plate reader (Fluostat, BMG Lab Technologies, Offenburg, Germany).

2.22 Migration assay

To determine the migration of endothelial cells, HUVEC were detached with trypsin, harvested by centrifugation, resuspended in 500 μ l EBM with 0.1% BSA, counted and placed in the upper chamber of a modified Boyden chamber (5×10^4 cells per chamber, pore size 8 μ m, BD Biosciences) coated with 2.5 μ g/ml fibronectin. The chamber was placed in a 24-well culture dish containing EBM with 0.1% BSA in presence or absence of human vascular endothelial growth factor (VEGF, 50 ng/ml, Peprotech). After incubation for 5 h at 37°C, the non-migrating cells on the upper side of the chamber were mechanically removed and the remaining cells on the lower side were fixed with 4% formaldehyde. For quantification, cell nuclei were stained with 4',6-diamidino-phenylidole (DAPI). Migrating cells on the bottom side of the chamber were counted manually in five random microscopic fields.

2.23 Cytokine and receptor array

24 h after transfection, cells were starved for 20 h in EBM + 0.05% BSA. Supernatants were collected and concentrated 10-fold using Vivaspin columns. 10x supernatants were subjected to a human cytokine antibody array (Ray Bio) according to the instructions of the manufacturer. For the receptor array, cells were harvested 48 h after the transfection, protein was isolated as described above and subjected to a receptor antibody array (Ray Bio) according to the manufacturer's protocol.

2.24 Flow cytometry analysis

For permeabilization, HUVEC transfected with pre92 or control were detached with trypsin, fixed in 4% formaldehyde for 10 minutes and treated with 0.1% TritonX-100. Cells (permeabilized and non-permeabilized) were blocked using 1% BSA and stained with Integrin α 5 (Anti-CD49e-FITC 1:10, Immunotech) antibody. Cells were analyzed on a FACS Canto II device (BD).

2.25 Proliferation assay

24 h after transfection, medium was changed and HUVEC were grown in the absence of serum (starving medium, EBM with 0.05% BSA) for 12 h. Cells were collected and stained with BrdU. FACS analysis was performed using a FACS Canto II device.

2.26 Annexin V staining of cardiomyocytes

Rat neonatal cardiomyocytes were pre-incubated with antagomir-92a for 48 h. Then, cells were washed and medium was replaced by medium without FCS („starving“) and antagomir-92a (150 nM) or PBS was added again for 24 h. Apoptotic cells were detected by annexin V staining by FACS.

2.27 Luciferase cloning and transfection

Synthetic oligonucleotides bearing 4x the Integrin α 5 binding sequence or a mutated sequence of miR-92a containing HindIII and SpeI restriction sites (Table 2.4) were cloned into firefly Luciferase reporter plasmid pMIR-Report (Ambion) according to the manufacturers protocol. For measuring luciferase activity Hek293 cells were grown

in 24-well plates until 60-70% confluence. 0.01 ng Luciferase plasmid was co-transfected with 0.1 ng pGL4 Renilla plasmid (Promega) as control for the transfection efficiency and 30 pmol pre92 or control using Lipofectamine 2000 (Invitrogen). The activity of Luciferase and Renilla was assessed after 24 h or 48 h with the Dual-Luciferase(R) Reporter 1000 Assay System (Promega).

2.28 Plasmid preparation

Plasmid preparations were performed using commercially available kits for spin-, midi- or maxi preparation of plasmid DNA (Qiagen, Hilden). The concentration and purity of the DNA was determined photometrically.

2.29 *In vivo* Matrigel plug assay with transfected HUVEC

This assay was carried out as described previously (Potente et al., 2005) with the following modifications: HUVEC were transfected with pre92 or control as described above. 18 h after transfection, cells were labeled with cell tracker CM-Dil (Invitrogen), were detached, washed and counted. 1×10^6 cells were resuspended in 30 μ l PBS and mixed with 500 μ l Matrigel Basement Membrane Matrix (BD Biosciences) containing 15 units of heparin (Sigma-Aldrich). The cell-matrigel-mixture was injected subcutaneously into 6-8 wk old female athymic nude mice (Harlan) along the abdominal midline. After 6 days, invading cells in Matrigel plugs were quantified by analysis of H&E stained sections using microscopy. In order to analyse perfused capillaries, 200 μ l FITC-conjugated lectin (1 mg/ml; Sigma) was injected *i.v.* 30 min before killing the mice. For hemoglobin analysis, the matrigel plug was removed after 6 days and homogenized in 130 μ l de-ionized water. After centrifugation, the supernatant was used in the Drabkin assay (Sigma-Aldrich) to measure hemoglobin concentration. Stock solutions of hemoglobin are used to generate a standard curve. Results are expressed relative to total protein in the supernatant.

2.30 Antagomirs

The single-stranded RNA used in this study consisted of a 21–23-nucleotide length were synthesized by VBC Biotech, Vienna as previously described (Kruzfeldt et al., 2005). Antagomir sequences are listed in table 2.7. All animal models were maintained in a C57BL/6 background. Eight-week-old mice were injected subcutaneously with 2 matrigel basement matrix plugs at day 0 and received tail-vein injections of saline or antagomir-92a at day 1, 3 and 5. Antagomir-92a was administered at doses of 8 mg per kg body weight in 0.2 ml per injection. Tissue and matrigel plugs were harvested at day 6. Tissue was snap-frozen and stored in -80°C for RNA analysis. Hemoglobin, H&E staining and blood vessel infiltration were measured as described above. Additionally smooth muscle cells were stained using anti-SMA-Cy3 (Sigma).

Antagomirs	Sequence	Company
Antagomir-92a	CAGGCCGGGACAAGUGCAAUA	VBC Biotech
Antagomir-Co	AAGGCAAGCUGACCCUGAAGUU	VBC Biotech
Antagomir-Co 2	AAAUCCUUUAGACCGAGCGUGUGUU	VBC Biotech

Table 2.7 Antagomirs

2.31 *In vivo* matrigel experiments

Eight-week-old mice were injected subcutaneously with 2 matrigel basement matrix plugs at day 0 and received tail-vein injections of saline, antagomir-Co or antagomir-92a at day 1, 3 and 5. Antagomir-92a or antagomir-Co was administered at doses of 8 mg per kg body weight in 0.2 ml per injection. Tissue and matrigel plugs were harvested at day 6. Capillaries were stained with anti-vWF and anti-rabbit Alexa 488 (Invitrogen). In order to analyse perfused capillaries, 200 µl FITC-conjugated lectin (1 mg/ml) was injected *i.v.* 30 min before harvest. Hemoglobin, H&E staining and blood vessel infiltration were measured as described above. Additionally, smooth muscle cells were stained using anti-SMA-Cy3 (Sigma).

2.32 Murine ischemic hind limb model

The effect of antagomir-92a on ischemia-induced neovascularization was investigated in a murine model of hind limb ischemia using C57/Bl6 mice. 8 mg/kg bw antagomir-92a, antagomir-Co or PBS was injected at day 0, 2, 4, 7 and 9 after causing hind limb ischemia by ligation of the superficial and deep femoral artery and vein. Two weeks after induction of hind limb ischemia, the morphology of the limb was determined and blood flow ratio of the ischemic to normal limb was measured by using a laser Doppler blood flow meter (Laser Doppler Perfusion Imager System, MoorLDI-Mark 2, Wilmington, DE). The perfusion of the ischemic and non-ischemic limb was calculated on the basis of colored histogram pixels. Red indicates high, blue indicates low perfusion. To minimize variables including ambient light and temperature and to maintain a constant body temperature, mice were exposed to infrared light for 10 min before laser Doppler scans. During the scan, mice were lying with their back on a heating pad with their legs stretched and fixed. The calculated perfusion was expressed as the ratio of ischemic to nonischemic hind limb perfusion. The necrosis of tips and toes was determined by the following rating: 0=none; 1=1-3 tips; 2=4-5 tips; 3=1-3 toes; 4=4-5 toes; 5=1/3 foot; 6=2/3 foot; 8=whole foot; 10=1/3 leg; 12=2/3 leg and 14=whole leg. For morphological analysis, 10- μ m frozen sections of the muscle and semimembraneous muscles were used. Myocyte membranes were stained using anti-laminin (Abcam) followed by anti-rabbit-Alexa 488 (Molecular Probes) and anti-CD31-PE (BD). Arterioles were visualized using anti-SMA-Cy3 (Sigma). For double staining, capillaries were visualized with biotinylated anti-lectin and SAV-Alexa 488 and arterioles by anti-SMA-Cy3 (Sigma). Integrin α 5 was stained using anti-Integrin α 5 (BD) and anti-rat Alexa 594 followed by anti-CD31-FITC (BD) to visualize capillaries.

2.33 Induction of myocardial infarction and functional evaluation

Myocardial infarction was induced by permanent ligation of the left coronary artery in 10-12 week old C57/Bl6 mice. Left coronary artery ligation was performed as

described previously with modification (Patten et al., 1998). Mortality during or directly after operation was 22 %. After operation, mice were randomized in a blinded manner to the antagomir-92a, antagomir-Co or PBS group. 8 mg/kg bw antagomir 92a, antagomir-Co or PBS was injected at day 0 (after operation), day 2, 4, 7 and 9 after ligation of the coronary artery. In the PBS group n=2 mice died during the first week, in the antagomir-Co group n=1 mouse died, whereas no mouse died in the antagomir-92a group. On day 14, cardiac catheterization was performed for functional analysis by using 1.4F micromanometertipped conductance catheter (Millar Instruments Inc). Left ventricular (LV) pressure and its derivative (LV dP/dt) were continuously monitored with a multiple recording system. All data were acquired under stable hemodynamic conditions in a blinded manner. Functional difference between the groups were controlled in a second set of experiment by echocardiography (Vevo 770, VisualSonics, Toronto, Canada) showing an improvement of wall motion score index from day 0 to day 14 in the antagomir-92a group compared to antagomir-co. In order to analyze perfused capillaries, 200 µl FITC-conjugated lectin (1 mg/ml) was injected *i.v.* 30 min before harvesting the hearts. Morphological analysis after myocardial infarction was performed using 4-µm paraffin sections of the heart at day 14. Fibrosis was detected by Sirius Red staining. Therefore, sections were deparafinized and stained for 1h in 0.1% Picro Sirius Red (Sirius Red F3B in saturated aqueous solution of picric acid). Sections were washed 2 times with acidified water, dehydrated using 100% ethanol and mounted in mounting medium (Dako). Arteries were visualized by smooth muscle actin staining. Apoptotic cells were detected in sections and cultured rat neonatal cardiomyocytes using *in situ* cell death detection kit TMR-Red (Roche) according to the manufacturer's protocol.

2.34 Detection of miRNA and mRNA expression

To analyze the specificity and efficacy of Antagomir-92a, tissue was snap-frozen and stored at -80°C for RNA analysis. RNA isolation, cDNA synthesis and real time PCR were performed as described above.

2.35 *In situ* hybridization

To detect miR-92a expression, tissue was processed according to Obernosterer et al. (Obernosterer et al., 2007) and was stored at -80 °C. 10 µm sections were cut and thawed for 30 min at room temperature. After fixation with paraformaldehyde (4%) for 10 min, sections were washed 3 times for 5 min and incubated with protein kinase K (Sigma) for 5 min. After washing 3 times with PBS, sections were incubated with hybridization buffer for 4 h at room temperature. Meanwhile, probes (0.5 µl 3'-DIG labeled LNA probes, Exiqon) were mixed with 150 µl denaturation buffer, heated to 80 °C for 5 min, chilled on ice and added to the sections followed by incubation overnight at 56 °C. After incubation for 1 h in 50 % formamide / 1x SSC at 56 °C, 1h in 0.2 SSC at 56 °C and 10 min in solution B1, sections were blocked for 1h at room temperature in blocking reagent. Then, anti-DIG AP (Roche) was added at a dilution of 1:500 for 1h at 37 °C. After washing with solution B1, sections were equilibrated in 1 M Tris, pH=8.3 for 10 min at room temperature and subsequently incubated for 15 min with Fast Red substrate (Dako) containing 1 drop levamisole. After washing in PBS/0.5% Tween-20, sections were mounted in DAPI mounting medium (Vector).

2.36 TUNEL staining

MiR-92a was inhibited by injecting antagomir-92a (8 mg/kg bw, injected at days 0, 2, 4, 7, 9) or antagomir-Co after ligation of left coronary artery. In order to quantify *in vivo* apoptosis after myocardial infarction TUNEL staining (*in situ* cell death detection kit, Roche) was performed using 4-µm paraffin sections of the heart at day 14.

2.37 Affimetrix mRNA profiling

HUVEC were transfected with pre92, control or siRNA for Integrin α 5 and scrambled siRNA. Total RNA was isolated after 48 h, and the gene expression profile was assessed with the Affymetrix gene chip expression assay.

2.38 Statistical analysis

Data are expressed as mean \pm SEM. Two treatment groups were compared by Mann-Whitney test or student's t-test, three or more treatment groups were compared by one-way analysis of variance followed by post-hoc analysis adjusted with a least significant difference correction for multiple comparisons (SPSS Inc.). Results were considered statistically significant when $P < 0.05$.

3 Results

MicroRNAs have been shown to play a crucial role in almost all biological processes. In order to study the general role of microRNAs in endothelial cells, we first analysed the expression and localization of the major microRNA-regulating enzymes Dicer and Drosha. Furthermore, the effect of siRNA, reducing the expression of Dicer and Drosha, on endothelial cell functions such as sprouting, viability and migration was analyzed. Since Dicer and Drosha are critically involved in microRNA biogenesis, we subsequently analysed microRNA expression after inhibition of Dicer and Drosha. In the second part of the thesis, we focused on the involvement of selected microRNAs on endothelial cell function such as proliferation, adhesion and their ability to improve recovery of ischemic tissues after hind limb ischemia or myocardial infarction *in vivo*.

3.1 Expression and localization of Dicer and Drosha in endothelial cells

Because the role of Dicer and Drosha in endothelial cells was unclear at the time when this study started, we first assessed the expression and localization of the two enzymes in endothelial cells using immunocytochemistry and confirmed these results by nuclear and cytoplasmic fractionation and subsequent western blot analysis.

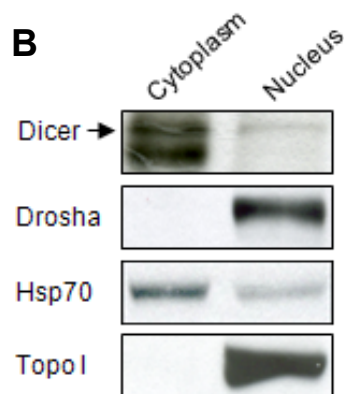
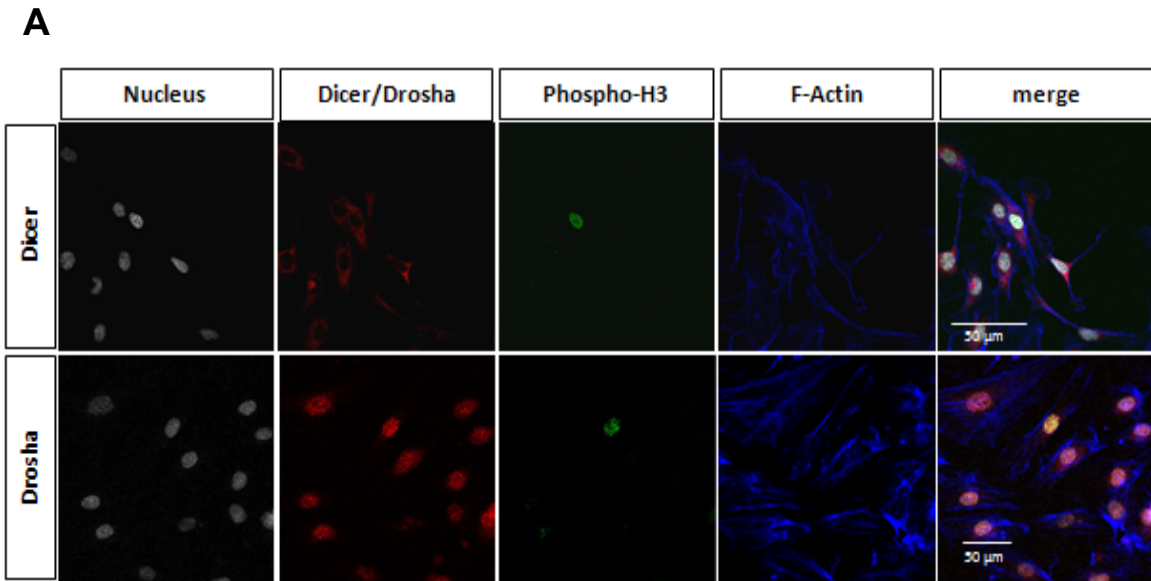


Figure 3.1 Expression and localization of Dicer and Drosha in endothelial cells

(A) Dicer and Drosha localization was assessed by immunocytochemistry. Dicer and Drosha staining is shown in red fluorescence, phospho-H3 is used as proliferation marker (green), cytoskeleton is visualized by F-actin staining (blue) and nuclei (Sytox blue) are shown in white. **(B)** Nuclear and cytoplasmic extracts were prepared as described in material and methods. Western blot analysis was performed using antibodies directed against Dicer, Drosha, Hsp70 and Topo I.

As shown for other cell types, Dicer is predominantly localized in the cytoplasm of endothelial cells, whereas the localization of Drosha is restricted to the nucleus (Fig. 3.1 A/B). To determine whether Dicer and Drosha localization might be different in proliferating cells, we additionally identified proliferating cells by phospho-histone-H3 staining. However, the proliferation status did not influence the localization of the two enzymes (Fig. 3.1 A/B).

3.2 Role of Dicer and Drosha for sprouting, tube formation and migration of endothelial cells

In order to investigate the influence of Dicer and Drosha on the angiogenic potential, EC were transfected with siRNA targeting Dicer and Drosha compared to scrambled siRNA. We performed two different *in vitro* angiogenesis assays, the three-dimensional spheroid assay and the two-dimensional matrigel vascular network formation assays. To exclude an unspecific effect of the siRNAs, we tested the efficiency and specificity using two different siRNAs termed Dicer I/ Dicer II and Drosha I/ Drosha II (Fig. 3.2 A). PCR as well as western blotting demonstrate the specific suppression of Dicer and Drosha by the respective siRNA oligonucleotides (Fig. 3.2 B). Subsequent experiments were performed using Dicer I and Drosha I siRNA.

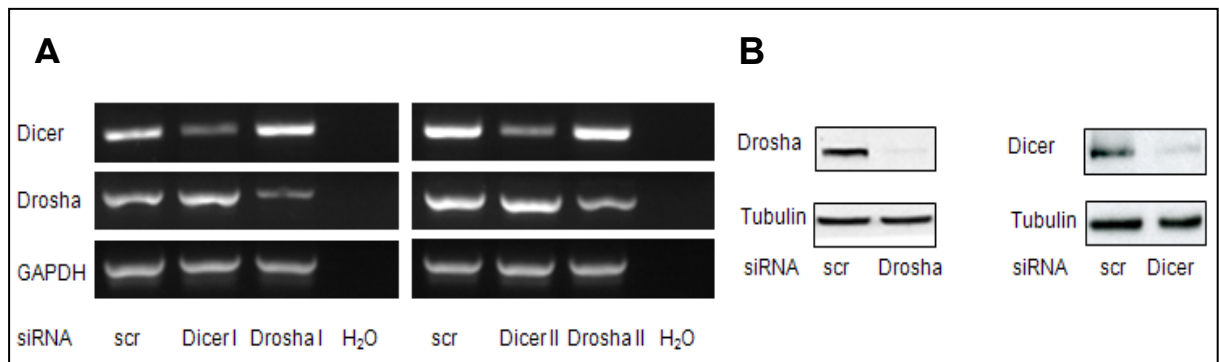


Figure 3.2 siRNA mediated knockdown of Dicer and Drosha

HUVEC were transfected with two different siRNAs targeting Dicer and Drosha, Dicer I and Dicer II as well as Drosha I and Drosha II or scrambled oligonucleotides. **A)** RT-PCR analysis of Dicer and Drosha mRNA expression after 24 h. A representative gel is shown. GAPDH served as loading control. **B)** 48 hours after transfection, cells were lysed and subjected to western blot analysis with antibodies against Dicer and Drosha. An antibody directed against tubulin was used as loading control.

The reduction of Dicer and Drosha significantly inhibits basal and bFGF-stimulated endothelial cell sprout formation as measured by capillary sprouting in a three-dimensional collagen-embedded spheroid culture assay (Fig. 3.3 A/B), while VEGF-induced sprout formation is selectively blocked by Dicer siRNA (Fig. 3.3 C). Next, we

tested whether the combined silencing of Dicer and Drosha further suppresses sprout formation. However, no additive effect was detected compared to the single reduction of Dicer or Drosha gene expression (Fig. 3.3 D/E).

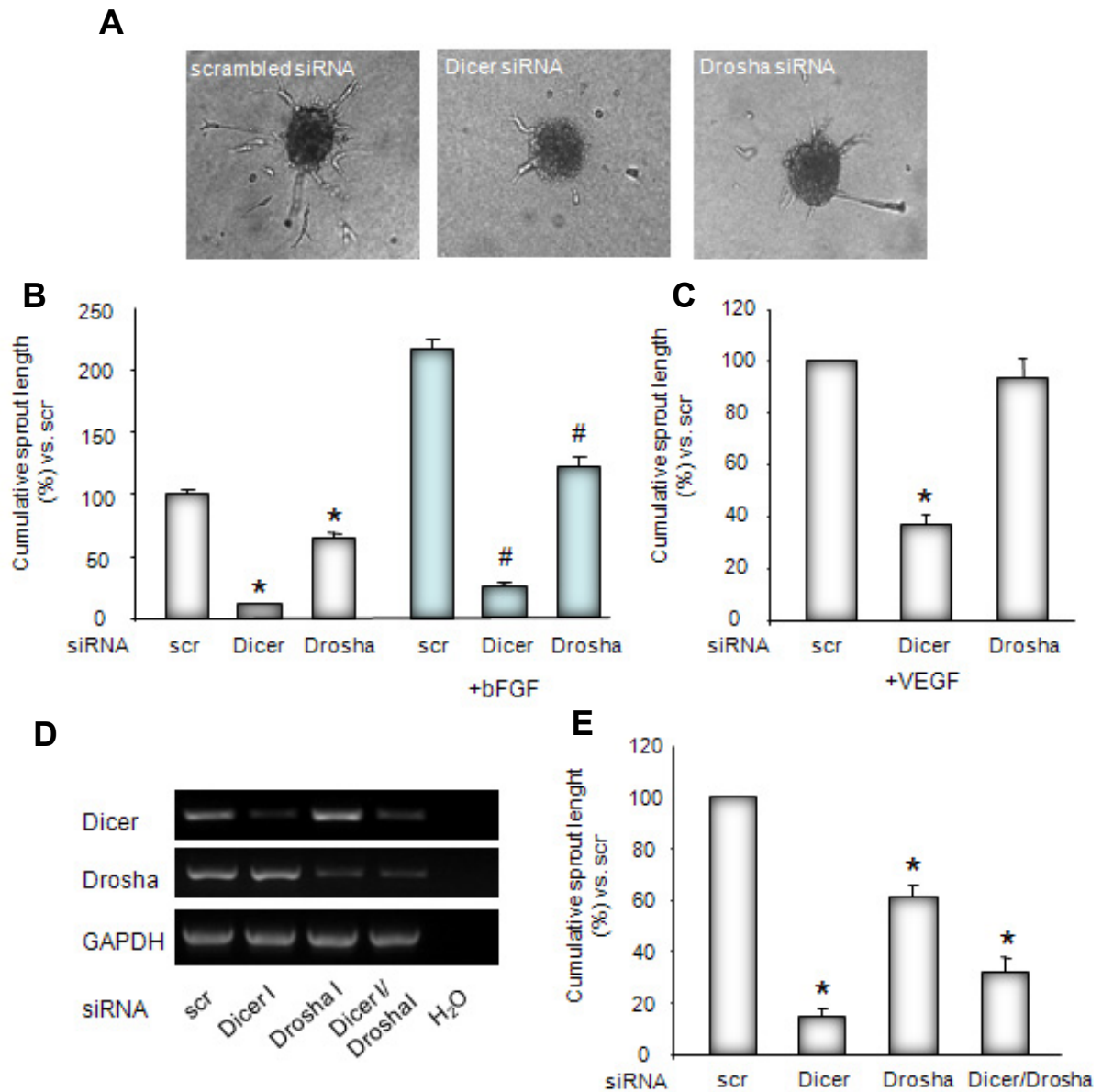


Figure 3.3 Dicer and Drosha regulate endothelial cell sprouting

(A/B) HUVEC were transfected with Dicer and Drosha siRNA or scrambled oligonucleotides. A spheroid assay was performed to analyze basal or bFGF stimulated endothelial sprouting capacity. **A)** Representative spheroids are shown. **B)** Analysis of endothelial sprouting capacity with or without bFGF (30 ng/ml), n=3-4. **C)** Spheroids were stimulated with VEGF (50 ng/ml), n=4. **D/E)** HUVEC were transfected with Dicer and Drosha siRNA in combination. PCR and analysis of endothelial sprouting is shown. Endothelial sprouting capacity is given as cumulative sprout length per spheroid. Data are shown as mean±SEM (% scrambled without stimulation), n=4.

To confirm the inhibitory effect of Dicer and Drosha knockdown assessed in the spheroid assay, we performed another *in vitro* angiogenesis assay detecting vascular network formation in matrigel. As shown in the spheroid model, suppression of Dicer and Drosha leads to a significant impairment of network forming activity (Fig. 3.4 A/B). Since migration of endothelial cells is a key process during angiogenesis, we addressed the question, whether the reduction of Dicer and Drosha contributes to reduced endothelial cell migration. For that purpose, we performed a migration assay using a modified Boyden chamber. While Dicer siRNA-mediated knockdown significantly decreases the migratory capacity, Drosha knockdown has no effect on cell migration (Fig. 3.4 C). Cell viability was measured using a MTT viability assay after 24 h (D) or 48 h (E), n=3.

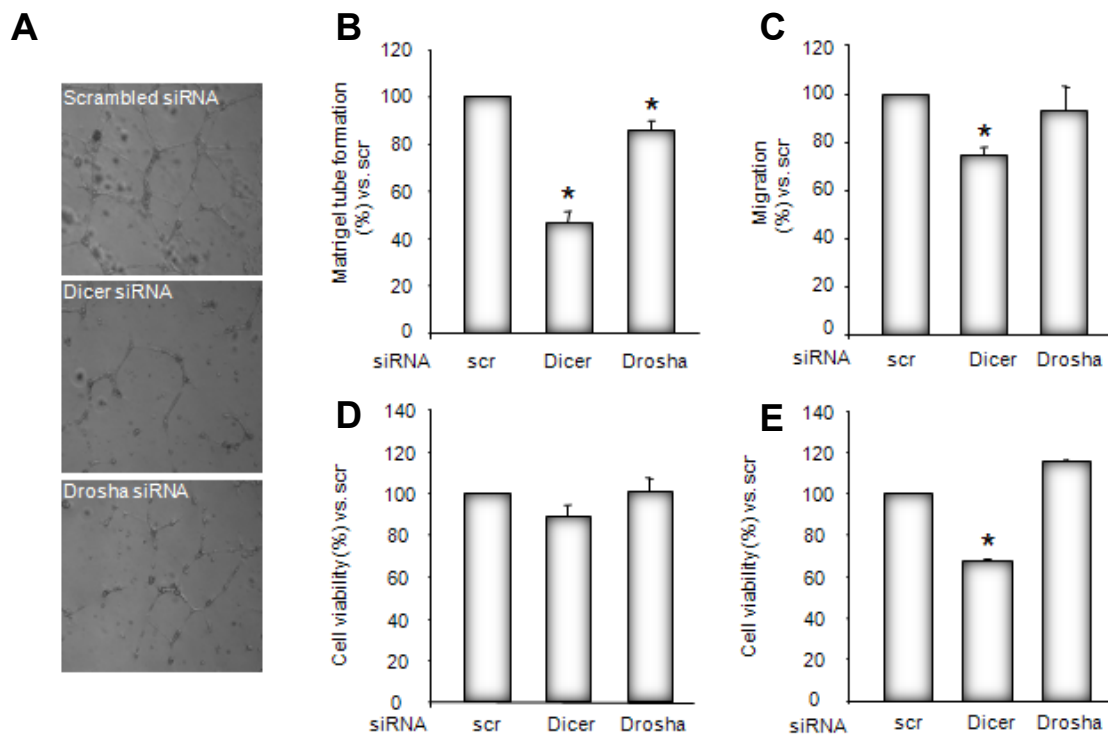


Figure 3.4 Effect of Dicer and Drosha on tube formation, migration and cell viability

(A-E) HUVEC were transfected with Dicer and Drosha siRNA or scrambled oligonucleotides. **(A/B)** HUVEC were seeded on a growth factor enriched Matrigel basement membrane matrix 24 hours after transfection. Representative micrographs and statistical summary of the tube forming activity, n=4. **(C)** Cell migration was measured using a modified Boyden chamber. Cells were seeded in the upper chamber of a modified Boyden chamber 24 hours after transfection. Endothelial cell migration was assessed using VEGF (50 ng/ml) as chemoattractant, n=3 **(D/E)** Cell viability was measured using a MTT viability assay after 24 h **(D)** or 48 h **(E)**, n=3.

To test whether the reduction of endothelial cell sprouting and tube formation is secondary to a nonspecific effect on cell growth or apoptosis, we analysed cell viability using a MTT assay. As shown in Figure 3.4 D, Dicer and Drosha knockdown does not impair cell viability after 24 h. After 48 h, Dicer siRNA transfection slightly reduces viability, whereas Drosha siRNA transfection does not affect viability (Fig. 3.4 E). In order to additionally investigate whether an induction of apoptosis mediates the anti-angiogenic effect of Dicer siRNA, apoptosis was blocked by the addition of the caspase-inhibitor zVAD. However, the reduced sprout forming activity of Dicer siRNA-transfected endothelial cells was not improved by zVAD addition (Fig. 3.5) indicating that the inhibition of sprout formation is independent of the induction of cell death.

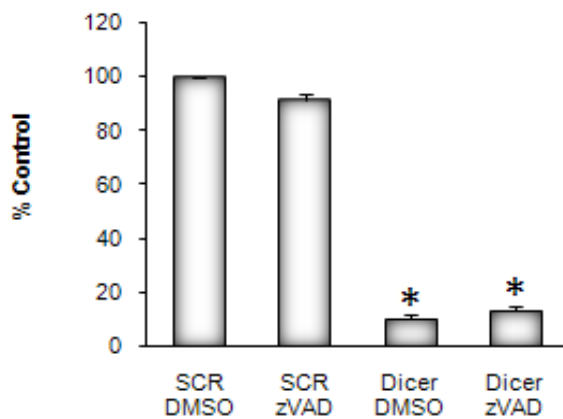


Figure 3.5 The anti-angiogenic effect of Dicer does not depend to induction of cell apoptosis

HUVEC were transfected with Dicer siRNA or scrambled oligonucleotides. After medium change cells were stimulated with 100 μ M zVAD or DMSO as control. 24 h after stimulation a spheroid assay under bFGF (30 ng/ml) stimulation was performed to analyze endothelial sprouting capacity, n=3.

3.3 Dicer is required for *in vivo* angiogenesis

Having shown that Dicer and Drosha contribute to *in vitro* angiogenesis, we further investigated the role of Dicer and Drosha on *in vivo* angiogenesis. Because Dicer-deficient mice are embryonic lethal and Drosha-deficient mice were not available for the study, we subcutaneously injected matrigel plugs mixed with siRNA-transfected HUVEC into nude mice and assessed the sprout formation.

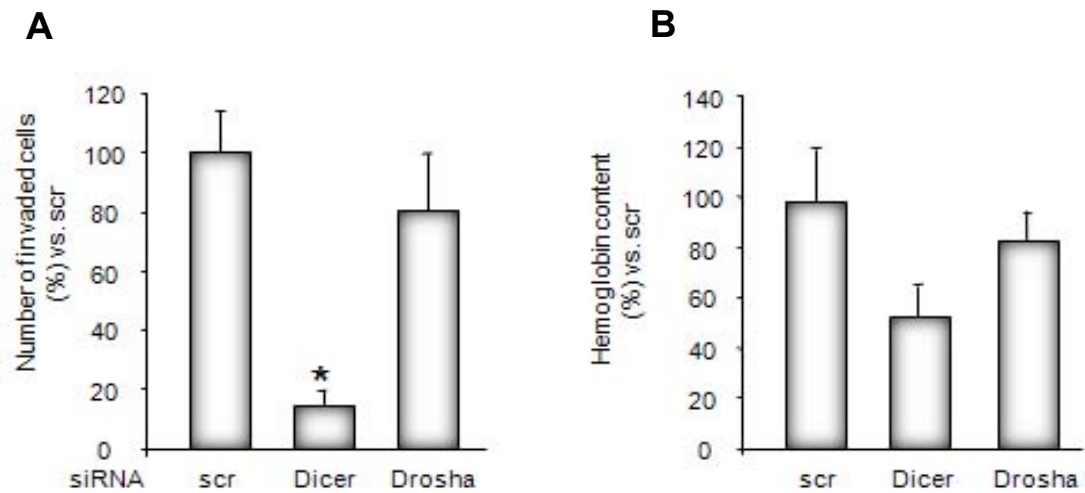


Figure 3.6 Dicer is required for *in vivo* angiogenesis

HUVEC were transfected with Dicer and Drosha siRNA or scrambled. 18 h after transfection cells were labelled with CM-Dil and mixed in matrigel basement membrane. The matrigel-cell mixture was injected subcutaneously in nude mice and plugs were harvested after 7 days. The number of invading cells was quantified by staining lectin or CD31 (**A**) and perfusion of matrigel plugs was analysed by measuring the hemoglobin content (**B**), n=3-6.

Vessel-like structures are significantly reduced in matrigel plugs with Dicer siRNA transfected HUVEC (Fig. 3.6 A). Silencing of Dicer additionally reduces matrigel plug hemoglobin concentrations indicating that the blood supply is reduced (Fig. 3.6 B). In contrast, Drosha siRNA transfection does not significantly affect sprouting angiogenesis and hemoglobin concentration of matrigel plugs *in vivo* (Fig. 3.6 A/B). In summary, our data provide evidence that Dicer and Drosha are critically involved in angiogenic processes *in vitro* and *in vivo*.

3.4 microRNAs enriched in endothelial cells

In order to detect microRNAs, which are highly enriched in EC, we performed a microRNA profiling. Since the high throughput expression profiling of microRNAs was still in its infancy at the beginning of the study, we performed two different profilings based on different methods. As shown in Fig. 3.7 A the expression of about 360 microRNAs in HUVEC was analysed using quantitative real-time PCR. In this approach, during reverse transcription the microRNA is elongated by a specific stem loop primer and subsequently subjected to real-time PCR using specific primer and

Taqman probes. In a second approach, 344 microRNAs expressed in HUVEC were quantified using microRNA microarray analysis (Fig. 3.7 B).

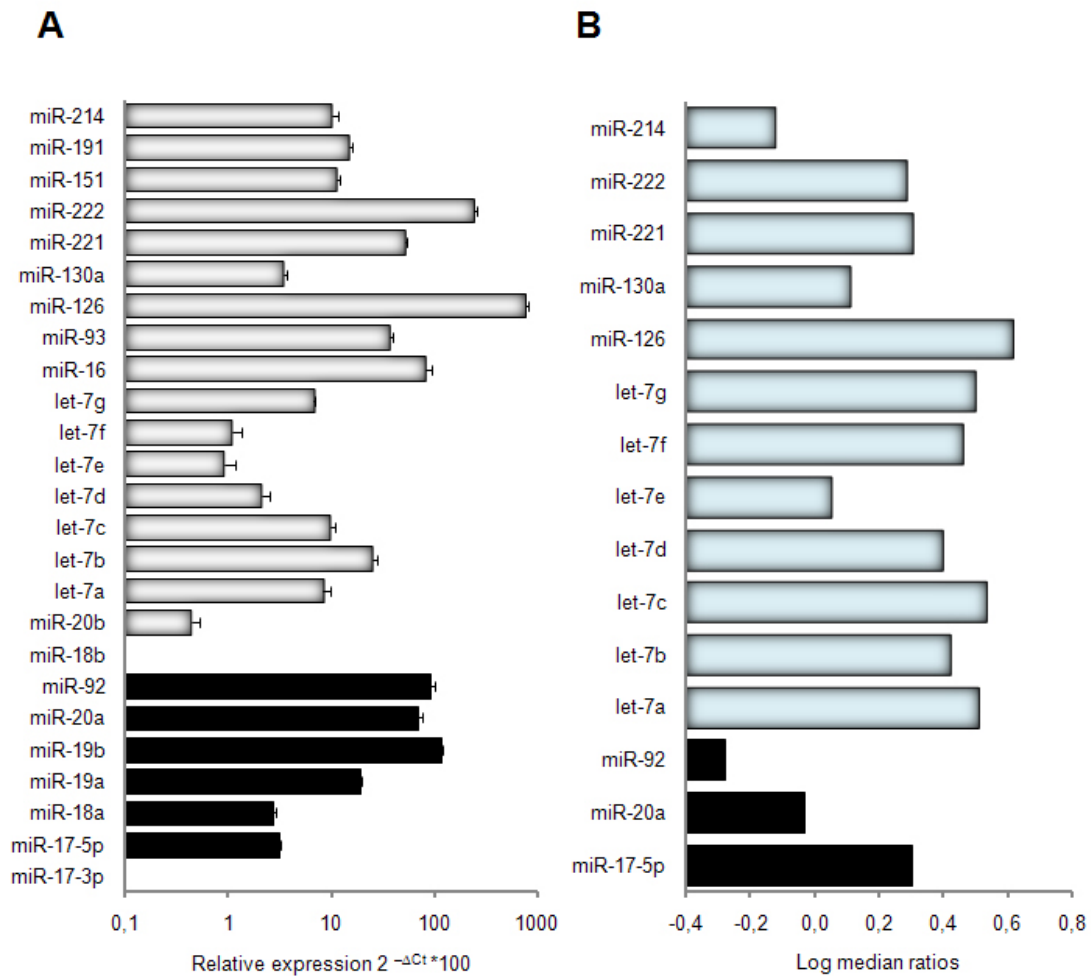


Figure 3.7 microRNA expression profile in HUVEC

A) The expression of 360 human microRNAs was profiled using real-time PCR. Comparative analysis was performed for 23 microRNAs, detected in all three samples. Raw data were normalized to RNU48 and converted using the formula $2^{-\Delta Ct}$ (relative expression). Data are mean \pm SEM, n=3. **B)** The expression analysis of 344 human microRNAs was performed from total RNA using miRCURY LNA arrays. Representative analysis is shown for 16 microRNAs, n=1.

Selected miRNAs highly expressed in both assays are summarized in Fig. 3.7. Recent studies demonstrate that some of these highly expressed miRNAs play a major role in vascular biology. MiR-221 and miR-222 target the stem cell factor ligand c-kit, thereby changing the angiogenic properties of HUVEC (Poliseno et al., 2006). Furthermore, two current studies in zebrafish and mouse models show that miR-126 stimulates angiogenesis *in vitro* and *in vivo* by targeting the negative regulator of

Ras/MAP signaling, SPRED1 (Fish et al., 2008; Wang et al., 2008). Interestingly, the whole miR-17-92 cluster encoding the miRNAs miR-17-5p, miR-17-3p, miR-18a, miR-19a, miR-20a, miR-19b and miR-92-a-1 is highly expressed in HUVEC, and particularly miR-92a, whose specific role in angiogenesis has not been investigated before. In contrast, the homologues miR-106a-363 cluster on the X-chromosome encoding miR-106a, miR-18b, miR-20b, miR-19b-2, miR-92-a-2 and miR-363 seems not to be processed in endothelial cells (Fig. 3.7 A).

3.5 Dicer and Drosha regulate the expression of miRNAs in endothelial cells

Since Dicer and Drosha are the major enzymes of microRNA biogenesis, we hypothesized that the observed defects on *in vitro* angiogenesis shown after knockdown of Dicer and Drosha described above might be due to the reduced expression of microRNAs. To identify microRNAs, which might be responsible for the functional defects, we analyzed the expression of 344 human miRNAs after siRNA-mediated knockdown of Dicer and Drosha using a microRNA array (Table 3.1 and Fig. 3.7 B). The expression of 202 miRNAs was below the detection limit of the assay. Unexpectedly, the selective analysis of the effect of Dicer and Drosha downregulation revealed that the expression of only two miRNAs is reduced to more than 30% by Dicer knockdown, while 29 miRNAs are reduced to more than 30% by Drosha knockdown, 31 miRNAs are regulated by both enzymes (Fig. 3.8). To identify microRNAs, which might be responsible for the functional defects, we analyzed the expression of 344 human miRNAs after siRNA-mediated knockdown of Dicer and Drosha using a microRNA array (Table 3.1 and Fig. 3.7 B). The expression of 202 miRNAs was below the detection limit of the assay.

miRNA	siRNA Dicer (%vs. scr)	siRNA Drosha (%vs. scr)
hsa-let-7a	64	56
hsa-let-7b	62	60
hsa-let-7c	63	56
hsa-let-7d	71	60
hsa-let-7f	59	52
hsa-let-7g	71	57
hsa-miR-10b	68	56
hsa-miR-126	83	54
hsa-miR-17-5p	73	60
hsa-miR-193a	67	42
hsa-miR-21	98	50
hsa-miR-22	73	45
hsa-miR-221	66	54
hsa-miR-23a	90	56
hsa-miR-24	87	64
hsa-miR-26a	93	53
hsa-miR-27b	64	below detection
hsa-miR-29a	82	58
hsa-miR-30c	72	56
hsa-miR-331	42	34
hsa-miR-365	81	60
hsa-miR-486	163	62

Table 3.1 microRNA expression profile after Dicer and Drosha suppression

Unexpectedly, the selective analysis of the effect of Dicer and Drosha downregulation revealed that the expression of only two miRNAs is reduced to more than 30% by Dicer knockdown, while 29 miRNAs are reduced to more than 30% by Drosha knockdown, 31 miRNAs are regulated by both enzymes (Fig. 3.8). These results are very surprising, since Dicer acts downstream of Drosha, therefore its

inhibition should have a similar effect on microRNA expression as the knockdown of Drosha.

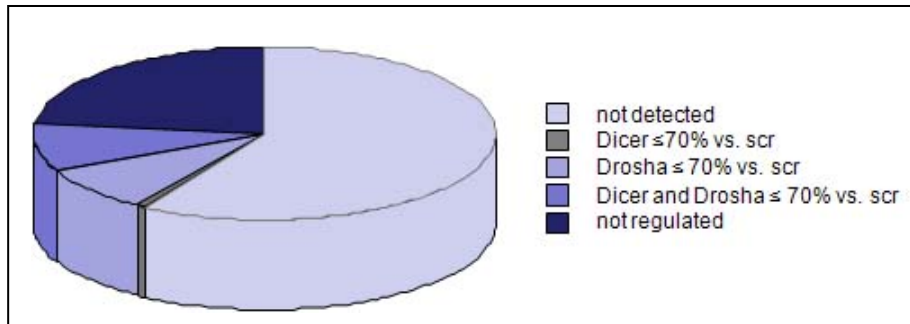


Figure 3.8 microRNA expression profile after Dicer and Drosha suppression

In order to confirm these data, we selected some highly downregulated miRNAs, miR-27b and let-7f, and performed RT-PCR. Indeed, both miRNAs were profoundly reduced after Dicer and Drosha knockdown as presented in Fig. 3.9 A/B. Based on the fact that miR-27b and let-7f potentially target the endogenous angiogenesis inhibitors Semaphorin 6a (Dhanabal et al., 2005) and thrombospondin-1 (only let-7f) (Iruela-Arispe et al., 1991), we further tested the functional effect of miR-27b and let-7f inhibition in endothelial cells. For that purpose, the miRNAs were blocked by specific inhibitors, so-called 2'-O-methyl antisense oligoribonucleotides and transfected EC were subjected to a spheroid assay. As shown in Fig. 3.9 C, inhibition of miR-27b as well as let-7f significantly reduces *in vitro* sprout formation to the same extent suggesting that these miRNAs are indeed pro-angiogenic by targeting anti-angiogenic genes.

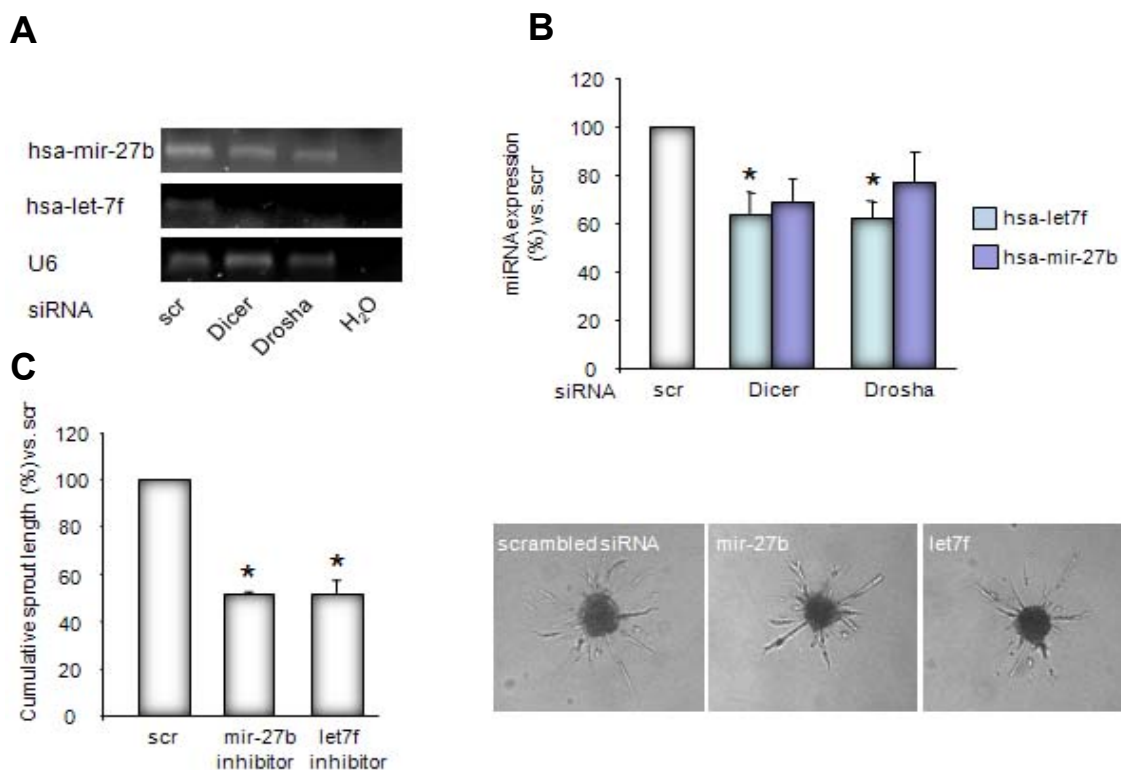


Figure 3.9 microRNA expression profile after Dicer and Drosha suppression

(A/B) HUVEC were transfected with Dicer and Drosha siRNA or scrambled oligonucleotides. The expression of miR-27b and let-7f was analyzed 48 h after transfection using RT-PCR. **A**) A representative gel is shown. The small nuclear ribonucleoprotein U6 serves as loading control. **B**) Quantitative analysis, n=5. **C**) Spheroid sprouts were detected 72 h after transfection with 2'-O-methyl antisense oligoribonucleotides against miR-27b and let-7f, n=4. Representative spheroids are shown.

3.6 Dicer and Drosha silencing induces the upregulation of thrombospondin-1 expression

Next, we assessed the expression of thrombospondin-1 (TSP1) after Dicer and Drosha siRNA transfection. As shown in Fig. 3.10 A, the reduction of Dicer and Drosha by siRNA transfection significantly increases the expression of TSP1 to $263 \pm 68\%$ in Dicer siRNA-transfected cells and to $358 \pm 95\%$ in Drosha siRNA-transfected cells, respectively.

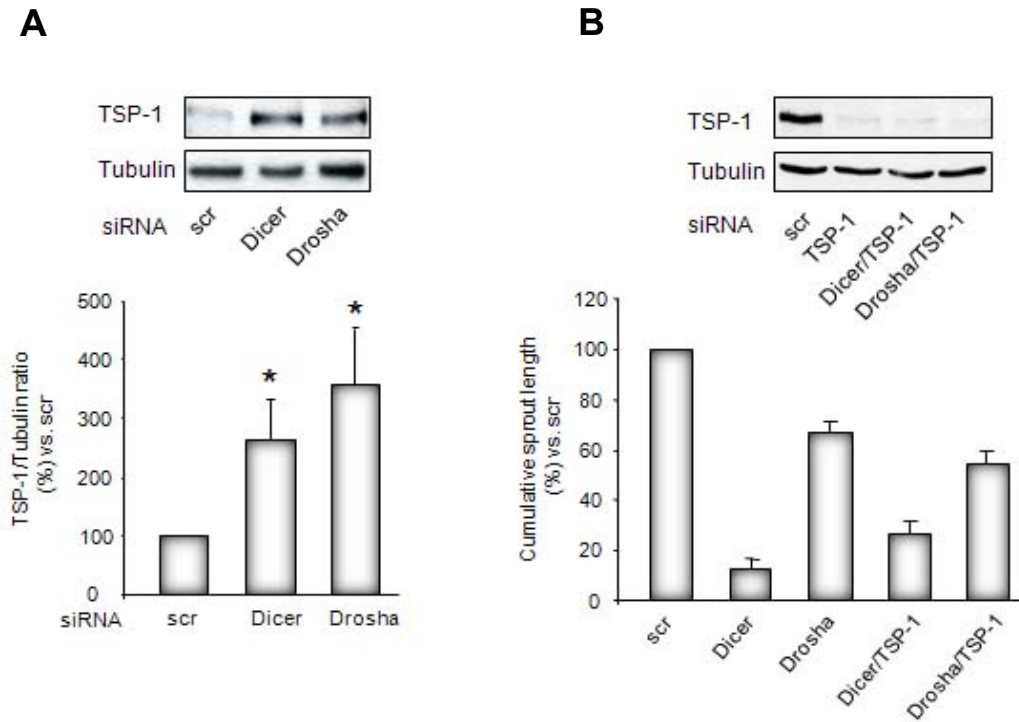


Figure 3.10 Dicer and Drosha regulate the expression of Thrombospondin-1

A) HUVEC were transfected with Dicer and Drosha siRNA or scrambled oligonucleotides. 48 hours after transfection, cells were lysed and subjected to western blot analysis with an antibody targeting thrombospondin-1. An antibody against tubulin was used as loading control. A representative western blot and quantitative analysis are shown, n=6. **B)** HUVEC were transfected with Dicer, Drosha and / or TSP1 siRNA or scrambled oligonucleotides. 18 hours after transfection, cells were lysed and subjected to western blot analysis with an antibody against thrombospondin-1. An antibody against tubulin was used as loading control. The angiogenic potential of transfected cells was analysed 72 h after transfection in response to bFGF stimulation using a spheroid model, n=3.

Based on the hypothesis, that the reduction in capillary sprout formation after Dicer and Drosha knockdown might be mediated by an increase of TSP1 expression, we simultaneously transfected HUVEC with Dicer or Drosha siRNA and siRNA targeting TSP1. However, simultaneous transfection of siRNA targeting TSP1 and Dicer or Drosha does not rescue the impaired sprout formation induced by Dicer or Drosha deficiency (Fig. 3.10 B) indicating that additional targets contribute to the Dicer and Drosha siRNA-mediated angiogenesis inhibition.

Since let-7f in comparison to other let-7 family members is most profoundly downregulated by Dicer and Drosha, we additionally investigated the effect of a let-7f inhibitor on TSP1 expression. However, inhibition of let-7f induces only a minor, not significant increase in TSP1 expression to $115 \pm 18\%$ (data not shown) suggesting that additional miRNAs are involved in the regulation of TSP1.

3.7 Effect of Dicer and Drosha silencing on cytokine expression and AKT signaling

Since the profound sprouting defect mediated by Dicer and Drosha siRNA was not explainable by the dysregulation of single genes, we elucidated the effect of Dicer and Drosha on the expression of several angiogenic growth factors and receptors by using a human receptor and cytokine array.

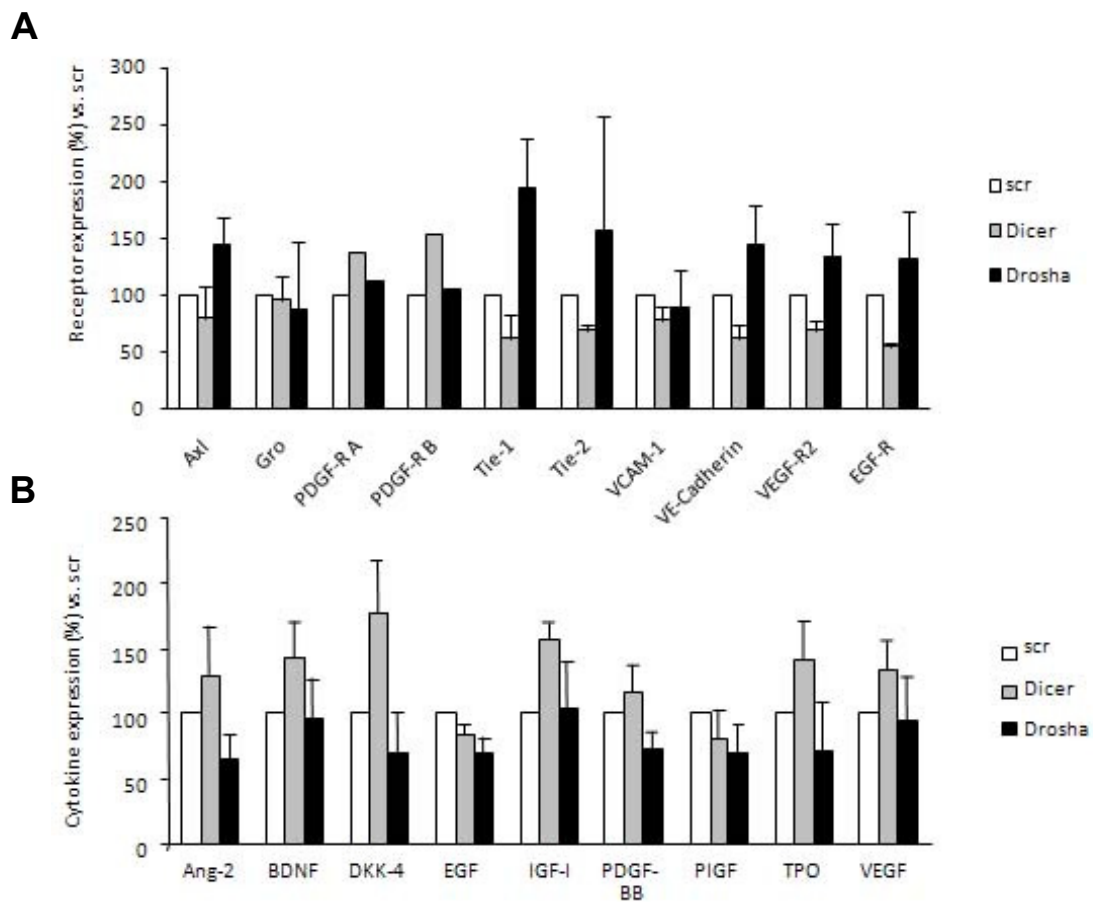


Figure 3.11 Effect of Dicer and Drosha silencing on cytokine and receptor expression

HUVEC were transfected with siRNA against Dicer and Drosha or scrambled oligonucleotides. **A)** 48 h after transfection cells were lysed and subjected to human receptor antibody array (Ray Bio). Quantitative analysis of receptor expression is shown, n=3. **B)** 24 h after transfection, cells were starved for 20 h in EBM + 0.05 % BSA. 10x supernatants were subjected to a human cytokine antibody array (Ray Bio), n=3. Quantitative analysis of cytokine expression is shown.

Although Dicer siRNA significantly suppresses angiogenesis, the expression of most of the pro-angiogenic receptors is not influenced in Dicer-silenced endothelial cells.

In contrast, Drosha knockdown enhances expression of some selected receptors important for endothelial function, such as VE-Cadherin, TIE2 and TIE1 (Fig. 3.11 A). On the other hand, suppression of Dicer leads to increased expression of pro-angiogenic cytokines like Angiopoetin-2, and DKK4, which could not be observed in Drosha siRNA transfected HUVEC (Fig. 3.11 B).

VEGF is an important pro-angiogenic factor, which activates the serine/threonine kinase AKT by binding to its receptor KDR. AKT has been shown to play a critical role in angiogenesis signaling, especially in proliferation, apoptosis inhibition and migration of endothelial cells (Dimmeler and Zeiher, 2000). In order to study the role of Dicer and Drosha in AKT signaling, we analysed the expression of the KDR and AKT-P in greater detail using Western blot analysis. However, no significant difference in KDR expression was detected after Dicer and Drosha inhibition (Fig. 3.12 A). However, the phosphorylation of AKT is selectively inhibited in Dicer siRNA compared to Drosha siRNA treated cells (Fig. 3.12 B) indicating an interference of Dicer with AKT activation.

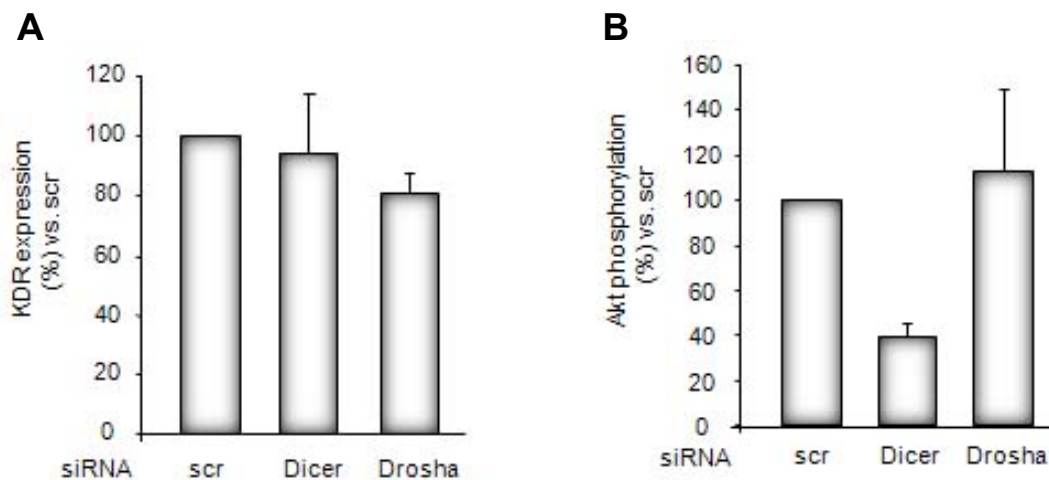


Figure 3.12. Dicer is involved in AKT signaling

HUVEC were transfected with siRNA against Dicer and Drosha or scrambled oligonucleotides. **A)** KDR expression was assessed by FACS staining. Quantitative analysis is shown, n=3. **B)** To assess AKT phosphorylation, cells were lysed and subjected to western blot analysis using an antibody against phospho-AKT. Total AKT was used as loading control, n=3. Quantitative analysis is shown.

In summary, the presented data shows that Dicer is critically involved in angiogenesis *in vitro* as well as *in vivo* by blocking expression of several microRNAs

and thereby inhibiting migration and cell viability. Furthermore, Dicer interferes with the AKT signaling pathway, which has been shown to play a crucial role in angiogenesis. In contrast, silencing of Drosha also inhibits *in vitro* angiogenesis, but has no effect on *in vivo* angiogenesis, migration and cell viability. Surprisingly, downregulation of Drosha more profoundly influenced the expression of several microRNAs compared to Dicer despite the fact that Dicer more efficiently contributes to angiogenesis.

3.8 Regulation of *in vitro* angiogenesis by highly expressed miRNAs

In the second part of this thesis, we focused on the relevance of specific microRNAs for endothelial cell biology. As shown in Fig. 3.7, we identified individual microRNAs highly expressed in HUVEC. In order to investigate the contribution of microRNAs to *in vitro* angiogenesis, we used 2'-O-methyl antisense oligoribonucleotides for inhibition of some of the highly expressed microRNAs and performed a spheroid assay (Fig. 3.13). The inhibition of miR-92a, miR-191 and miR-214 enhances capillary sprouting under basal conditions (Fig. 3.13 A) suggesting that these microRNAs might act anti-angiogenic. However, only a minor increase in sprouting was detected after stimulation with bFGF (Fig. 3.13 B).

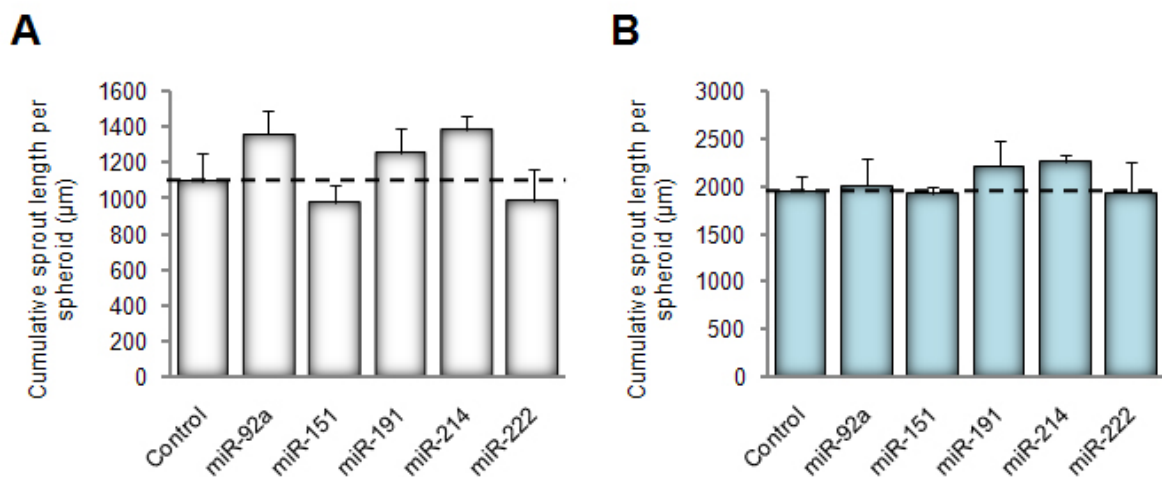


Figure 3.13 Role of highly expressed microRNAs in *in vitro* angiogenesis

HUVEC were transfected with 2'-O-methyl antisense oligoribonucleotides inhibiting microRNA expression. A spheroid assay was performed to analyze basal (A) and bFGF –stimulated (B) endothelial sprouting capacity. The cumulative sprout length of each spheroid was measured after 24 h in the collagen matrix, n=3.

MiR-92a is a member of the miR-17-92 cluster, which has been previously reported to be involved in tumorangiogenesis by targeting the anti-angiogenic protein TSP1 (Thrombospondin 1) and CTGF (Connective tissue growth factor) (Dews et al., 2006). However, the specific role of miR-92a in angiogenesis has not been studied so far.

Therefore, we investigated the effect of inhibition and overexpression of miR-92a *in vitro* on endothelial functionality and inhibited miR-92a *in vivo* to analyse the contribution to the recovery after ischemia in a hind limb ischemia and myocardial infarction model.

3.9 miR-92a impairs *in vitro* and *in vivo* angiogenesis

Overexpression of miR-92a using specific precursor molecules (termed pre92) in HUVEC results in >2-fold increase in the levels of miR-92a compared to control precursor (Fig. 3.14 A). In contrast to recent publications, which show that the miR-17-92 cluster has pro-angiogenic functions mainly exerted by miR-18a and miR-19a, miR-92a overexpression in endothelial cells unexpectedly blocks sprout formation in a three-dimensional model of *in vitro* angiogenesis (Fig. 3.14 B).

These results were confirmed by a second *in vitro* angiogenesis model, the vascular network formation in matrigel (Fig. 3.14 C). Representative images of the spheroid model and vascular network formation assay are shown in Fig. 3.14 D.

Migration and adhesion as well as apoptosis and proliferation of endothelial cells are key process during angiogenesis. Therefore, we addressed the question, whether the overexpression of miR-92a might contribute to these processes. Overexpression of miR-92a reduces EC adhesion to fibronectin after 15 min and 30 min (Fig. 3.14 E). Additionally, basal and VEGF-induced endothelial cell (EC) migration measured in a modified Boyden chamber is impaired (Fig. 3.14 F). In order to exclude a cytotoxic effect of miR-92a overexpression, we additionally analysed proliferation and viability of transfected cells. However, overexpression of miR-92a does not affect EC viability or proliferation under basal conditions or after serum depletion (Fig. 3.14 G/H). In an attempt to investigate the role of miR-92a overexpression *in vivo*, HUVEC transfected with pre92 or a control precursor were first stained with CM-DIL in order to discriminate later between the implanted HUVEC cells and the invaded host cells.

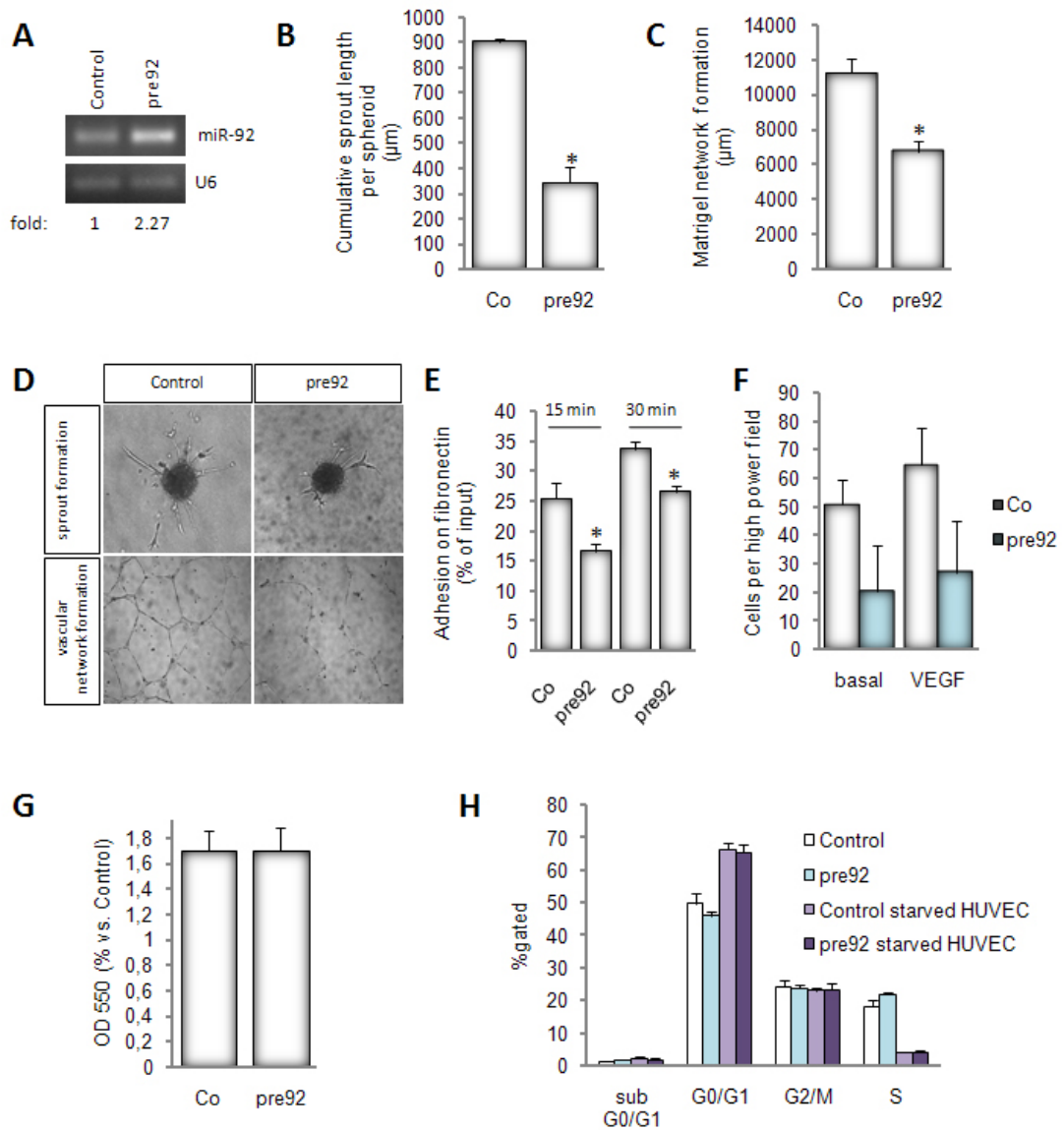


Figure 3.14 Overexpression of miR-92a impairs angiogenesis *in vitro*

HUVEC were transfected with a miR-92a precursor (pre92) or a control precursor. **A**) Expression of miR-92 in pre-miR-92a (pre92) transfected endothelial cells. **B**) A 3D spheroid assay was performed 24 h after transfection. The cumulative sprout length of each spheroid was measured after 24 h in the collagen matrix, n=3. **C**) Matrigel tube formation of transfected HUVEC was assessed after 48 h, n=3. **D**) Representative images of spheroid and matrigel assays are shown. **E**) Effect of pre92 on adhesion to fibronectin. Adhesion was measured with a fluorescence plate reader after 15 min and 30 min, n=4. **F**) Migratory capacity of pre92 transfected HUVEC was analysed using the modified Boyden chamber coated with fibronectin. Transmigrated HUVEC were stained after 5 h with DAPI and counted in 5 random high power fields, n=3. **G**) MTT viability assay was performed 48 h after transfection to exclude toxicity, n=4. **H**) 24 h after transfection, medium was changed and cells were grown in the absence of serum (starving medium, EBM with 0.05 % BSA) for 12 h. Cells were collected and stained with BrdU. FACS analysis was performed using a FACS Canto II device, n=3.

In a further attempt, HUVEC were mixed with matrigel and subcutaneously injected in nude mice. After 6 days, the overall number of invading cells is significantly decreased in matrigel plugs containing pre92 transfected HUVEC compared to control as shown in H&E staining (Fig. 3.15 A). Whereas control transfected HUVEC form vessel-like structures together with host-derived as shown by staining with von Willebrand factor (green), no host-derived cells were detectable in matrigel plugs containing pre92-transfected HUVEC (Fig. 3.15 B). In order to additionally quantify the number of perfused vessels, we infused FITC-conjugated lectin 30 min before explantation of the matrigel plugs. Matrigel plugs implanted with pre92-transfected HUVEC demonstrate a significantly lowered number of *in vivo* lectin-perfused vessels and impaired perfusion as determined by measuring the hemoglobin concentrations (Fig. 3.15 C/D). These results indicate that overexpression of miR-92a blocks angiogenesis *in vitro* and *in vivo*.

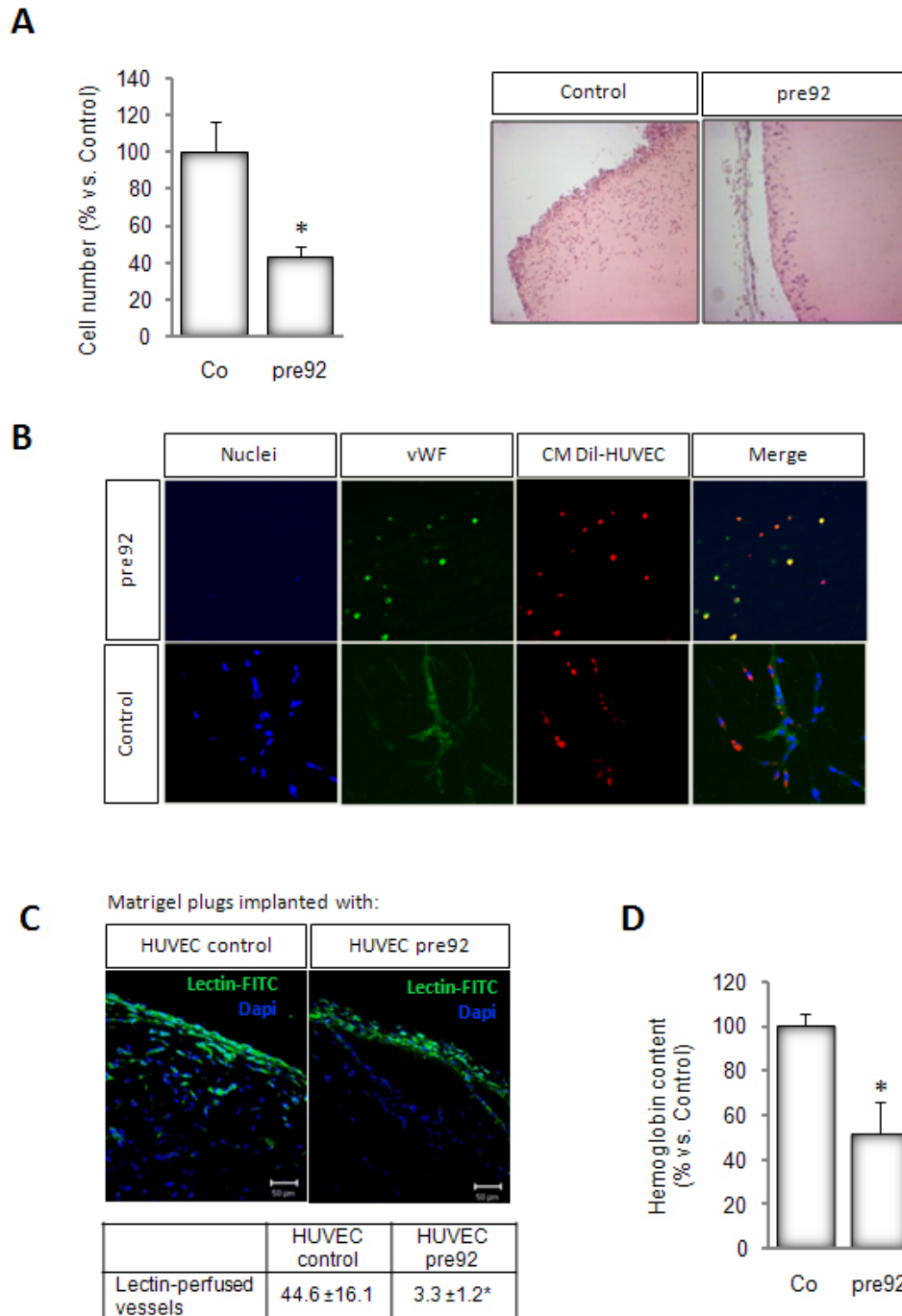


Figure 3.15 Overexpression of miR-92a impairs angiogenesis *in vivo*

HUVEC were transfected with pre92 or control oligonucleotides. 1×10^6 cells were stained with CM-DIL, mixed in matrigel and subcutaneously implanted *in vivo*. After 6 days, matrigel plugs were explanted and invading cells were detected in H&E sections (**A**) and after immunostaining with vWF antibody (green). CM-Dil labelled implanted HUVEC are red, Nuclei are stained with DAPI (blue), n=5-6 (**B**). *In vivo* perfused lectin-positive vessels were identified and counted after *i.v.* infusion of FITC-conjugated lectin, n=8 high power fields (**C**). Perfusion was determined by measuring the hemoglobin content, n=6-7 (**D**).

3.10 Inhibition of miR-92a enhances angiogenesis and neovascularization *in vitro* and *in vivo*

Next, we investigated whether inhibition of miR-92a might be useful to enhance vessel growth. As shown in Fig. 3.13 and Fig. 3.16, inhibition of endothelial miR-92a by 2'-O-methyl antisense oligonucleotides increases sprout formation *in vitro*.

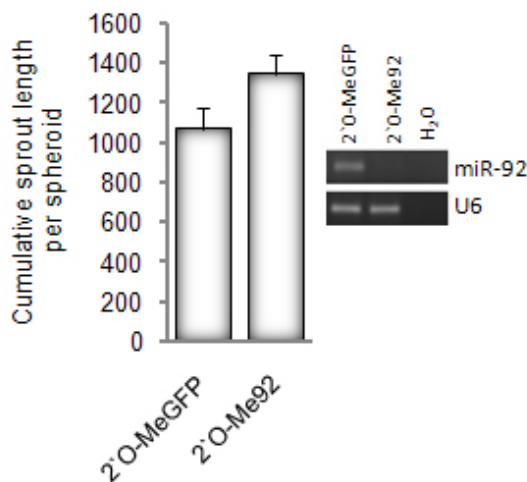


Figure 3.16 Inhibition of miR-92a enhances angiogenesis *in vitro*

miR-92a expression and sprout formation in HUVEC after transfection with 2'-O-methyl antisense oligoribonucleotides blocking miR-92a, n=4.

To inhibit miR-92a *in vivo*, we designed single-stranded RNA oligonucleotides complementary to specific miRNAs, also known as antagomirs. Antagomirs are chemically modified for improved stability by substitution of 2 phosphothioates at the 5' end and 4 phosphothioates at the 3' end. In addition, each nucleotide is conjugated with a 2'-O-methyl group for stronger binding of the miRNA and cholesterol is added to the 3' end for increased cell delivery (Kruzfeldt et al., 2005) (Fig. 3.17).

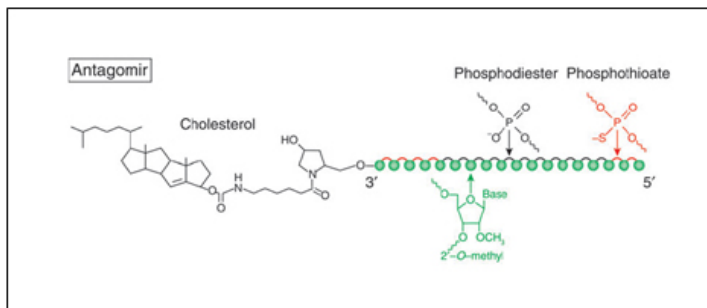


Figure 3.17 Antagomirs

Antagomirs are single-stranded RNA oligonucleotides complementary to specific miRNAs. They are chemically modified for stability and cholesterol conjugated for better delivery (Kruzfeldt et al., Nature 2006)

First, we analysed the uptake of antagomirs in different tissues and elucidated the antagomir concentration inducing a sufficient knockdown of miR-92a *in vivo*.

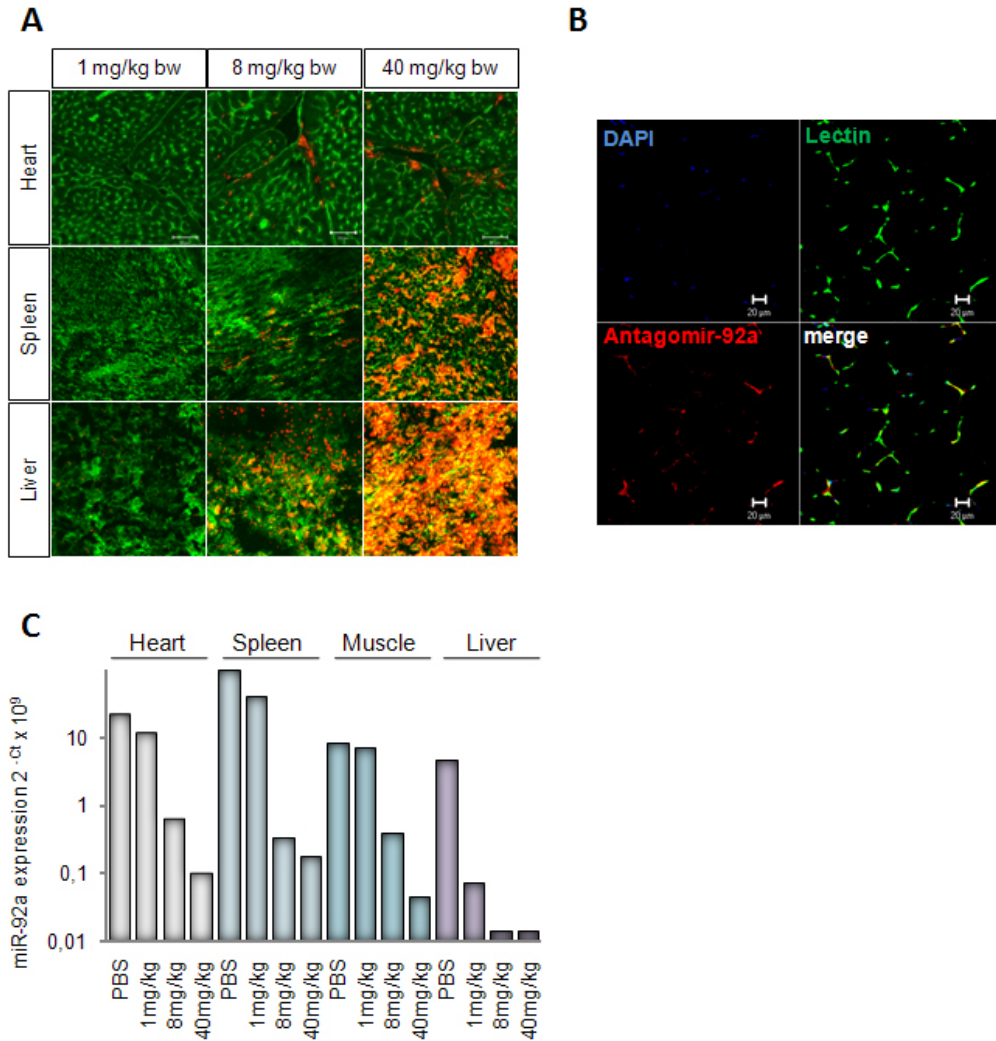


Figure 3.18 Dose-dependent downregulation of miR-92a by antagomir-92a

A) 48 h after *i.v.* infusion of Cy3-labelled antagomir-92a at concentrations of 1 mg/kg bw, 8 mg/kg bw and 40 mg/kg bw heart, spleen, and liver were harvested. The uptake of Cy3-labelled antagomir-92a was analysed in histological sections, capillaries were stained with Lectin. **B)** At day 1 after injection of Cy3-labelled antagomir-92a, skeletal muscle tissue was harvested and Cy3-labelled antagomirs were detected by confocal microscope in frozen 10- μ m sections. Cy3-labelled antagomir-92a is shown in red, *in vitro* counterstaining with lectin is shown in green. Nuclei are stained with DAPI (blue). **C)** RNA of different tissues was isolated 48 h after infusion of Cy3-labelled antagomir-92a by Trizol. Quantitative analysis of miR-92a expression was performed by real-time PCR, n=1-2.

Therefore, we *i.v.* injected antagomirs targeting miR-92a (from hereon antagomir-92a) carrying a Cy3 label at the 5' end at concentrations of 1 mg/kg, 8 mg/kg and 40 mg/kg and analysed the biodistribution in heart, spleen, muscle and liver two days after injection.

Whereas 1mg/kg Cy3-labelled antagomir-92a was not detectable in any tissue, we observed antagomir-92a in all tissues already at the relatively low concentration of 8 mg/kg (Fig. 3.18 A/B). Additionally, we isolated RNA from the different tissues 2 days after *i.v.* injection of Cy3-labelled antagomir-92a and analysed miR-92a expression using real-time PCR. As shown in Fig. 3.18 C, 1mg/kg antagomir-92a decreases miR-92a expression only to a minor extent in heart, spleen and muscle, whereas a significant knockdown is achieved in the liver. 8 mg/kg as well as 40 mg/kg antagomir-92a sufficiently blocks miR-92a expression in all analysed tissues. High resolution images of heart sections from mice treated with 8 mg/kg Cy3-labelled antagomir-92a and co-staining of perfused capillaries by injection of Lectin-FITC show that antagomir-92a is preferentially taken-up by vascular cells of the heart (Fig. 3.19) at the rather low concentration of 8 mg/kg bw used in the present study.

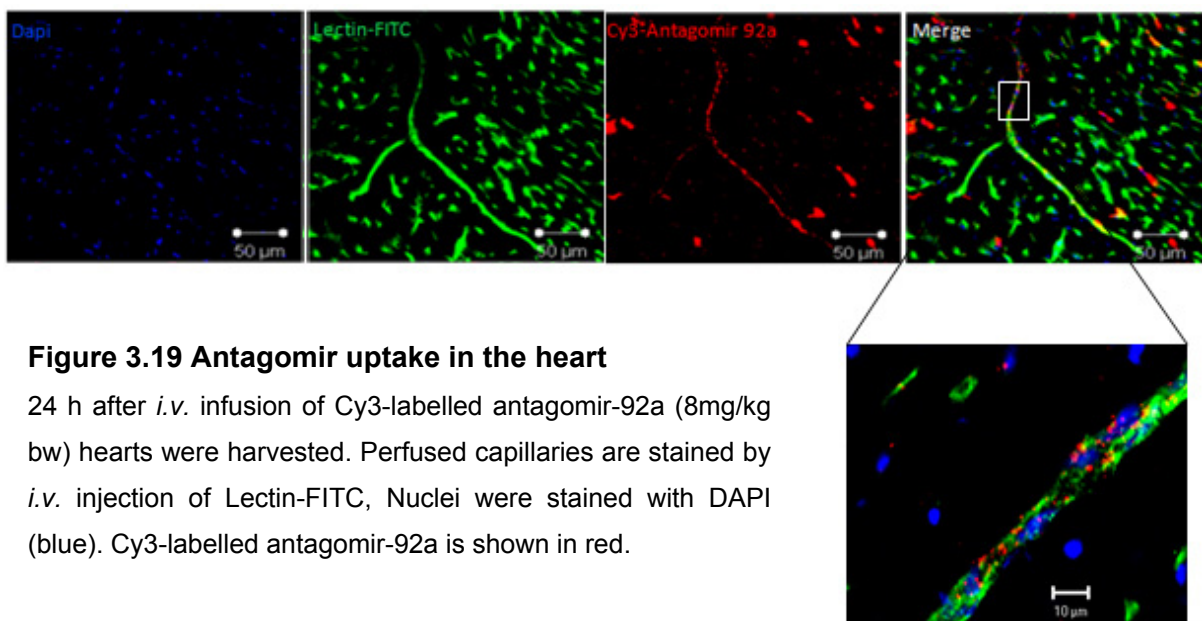


Figure 3.19 Antagomir uptake in the heart

24 h after *i.v.* infusion of Cy3-labelled antagomir-92a (8mg/kg bw) hearts were harvested. Perfused capillaries are stained by *i.v.* injection of Lectin-FITC, Nuclei were stained with DAPI (blue). Cy3-labelled antagomir-92a is shown in red.

Since we showed that a concentration of 8 mg/kg antagomir-92a sufficiently blocks miR-92a expression in different tissues (Fig. 3.18) one day after a single injection and is targeting mainly the vasculature (Fig. 3.19), we analysed the efficiency after repetitive treatment. Systemic application of 8 mg/kg antagomir-92a at day 1, 3 and 5 after implantation of matrigel plugs efficiently inhibits miR-92a expression in tissues like heart, spleen and liver harvested at day 6 (Fig. 3.20).

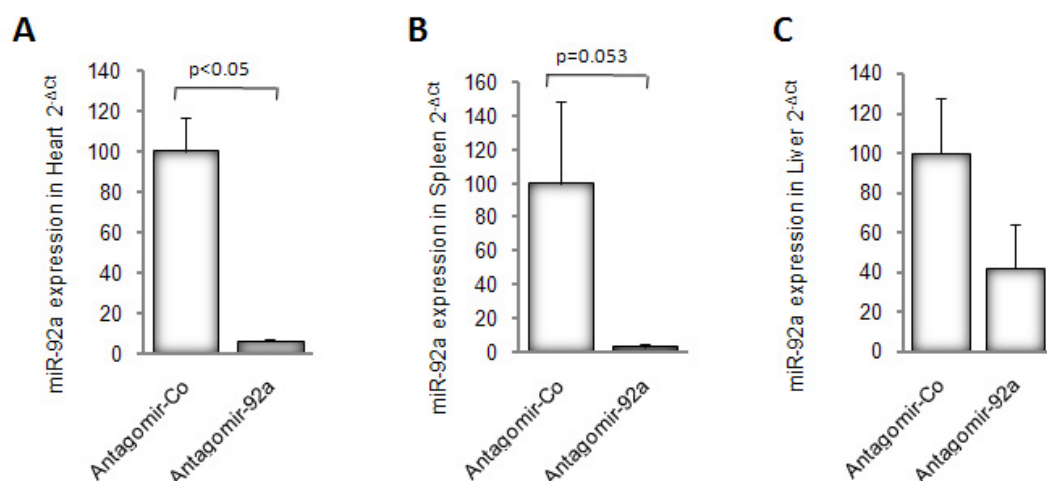


Figure 3.20 Inhibition of miR-92a expression in different tissues

Antagomir-92a or antagomir-Co were injected at day 1, 3, and 5. At day 6 different tissues were harvested and miR-92a expression was analysed in heart (A), spleen (B) and liver (C) using real-time PCR, n=3-5. MiR-92a expression was normalized to miR-24.

Having shown that repetitive antagomir-92a treatment efficiently blocks miR-92a expression in different tissues, we further analysed the effect of miR-92a inhibition on plug vascularization. Consistent with the hypothesis that inhibition of miR-92a augments angiogenesis, systemic application of antagomirs enhances the number of invading cells shown in a H&E staining (Fig. 3.21 A/B). Furthermore, the number of *in vivo* perfused lectin-positive vessels in implanted matrigel plugs (Fig. 3.21 C) and the hemoglobin content as a parameter for perfusion is significantly increased (Fig. 3.21 D).

To control for off-target effects of single-stranded RNA oligonucleotides and to confirm the specificity of antagomir-92a, we used two different control antagomirs, which both did not affect plug vascularization (Fig. 3.21 A).

These data clearly demonstrate a pro-angiogenic function of antagomir-92a *in vivo*. Antagomir-92a represses miR-92a expression *in vivo*, thereby promoting vascularization in matrigel plugs.

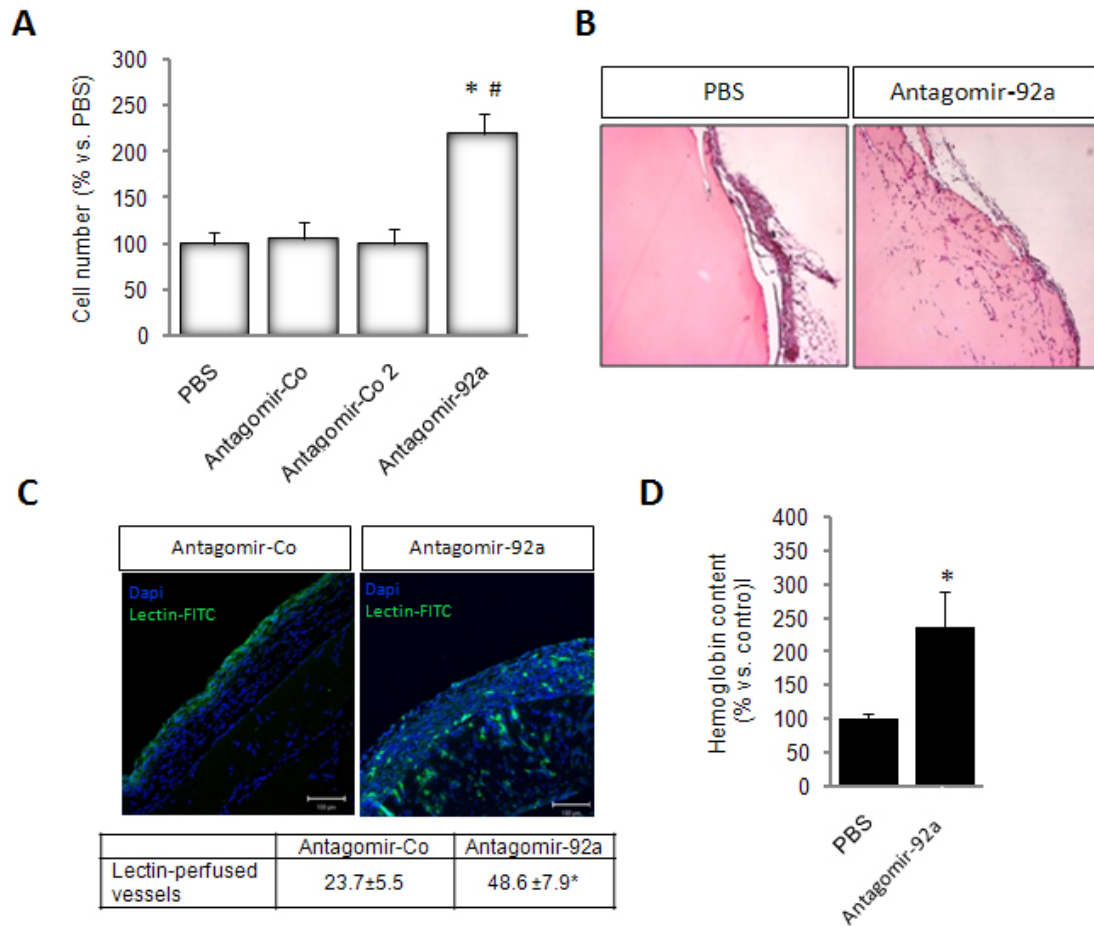


Figure 3.21 Inhibition of miR-92a enhances angiogenesis *in vivo*

Effect of systemic infusion of antagomirs targeting miR-92a (8 mg/kg bw, n=12), two different control antagomirs (Antagomir-Co and antagomir-Co2, each n=5-8) or PBS (n=11) at day 1, 3, 5. The number of invading cells was counted in H&E sections (**A/B**). Number of lectin-positive vessels was assessed by injection of FITC-conjugated lectin (**C**) and perfusion was measured by hemoglobin content (**D**). *p<0.05 compared to PBS, #p<0.05 compared to antagomir-Co for all panels.

3.11 MiR-92a is regulated by ischemic injury

We further addressed the question, whether antagomir-92a might be an attractive therapeutic tool to promote angiogenesis in ischemic diseases.

Therefore, we first determined the time-dependent expression of miR-92a in response to ischemia in two different models of ischemia, a model of hind limb ischemia and a myocardial infarction model (Fig. 3.22). RNA from the ischemic hind limb was isolated at the indicated time points and miR-92a as well as miR-92b and miR-93 expression was quantified using real-time PCR. Ischemic injury significantly

increases miR-92a expression with a maximal effect between 1-3 days (Fig. 3.22 A), suggesting a pathophysiological role for miR-92a *in vivo*. In accordance with the hind limb ischemia data, we could observe a significant increase in miR-92a expression in the infarcted vs. non-infarcted region one day after ligation of the left coronary artery.

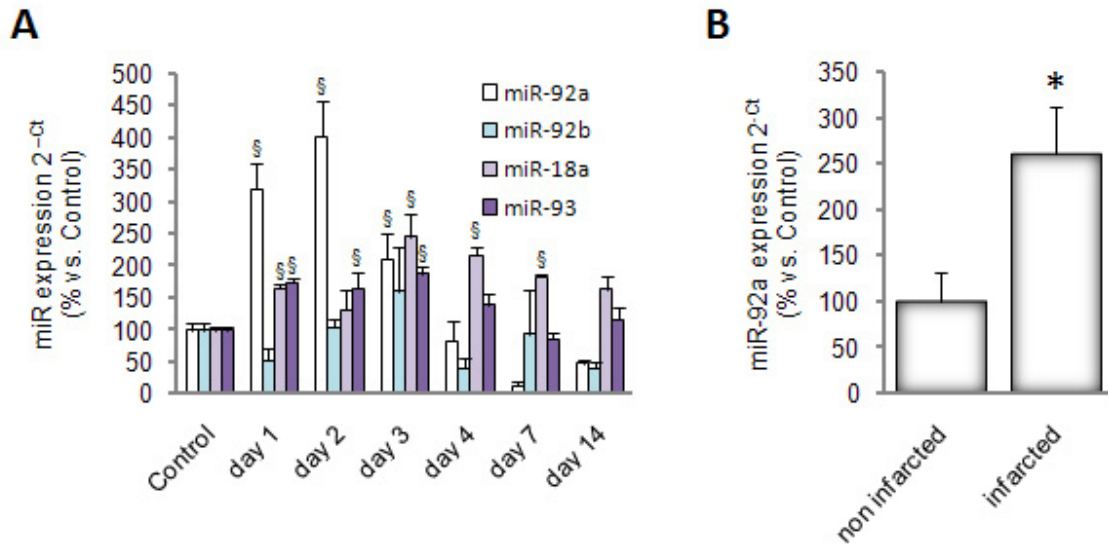


Figure 3.22 miR-92a is upregulated by ischemia

A) Expression of miR-92a, miR-92b, miR-18a and miR-93 was detected in ischemic muscle tissue at the respective days compared to non-ischemic control muscle. n=3. **B)** Day 1 after ligation of left coronary arteria, hearts were divided for infarcted and non-infarcted parts. Expression of miR-92a in infarcted vs. non infarcted region was analysed using real-time PCR, n= 4-5. *p<0.05 compared to PBS, §p<0.05 compared to non-ischemic control muscle. HLI operation was performed by Ariane Fischer. AMI operation was performed by Henrik Fox.

To test the efficiency and specificity of antagomir-92a treatment under ischemic conditions, we determined the expression of miR-92a and the closely related miR-92b, which differs only in 2 nucleotides, under ischemic conditions and simultaneous treatment with antagomir-92a. Additionally, we analysed expression of other members of the miR-17~92 cluster, namely miR-18a and miR-19a, and the unrelated miR-93 in ischemic and non-ischemic muscle. Whereas one single injection of antagomir-92a significantly suppresses miR-92a expression in non-ischemic and ischemic limbs, miR-92b is only slightly and non-significantly reduced. Moreover,

none of the other miRNAs studied is suppressed by antagomir-92a treatment (Fig. 3.23 A). Likewise, a specific and efficient knockdown of miR-92a by antagomir-92a treatment was demonstrated also in the heart (Fig. 3.23 B).

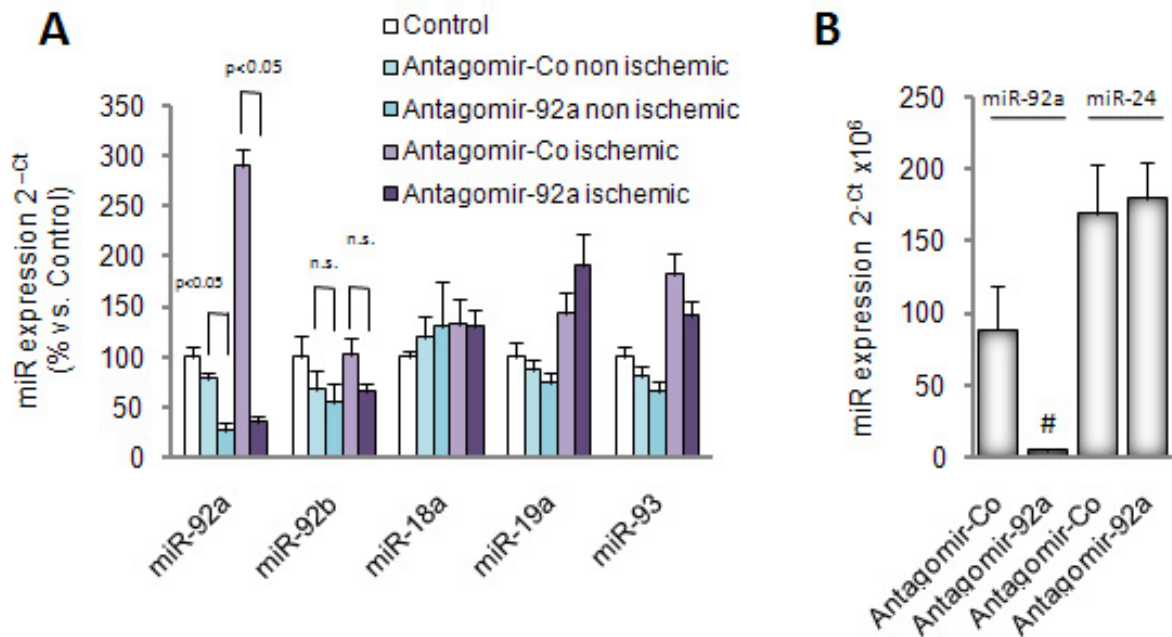


Figure 3.23 miR-92a is specifically downregulated by antagomir-92a

A) Antagomir-92a (8 mg/kg bw, *i.v.* injected once directly after induction of ischemia) specifically reduces miR-92a expression in ischemic and non-ischemic muscle tissue 2 days after induction of hind limb ischemia. Expression of miRs was determined by real time PCR as indicated in antagomir-92a or control antagomir-treated mice and was compared to non-treated controls, n=4. **B)** miR-92a expression in hearts 6 days after antagomir-92a treatment compared to control antagomirs, n=3-8. miR-24 expression was detected as control.

3.12 Antagomir-92a improves functional recovery after hind limb ischemia

We have shown that miR-92a is upregulated by ischemia and specifically downregulated by antagomir-92a. Furthermore, inhibition of miR-92a improves

vessel formation in matrigel plugs. Therefore, we tested whether antagomir-92a promotes blood vessel growth and improves functional recovery *in vivo* under pathophysiological conditions using a model of hind limb ischemia.

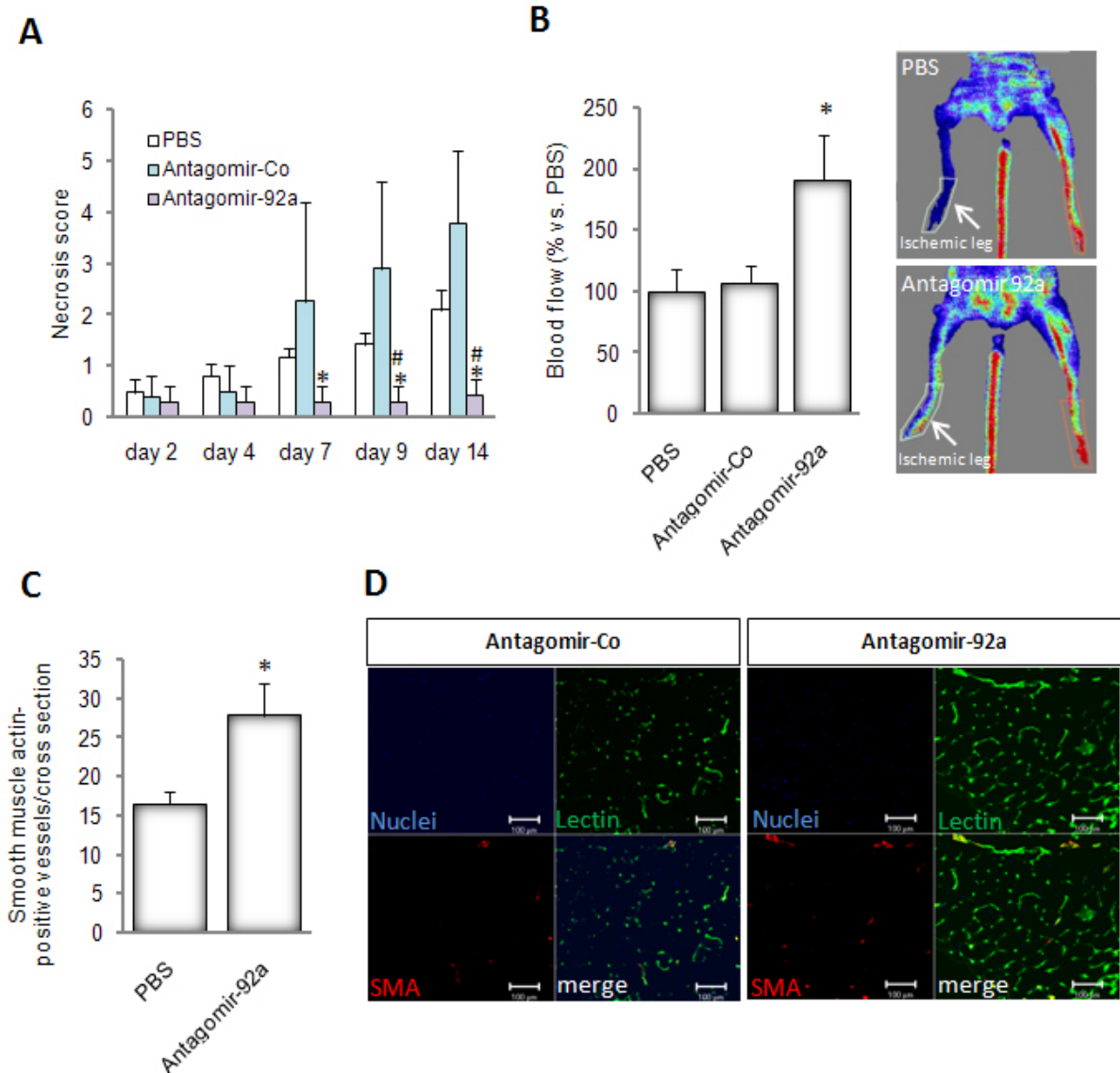


Figure 3.24 Antagomir-92a improves recovery after hind limb ischemia

Antagomir-92a, control antagomir (Antagomir-Co) (8 mg/kg bw) or PBS was injected at days 0, 2, 4, 7, 9 after induction of hind limb ischemia. **A)** At day 14, necrosis of tips and toes was determined by the following rating: 0=none; 1=1-3 tips; 2=4-5 tips; 3=1-3 toes; 4=4-5 toes; 5=1/3 foot; 6=2/3 foot; 8=whole foot; 10=1/3 leg; 12=2/3 leg and 14=whole leg, n=5. **B)** Blood flow ratio of the ischemic to normal limb was measured by using a laser Doppler blood flow meter at day 14, n=5 **C/D)** Muscle tissue was harvested at day 14 and stained with smooth muscle actin (red) and lectin *in vitro* (green). **C)** Quantitative analysis of smooth muscle actin-positive vessels (50-100 μ m) and **D)** representative images, n=4. HLI operation was performed by Ariane Fischer.

Intravenous infusion of antagomir-92a at day 0, 2, 4, 7 and 9 leads to a significant reduction in toe necrosis compared to antagomir-Co and PBS-treated control mice 14 days after induction of hind limb ischemia (Fig. 3.24 A). Consistent with the idea that these effects are due to improved neovascularization of ischemic limbs, the recovery of blood flow is improved by antagomir-92a compared to PBS or control antagomirs (Fig. 3.24 B). Likewise, the number of capillaries and the number of smooth muscle actin-positive arterioles is increased after antagomir-92a treatment (Fig. 3.24 C/D) indicating that antagomir-92a enhances perfusion and functional recovery of ischemic limbs.

3.13 Antagomir-92a improves functional recovery after acute myocardial infarction

To determine the effect of antagomir-92a treatment on functional recovery after acute myocardial infarction, the left coronary artery was occluded and left ventricular (LV) function was determined by Millar catheterization after 14 days (Table 3.2). Antagomir-92a treatment improves LV systolic and diastolic function as evidenced by increases of dp/dt_{max} and dp/dt_{min} , and significantly reduced enddiastolic pressure as well as tau as a parameter for isovolumic relaxation compared to vehicle controls and control antagomir treatment (Table 3.2 and Fig. 3.25 A-C). Representative pressure-volume loops reflect the functional recovery after antagomir-92a injection compared to PBS and antagomir-Co treated mice (Fig. 3.25 D).

	Sham (N=5)	AMI+PBS (N=7)	AMI+ Antagomir-Co (N=6)	AMI+ Antagomir-92a (N=8)
Age (weeks)	12	12	12	12
Weight (g)	21.4 ± 0.5	21.4 ± 0.4	22.3 ± 0.2	21.6 ± 0.2
HR (bpm)	480 ± 41	461 ± 15	414 ± 21	474 ± 18
LVESP (mmHg)	93 ± 4	85 ± 3	92 ± 3	89 ± 3
LVEDP (mmHg)	6.7 ± 0.8	16.7 ± 1.7*	15.0 ± 2.0*	8.0 ± 0.6 ^{†,##}
dp/dt max (mmHg/sec)	9745 ± 862	6714 ± 440*	6587 ± 939*	8932 ± 550 ^{†,#}
dp/dt min (mmHg/sec)	9234 ± 654	5903 ± 404*	6591 ± 727*	7910 ± 294 ^{††}
tau-Weiss (msec)	6.1 ± 0.5	8.7 ± 0.8*	9.0 ± 0.7*	6.9 ± 0.2 ^{†,#}

Tabel 3.2 Antagomir-92a improves recovery after acute myocardial infarction

Antagomir-92a, antagomir-Co or PBS were infused *i.v.* at day 0, 2, 4, 7 and 9 after ligation of the left coronary artery. On day 14, cardiac catheterization was performed for functional analysis by using 1.4F micromanometertipped conductance catheter (Millar Instruments Inc). Left ventricular (LV) pressure and its derivative (LV dP/dt) were continuously monitored with a multiple recording system. AMI operations was performed by Masayoshi Iwasaki and Jana Burchfield.

All data were acquired under stable hemodynamic conditions.

AMI: acute myocardial infarction, Antagomir-Co: control antagomir,

HR: heart rate, LVESP: left ventricular end systolic pressure, LVEDP: left ventricular end diastolic pressure

* indicates $p < 0.01$ vs sham.

[†] and ^{††} indicate $p < 0.05$ and $p < 0.01$ vs AMI+PBS, respectively.

[#] and ^{##} indicate $p < 0.05$ and $p < 0.01$ vs AMI+Antagomir-co, respectively.

Furthermore, antagomir-92a treatment reduces the infarct size by $44 \pm 3\%$ (Fig. 3.26 A) and significantly augments the number of *in vivo* perfused lectin-positive vessels particularly in the remote and border zone (Fig. 3.26 B). Antagomir-92a treatment also increases the number of smooth muscle actin positive vessels by ~ 1.4 -fold (Fig. 3.26 C).

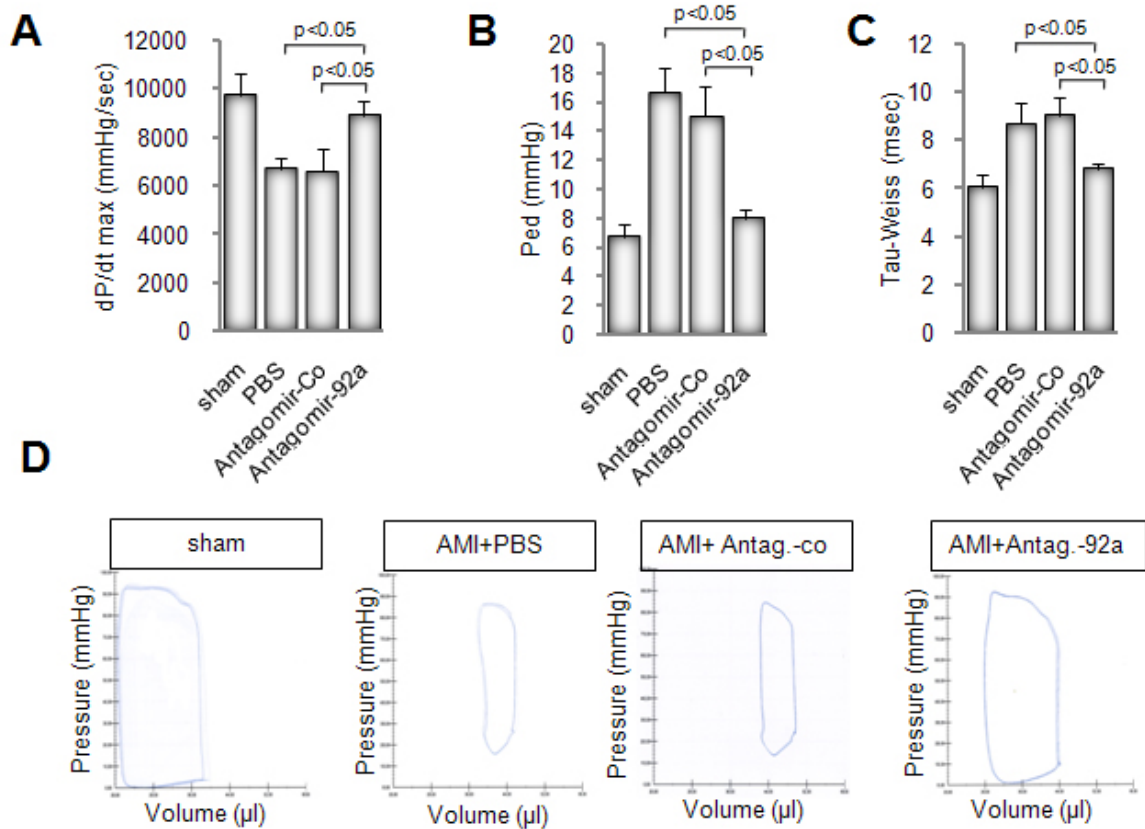


Figure 3.25 Antagomir-92a improves functional recovery after acute myocardial infarction

(A-D) 8 mg/kg bw antagomir -92a (n=8), control antagomirs (n=6), or PBS (n=7) were injected at days 0, 2, 4, 7, 9 after induction of myocardial infarction. On day 14, cardiac catheterization was performed for functional analysis compared to sham controls as shown in panels A-C, n=5-8. Panel D shows representative pressure volume loops. AMI operation was performed by Masayoshi Iwasaki and Jana Burchfield.

Having shown that inhibition of miR-92a improves recovery after myocardial infarction, we further investigated, if antagomir-92a treatment might have an anti-apoptotic effect on cardiomyocytes by increasing the number of capillaries and smooth muscle actin-positive cells.

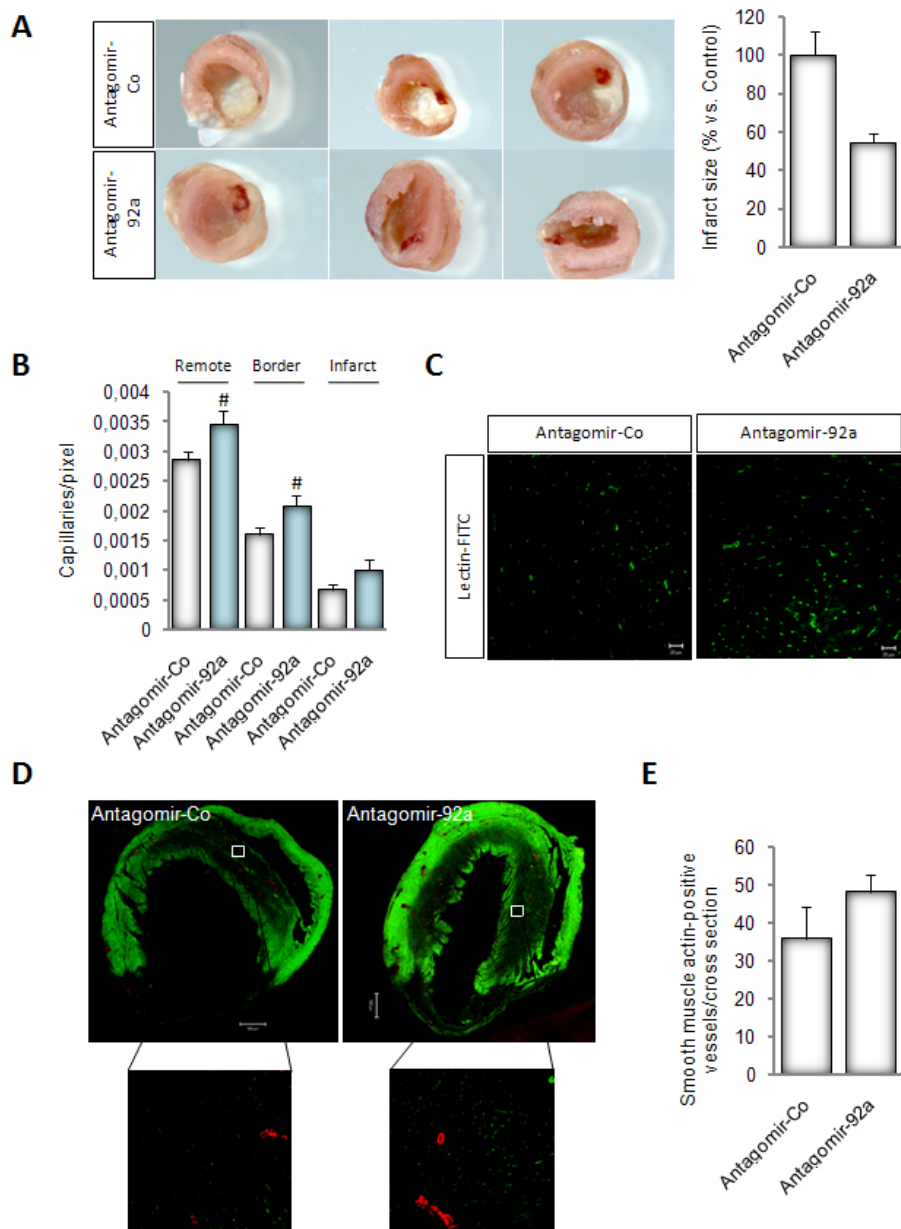


Figure 3.26 Antagomir-92a reduces infarct size and increases capillary density after acute myocardial infarction

8 mg/kg bw antagomir 92a, control antagomirs, or PBS were injected at days 0, 2, 4, 7, 9 after induction of myocardial infarction. On day 14, infarct size was measured, n=3-5. Representative images of the apex are shown (A). Capillary density was determined after *i.v.* infusion of FITC-conjugated lectin and was quantified in the remote, border and infarct regions of the hearts. (B) Quantification of n=6 high power fields per region per group, and (C) representative images of the remote region. Arteries were visualized by smooth muscle actin (SMA) staining and quantified per cross section, n=3-6. (D) Representative images of smooth muscle actin (red) and lectin (green) and (E) quantitative analysis of SMA-positive vessels are shown.

Therefore, freshly isolated rat neonatal cardiomyocytes were incubated with antagomir-92a or antagomir-Co for 48 h. Then, cardiomyocytes were serum-deprived for 24 h by incubation with medium depleted from FCS to induce apoptosis, but containing antagomir-92a or antagomir-Co to determine the impact of miR-92a on cell death. Apoptotic cells were measured by FACS analysis. However, antagomir-92a has no effect on cardiomyocyte apoptosis *in vitro* (Fig. 3.27 A). Additionally, we analysed the effect of antagomir-92a treatment on cardiomyocytes in the infarct zone *in vivo* using TUNEL staining. Whereas antagomir-92a shows no effect on cardiomyocyte apoptosis *in vitro*, we observed a significant downregulation of apoptosis *in vivo* (Fig. 3.27 B).

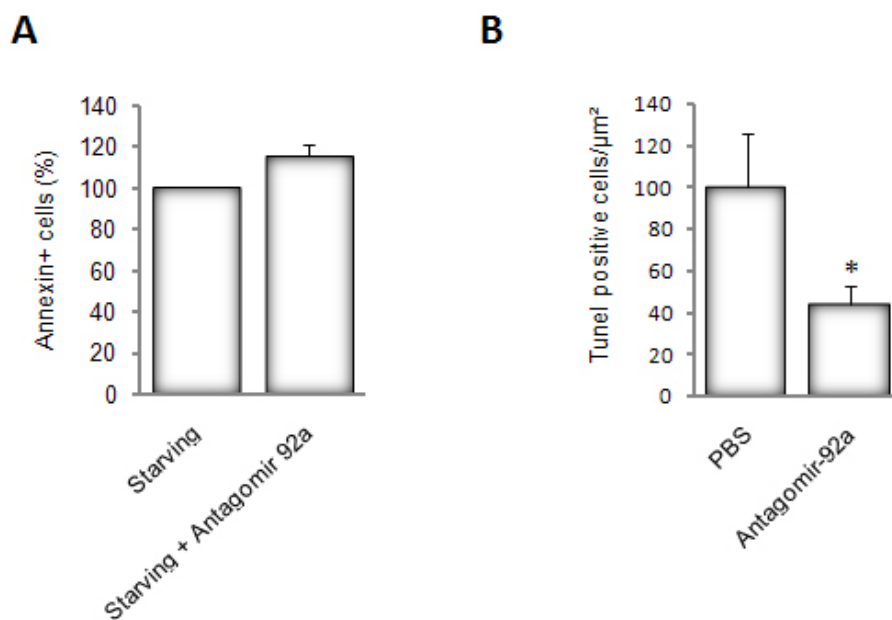


Figure 3.27 Effect of antagomir-92a treatment on apoptosis *in vitro* and *in vivo*

A) Rat neonatal cardiomyocytes were pre-incubated with antagomir-92a for 48 h. Then, cells were washed and medium was replaced by medium without FCS („starving“) and antagomir-92a or control antagomir (each 150 nM) was added again for 24 h. Apoptotic cells were detected by annexin V staining by FACS, n=3. **B)** miR-92a was inhibited by injecting antagomir-92a (8 mg/kg bw at days 0) or antagomir control after ligation of left coronary artery. In order to quantify *in vivo* apoptosis after myocardial infarction in the infarct zone TUNEL staining was performed using 4-μm paraffin sections of the heart at day 14, n=4-5.

These data indicate that antagomir-92a improves functional recovery after acute myocardial infarction by increasing the number of capillaries and smooth muscle actin positive vessels and reducing the number of apoptotic cardiomyocytes in the infarct zone. We further addressed the question, if miR-92a expression and activity is restricted to endothelial cells exerting anti-apoptotic effects on cardiomyocytes in a paracrine manner or if miR-92a has also a functional role in cardiomyocytes. In order to clarify this question, we performed an *in situ* hybridization using frozen sections from the heart. A specific 3'DIG labelled LNA probe as well as a scrambled probe as negative control and a U6 probe as positive control were used.

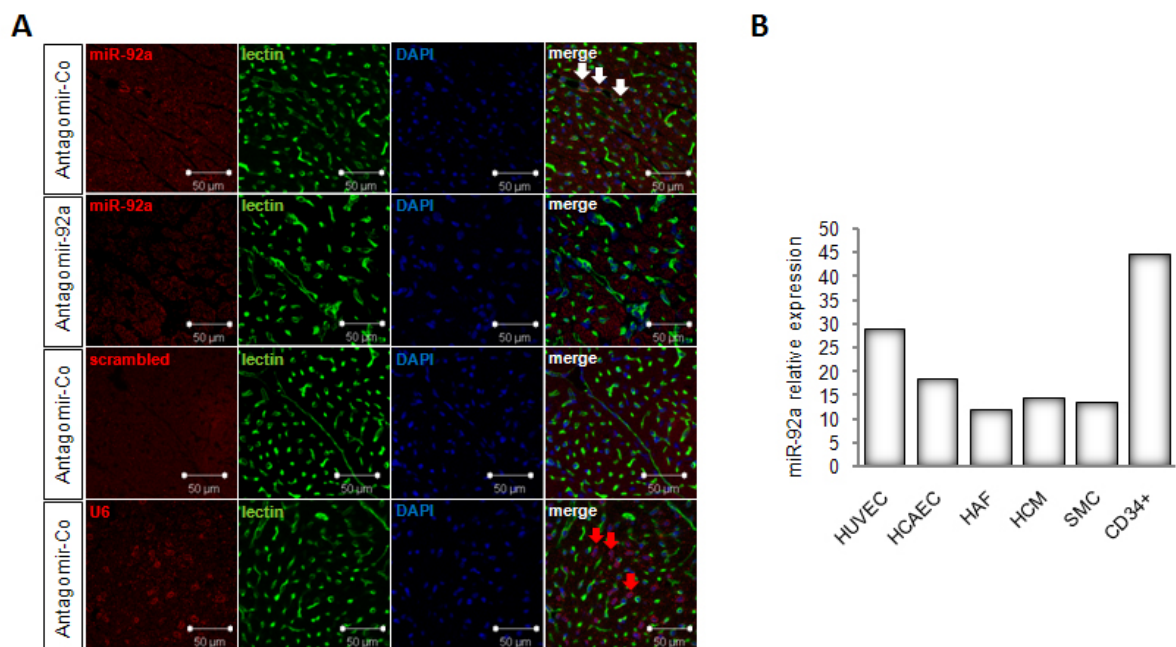


Figure 3.28 Expression profile of miR-92a

A) After ligation of the left coronary artery, antagomir-92a or control antagomir (Antagomir-Co) were injected *i.v.* at a concentration of 8 mg/kg bw at day 0. Hearts were harvested at day 2 and *in situ* hybridization on frozen sections was performed using a specific 3'DIG-labelled probe for miR-92a. U6 served as positive control, a scrambled probe was used as negative control. Sections were counterstained with lectin *ex vivo* (green) and DAPI (blue). White arrows indicate miR-92a expressing endothelial cells in control antagomir-treated mice, red arrows indicate U6-positive non-endothelial cells. Scale bar indicates 20 μ m. **B)** Human umbilical vein endothelial cells (HUVEC), human coronary artery endothelial cells (HCAEC), human aortic fibroblasts (HAF), human cardiac myocytes (HCM), human smooth muscle cells (SMC) and CD34+ cells were cultured *in vitro*. RNA was isolated and expression of miR-92a was assessed by real time PCR. U48 served as loading control.

Co-staining with Lectin to visualize capillaries indicates a higher expression of miR-92a in endothelial cells compared to cardiomyocytes (Fig. 3.28 A). Administration of antagomir-92a abolished the staining demonstrating that the miR-92a probe is specific. Moreover, we analysed the expression of miR-92a in various cell types such as different endothelial cells, smooth muscle cells, fibroblasts and cardiomyocytes. As shown in Fig. 3.28 B, human umbilical vein endothelial cells express miR-92a on a much higher level in comparison to microvascular or artery endothelial cells as well as smooth muscle cells, fibroblasts and cardiomyocytes.

3.14 Genes regulated by miR-92a

Having shown, that miR-92a is critically involved in angiogenic processes *in vitro* and *in vivo*, we further addressed the question, which potential miR-92a targets might be responsible for the observed effects.

Predicted target	Function	Phenotype	Reference
Integrin $\alpha 5$	Cell-matrix interaction	Embryonic lethal	Yang et al., Development 1993
Integrin αv	Cell-matrix interaction	Improves angiogenesis	Bader et al., Cell 1998
SIRT1	Histone deacetylase	Lethal just before or after birth	Cheng et al., PNAS 2003
Rap1b	GTP-binding protein	Embryonic lethal	Chzanowska-Wodnicka et al., Blood 2008
MKK4	Mitogen activated map kinase	Embryonic lethal	Yang et al., PNAS 1997
EDG1	sphingosin-1-phosphate receptor	Embryonic lethal	Liu et al., JCI 2000

Tabel 3.3 Potential miR-92a targets

Targets were predicted *in silico* using TargetScan, PicTar or miRanda software.

As shown in Table 3.3, *in silico* target prediction of miR-92a revealed several targets involved in angiogenesis, whose deletion causes, in most cases, embryonic lethality by a defect in vascular development.

The targets predicted in silico included several regulators of endothelial cell functions and vessel growth, such as the Integrin subunits $\alpha 5$ and αv , which mediate cell-matrix interactions, anti-apoptotic signaling and cell migration (Francis et al., 2002; Urbich et al., 2002; Yang and Korsmeyer, 1996). Furthermore, other predicted pro-angiogenic targets include the histone deacetylase SIRT1 (Imai et al., 2000; Potente et al., 2007), the small GTP-binding protein RAP1, an angiogenesis-mediating protein involved in Integrin signaling (Chrzanowska-Wodnicka et al., 2008), the sphingosin-1-phosphate receptor 1 (S1P₁) (Paik et al., 2001) and the mitogen activated kinase kinase 4 (MKK4). In order to determine whether the predicted targets are indeed regulated by miR-92a, we overexpressed miR-92a in HUVEC using pre92 or control, isolated RNA after 48h and performed an Affymetrix mRNA gene expression array. Upregulation of miR-92a causes a more than 1.25-fold downregulation of ~7000 genes (53.000 genes were analysed in total) in comparison to control (data not shown). Quantification of the mRNA expression revealed, that many genes involved in angiogenic signaling are downregulated by miR-92a overexpression (Fig. 3.29 A).

In order to confirm these results on protein level, we performed Western blotting 48 h after transfection with pre92 or control precursor and demonstrate that especially Integrin $\alpha 5$ and eNOS are significantly reduced in HUVEC overexpressing miR-92a (Fig.3.29 B). Additionally, we observed a downregulation of MKK4 and SIRT1 protein (Fig. 3.29 B). Accordingly, overexpression of miR-92a results in the decrease of Integrin $\alpha 5$ protein on the cell surface as well as in total lysates as measured by FACS analysis (Fig. 3.29 C).

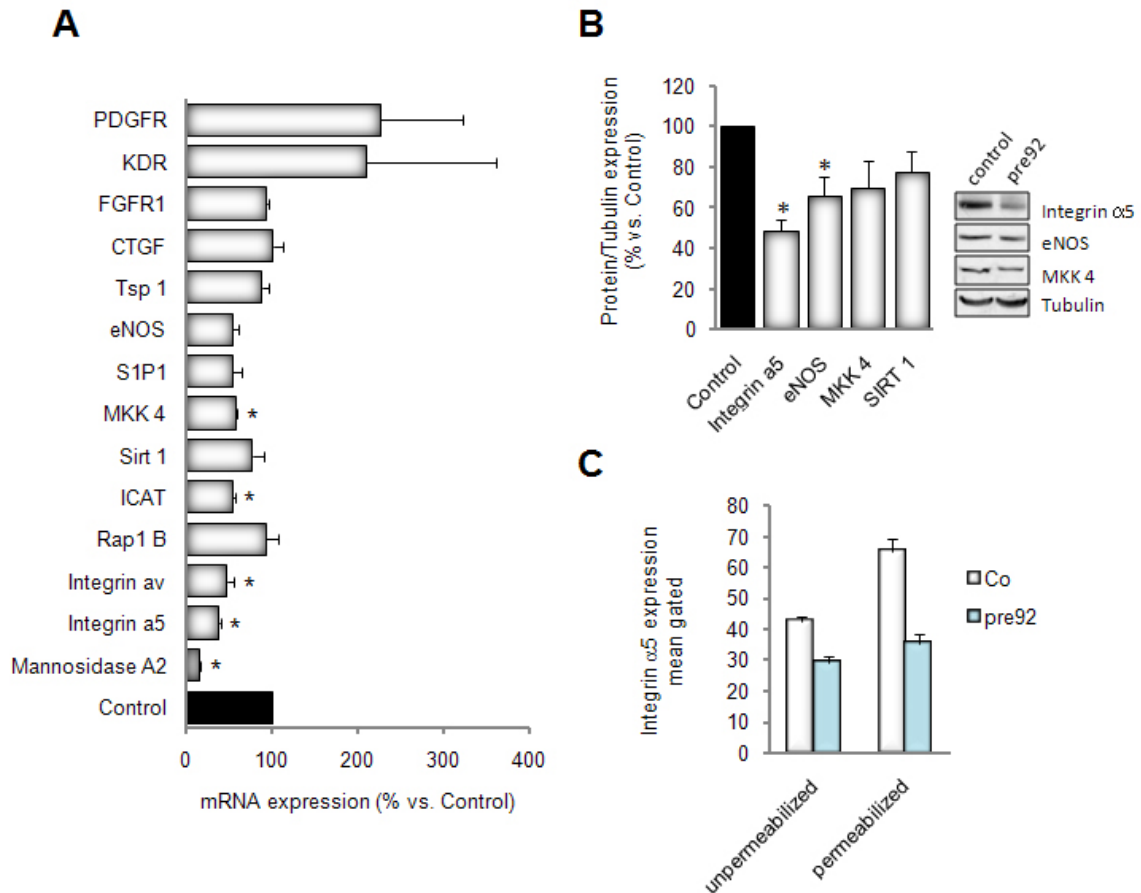


Figure 3.29 Target genes downregulated on protein level

HUVEC were transfected with pre92 or control. **A)** Protein expression determined by Western blotting using antibodies against Integrin α 5, eNOS, MKK4 and SIRT1. Quantitative analysis and representative images are shown, n=3-4. **B)** Integrin α 5 expression on the surface was measured using FACS analysis, n=3.

3.15 Integrin α 5 is a direct target of miR-92a

Given the pivotal role of Integrin α 5 in vascular development and angiogenesis and its profound regulation by overexpression of miR-92a, we investigated whether Integrin α 5 is a direct target of miR-92a. The 3'UTR of Integrin α 5 contains one conserved predicted binding site for miR-92a (Fig. 3.30 A). We therefore cloned a fragment of the Integrin α 5 3'UTR sequence containing 4x the binding sites of miR-92a or a fragment containing the mutated seed sequence in the 3'UTR of the Luciferase reporter and examined luciferase activity after co-transfection with miR-

92a in HEK293 cells. Indeed, miR-92a overexpression reduces luciferase activity (Fig. 3.30 B), indicating that Integrin $\alpha 5$ is a direct target of miR-92a.

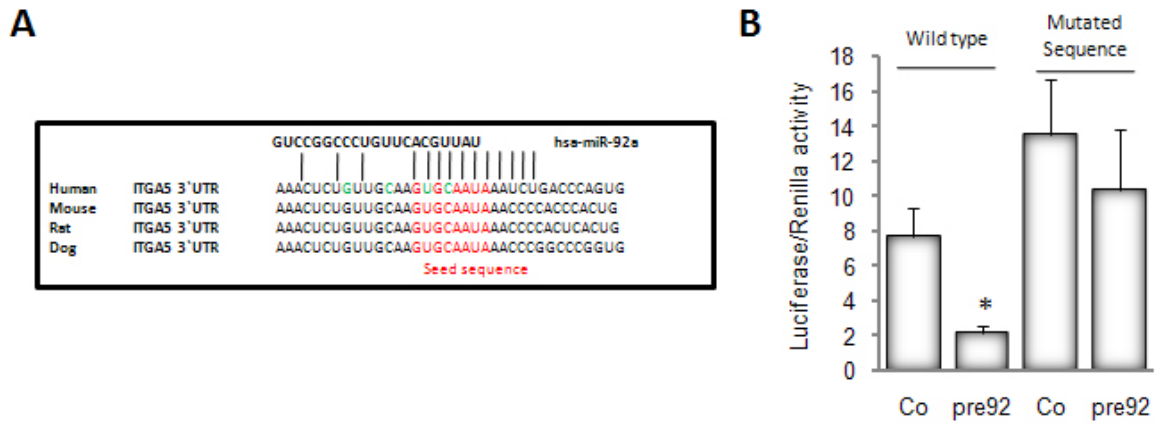


Figure 3.30 Integrin $\alpha 5$ is a direct target of miR-92a

A) Schematic illustration of miR-92a seed sequence in the Integrin $\alpha 5$ 3'UTR. Green indicates the mutated nucleotides. **B)** Luciferase normalized to Renilla activity measured in homogenates of HEK cells transfected with the wild type (wt) or mutated luciferase constructs and pre92 or control precursor, n=3-4.

Mutation of the target sequence results in a higher basal expression indicating stabilization possibly by protecting against endogenous miR-92a and reduces the downregulation by pre-miR-92a (Fig. 3.30 B).

Having shown that Integrin $\alpha 5$ is a direct target of miR-92a, we further addressed the question, if the reduced expression of Integrin $\alpha 5$ by miR-92a may contribute to the inhibition of sprout formation *in vitro*.

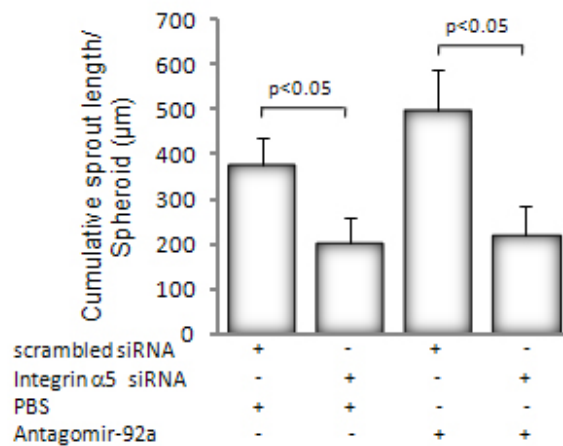


Figure 3.31 Impaired sprouting by miR-92a overexpression is mediated by Integrin $\alpha 5$

HUVEC were cotransfected with Integrin $\alpha 5$ or scrambled siRNA and PBS or antagomir-92a. The cumulative sprout length per spheroid was measured 24 h after embedding spheroids in the collagen matrix.

Therefore, we inhibited miR-92a expression using antagomir-92a and co-silenced Integrin $\alpha 5$ by siRNA and found that antagomir-92a only stimulates sprouting in the presence but not in the absence of Integrin $\alpha 5$ (Fig. 3.31).

In order to investigate the regulation of Integrin $\alpha 5$ by miR-92a *in vivo*, we inhibited miR-92a expression by *i.v.* injection of antagomir-92a or control antagomir. Two days after injection, Integrin $\alpha 5$ expression in the muscle was quantified using real-time PCR and histological sections. In accordance with our *in vitro* data, inhibiting miR-92a by antagomir-92a treatment *in vivo* increases the expression of Integrin $\alpha 5$ mRNA (Fig. 3.32 A) and protein (Fig. 3.32 B) in the vasculature of non-ischemic muscle tissue as shown by staining with a specific Integrin $\alpha 5$ antibody.

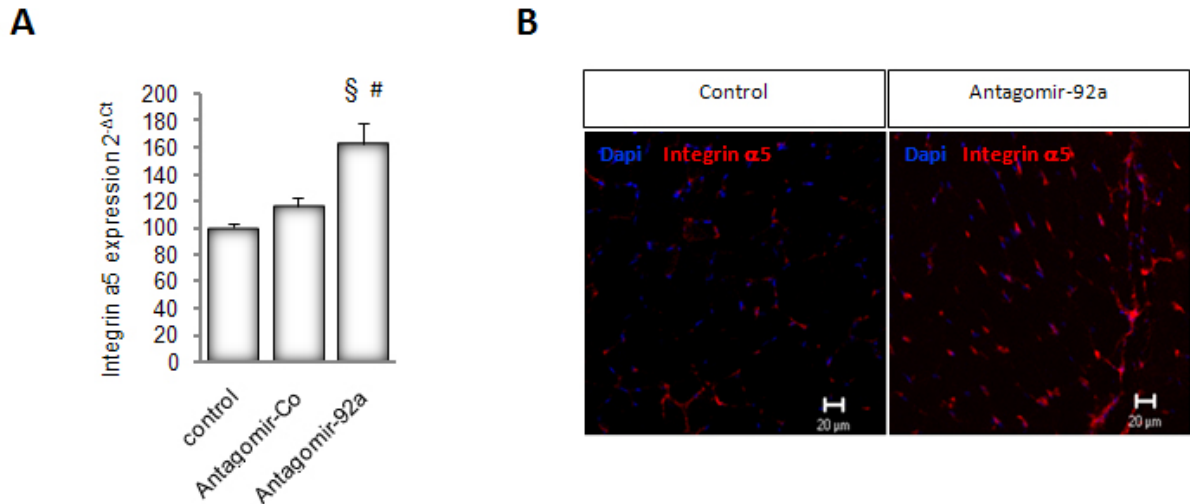


Figure 3.32 Antagomir-92a upregulates Integrin α 5 expression *in vivo*

A) Antagomir-92a (8 mg/kg bw, *i.v.*) or antagomir-Co were injected once directly after induction of ischemia. The expression of Integrin α 5 was determined by real time PCR in non-ischemic muscle in antagomir-92a or control antagomir-treated mice and was compared to non-treated controls, n=6-8. \S p<0.05 versus non-treated control muscle, $\#$ p<0.05 compared to antagomir controls. **B)** Immunostaining against Integrin α 5 (red) of non-ischemic muscle sections from mice treated with antagomir-92a or controls.

In summary, these data indicate that Integrin α 5 is a key regulator of antagomir-92a-mediated improved angiogenesis and therefore recovery after hind limb ischemia and acute myocardial infarction.

To identify genes, which might be secondarily regulated by Integrin α 5, we performed an additional Affimetrix profiling using RNA from HUVEC treated with Integrin α 5 siRNA (Table 3.4) and compared the results with the previously performed pre92 Affimetrix chip.

Several genes were identified, which are downregulated by pre92 and Integrin α 5 siRNA suggesting that these genes are indirectly regulated by miR-92a-dependent downregulation of Integrin α 5. The most prominent example is the regulation of eNOS expression, which is downregulated by miR-92a and Integrin α 5 siRNA indicating that eNOS downregulation in response to miR-92a overexpression may occur as a consequence of Integrin α 5 mRNA degradation.

Genbank	Common	Product	Pre92/ control	Predicted miR- 92a target	Downregulat ed by Integrin α 5
NM_002205	CD49e	Integrin α 5	0.39	yes	yes
NM_001400	EDG1	Endothelial differentiation, sphingolipid G-protein-coupled receptor, 1	0.54	yes	no
NM_003010	MEK4	Mitogen-activated protein kinase kinase 4	0.59	yes	no
NM_012238.3	Sirt1	Sirtuin 1	0.77	yes	no
NM_002372	MANA2	Mannosidase, alpha, class 2A, member 1	0.16	yes	no
NM_013253	DKK-3	Dickkopf (Xenopus laevis) homolog 3	0.28	yes	no
NM_002428	MT2-MMP	Matrix metalloproteinase 15	0.24	no	yes
AK024172	UBC9	Ubiquitin-conjugating enzyme E2I	0.31	no	yes
NM_001721	ETK	BMX non-receptor tyrosine kinase	0.43	no	yes
NM_004995	MT1-MMP	Matrix metalloproteinase 14	0.44	no	yes
AF270513	EMILIN-2	Extracellular glycoprotein EMILIN-2 precursor	0.45	no	yes
NM_005258	GFRP	GTP cyclohydrolase I feedback reg. Pro.	0.47	no	yes
NM_018728	MYO5C	Myosin 5C	0.54	no	yes
NM_000603	eNOS	Nitric oxide synthase 3 (endothelial cell)	0.54	no	yes
NM_016580	VECAD2	Protocadherin 12	0.63	no	yes
M37780	CD31	Platelet/endothelial cell adhesion molecule	0.63	no	yes
NM_000552	VWF	Von Willebrand factor	0.66	no	yes
NM_003379	VIL2	Villin 2	0.71	no	yes
NM_000450	CD62E	Selectin E (endothelial adhesion molecule 1)	0.13	no	no
NM_000259	MYO5A	Myosin VA (heavy polypeptide 12, myosin)	0.50	no	no
AK023795	ADAMTS1	A disintegrin-like and metalloprotease	0.22	no	no
NM_007361	NID2	Nidogen 2	0.29	no	no
U65404	EKLF	Kruppel-like factor 1 (erythroid)	0.32	no	no
NM_000361	CD141	Thrombomodulin	0.36	no	no
NM_001200	BMP2A	Bone morphogenetic protein 2	0.37	no	no
NM_005562	EBR2	Laminin, gamma 2	0.40	no	no
NM_000201	ICAM1	Intercellular adhesion molecule 1 (CD54)	0.44	no	no
NM_001147	ANG2	Angiopoietin 2	0.52	no	no
NM_000584	IL8	Interleukin 8	0.54	no	no
NM_002253	FLK1	Kinase insert domain receptor	0.61	no	no
NM_000459	TIE2	TEK tyrosine kinase, endothelial	0.66	no	no
M27968	BFGF	Fibroblast growth factor 2 (basic)	0.70	no	no

Table 3.4 Summary of genes downregulated by miR-92a and Integrin α 5

HUVEC were transfected with pre92 and control or siRNA against Integrin α 5 and scrambled siRNA. 48 h after transfection RNA was isolated and subjected to an Affimetrix mRNA chip. Selected genes which are downregulated by pre92 are shown. Light blue represents directly predicted targets, which are not regulated by Integrin α 5 siRNA, blue represents genes, which are downregulated by pre92 and Integrin α 5 siRNA indicating that these targets might be indirectly regulated by miR-92a-dependent downregulation of Integrin α 5. Dark blue represents genes downregulated by pre92, which are not predicted as direct targets and are not regulated by Integrin α 5

Furthermore, we identified a large group of regulated genes, which are not predicted to be miR-92a targets and are not regulated by Integrin α 5 siRNA suggesting that these genes might be regulated by other direct miR-92a target genes.

4 Discussion

MicroRNAs are a recently discovered class of highly conserved, non-coding small RNAs that regulate gene expression on the post-transcriptional level by binding to the target mRNA leading either to translational repression or mRNA degradation (Bartel, 2004). MicroRNAs control various physiological and pathophysiological processes such as cardiogenesis and oncogenesis (Bartel, 2004; van Rooij et al., 2007; Ventura et al., 2008; Zhao et al., 2007). Additionally, several studies have dissected the role of miRNAs in skeletal muscle proliferation and differentiation, brain morphogenesis, and hematopoietic lineage differentiation (Chen et al., 2004; Giraldez et al., 2005; Zhao et al., 2005). However, at the beginning of this study, the involvement of miRNAs in vascular signaling and function was unknown. Therefore, the major aim of this study was the analysis of the general role of microRNAs for endothelial cell biology. Moreover, the function of specific microRNAs highly expressed in EC should be investigated in detail.

4.1 MicroRNAs are crucial regulators of endothelial cell biology

4.1.1 Role of Dicer and Drosha in endothelial cells

The present study demonstrates for the first time that the enzymes Dicer and Drosha, which are the major enzymes involved in miRNA biogenesis, play a decisive role in endothelial cell biology. Immunostainings and Western blot analysis revealed that Dicer and Drosha are expressed in endothelial cells, whereby Drosha is restricted to the nucleus and Dicer is mainly localized in the cytoplasm. Transient silencing efficiently blocking Dicer and Drosha on mRNA and protein level demonstrates that both enzymes are involved in the regulation of angiogenesis *in vitro*. Additionally, inhibition of Dicer specifically impairs migration and viability of endothelial cells and reduces *in vivo* angiogenesis.

In summary, our data provide evidence for an important role of Dicer and Drosha for endothelial cell functions. The profound impairment of *in vitro* angiogenesis in Dicer deficient endothelial cells is consistent with findings, which were published

simultaneously with the data of the present study (Giraldez et al., 2005; Suarez et al., 2007; Yang et al., 2005).

However, there have been also several inconsistencies between the different studies. While the migration of Dicer-deficient endothelial cells on collagen matrix is not affected in the study of Suarez and his colleagues (Suarez et al., 2007), migration is significantly impaired when fibronectin was used as matrix as shown in our study. It is conceivable that depletion of Dicer differentially modifies Integrin receptors, thereby selectively impairing fibronectin matrix-dependent cell functions. Furthermore, Dicer knockdown causes profound dysregulation of angiogenesis-related genes *in vitro* and *in vivo*. Despite the requirement of Dicer for vascularization, crucial regulators of angiogenesis, for instance vascular endothelial growth factor (VEGF) and its receptors FLT1 and KDR have been shown to be upregulated (Suarez et al., 2007; Yang et al., 2005). In contrast, our study did not reveal a role of Dicer in the regulation of KDR expression, which might suggest that this regulation is a highly dynamic process. Furthermore, protein levels of TIE1 are decreased in Dicer^{ex1/2} embryos (Yang et al., 2005), whereas its expression is strongly enhanced in Dicer-depleted cultured endothelial cells (Suarez et al., 2007). This phenomenon might be explained by the complex mixture of miRNAs being spatiotemporally expressed during development compared to isolated endothelial cells in culture.

Interestingly, the knockdown of Dicer exerts more profound effects on endothelial sprout formation *in vitro* and *in vivo* compared to Drosha, although Drosha acts upstream of Dicer in miRNA biogenesis. To exclude that the distinct biological response is caused by a methodological problem, control experiments were performed to confirm a similar efficiency of the downregulation on protein and mRNA level. Moreover, the findings were reproduced using a second siRNA sequence excluding a nonspecific effect of one of the sequences. Furthermore, the genetic downregulation of Drosha efficiently reduced the expression of about 42% of the detected miRNAs as shown in a microRNA profiling indicating that the minor phenotypic alteration in Drosha siRNA-transfected cells is not related to an insufficient reduction of Drosha enzymatic activity.

An explanation for the profound differences between Dicer and Drosha silenced cells could likely be due to the selective impairment of AKT signaling in Dicer siRNA treated cells. Moreover, the distinct effects of Dicer versus Drosha may be related to

other biological properties of Dicer, namely its role in the formation and maintenance of heterochromatin (Volpe et al., 2002), which might also affect endothelial cell functions independent of the reduction of miRNA processing. Moreover, a recently described Drosha-independent microRNA processing pathway could compensate for the loss of Drosha (Okamura et al., 2007; Ruby et al., 2007). Additionally, the minor role of Drosha compared to Dicer on sprouting might alternatively be explained by a concomitant effect on anti-apoptotic or pro-angiogenic genes, which might be less affected by Dicer siRNA. A downregulation of miRNAs targeting anti-apoptotic or pro-angiogenic genes might lead to an upregulation of protective and pro-angiogenic proteins in Drosha-silenced endothelial cells and may partially compensate for the increase in angiogenesis inhibitors. It is well established that angiogenesis is regulated by a balance of pro- or anti-angiogenic genes. A disturbance of this critical balance by interfering with various miRNAs, each of which inhibiting translation or transcription of multiple target mRNAs, may well explain differences in the phenotype.

Profiling of miRNA expression in endothelial cells, as it has been performed in the present study, additionally provides a tool to identify potential important miRNAs in endothelial cell biology. Strikingly, the relative expression of about 60% of the miRNAs was below the detection limit indicating that the majority of the miRNAs are downregulated in endothelial cells. This is consistent with the concept that miRNAs are differentially expressed during development and control lineage commitment (Chen et al., 2004; Giraldez et al., 2005; Sempere et al., 2004; Wienholds et al., 2005). A cell type specific regulation of miRNA expression may contribute to tissue and cell type specific patterning of gene expression. However, to exclude that the results are due to false-negative detection, the data were selectively confirmed by RT-PCR demonstrating that several miRNAs such as miR-142-3p are not detectable in EC (data not shown). The high expression of miR-221 is in accordance with a recent study demonstrating that miR-221 may affect the angiogenic properties of endothelial cells by regulating c-kit, the receptor for the cytokine stem cell factor (SCF) (Poliseno et al., 2006). Consistently, c-kit expression was significantly increased in Dicer and Drosha siRNA transfected cells. Moreover, according to other recently published studies miR-126 and miR-130, which has been shown to play a crucial role in angiogenic processes, are highly expressed in endothelial cells (Chen

and Gorski, 2008; Fish et al., 2008; Wang et al., 2008). Thus, the data of the present miRNA array analysis allows to selectively evaluate the function and regulation of endothelial cell-enriched miRNAs in future studies.

Surprisingly, the downregulation of Drosha and Dicer only affects a subset of miRNAs. Based on the assumption that these two enzymes are essential for miRNA processing, one would have expected to see a downregulation of the majority of miRNAs. However, in accordance with our data, others also reported that only a subset of miRNAs is reduced after Dicer downregulation (55% (Cummins et al., 2006) and 15-59% (Giraldez et al., 2005)). The incomplete inhibition of miRNAs might be explained by an insufficient downregulation of the enzymes or a higher stability of some of the miRNAs exceeding the transient effect of Drosha or Dicer downregulation by siRNA. Finally, the data should be interpreted with caution due to the limitation of the miRNA array technology. Although the assays preferentially detect mature miRNAs, the discrimination of pri-, pre- and mature miRNAs requires confirmation by Northern blotting. The low sensitivity of Northern blot, however, limits its general use.

4.1.2 Let-7f and miR-27b are regulated by Dicer and Drosha

Based on the miRNA profiling performed after inhibition of Dicer and Drosha we could identify several miRNAs including the let-7 cluster and miR-27b, which were downregulated by both, Dicer and Drosha knockdown.

Using *in silico* prediction of targets for the highly expressed, and by Drosha and Dicer siRNA downregulated let-7 cluster, we identified several potential interesting genes including thrombospondin-1 (TSP1). TSP1 is a potent endogenous inhibitor of angiogenesis (Iruela-Arispe et al., 1991). Upregulation of TSP1 in endothelial progenitor cells contributes to impaired vasculogenesis in diabetic mice (li et al., 2006). Consistent with a predicted regulatory role of the let-7 cluster for targeting TSP1, Drosha and Dicer silencing augmented TSP1 expression. Given that TSP1 is a potent angiogenesis inhibitor, its upregulation might contribute to the impairment of angiogenesis after Drosha or Dicer downregulation. Because of its most significant downregulation by Dicer and Drosha compared to other let-7 cluster members we selected let-7f for further studies. A let-7f inhibitor, however, increased TSP1

expression only about 15% indicating that other factors (e.g. other let-7 family members) may in part compensate for the loss of let-7f (data not shown).

The angiogenesis suppressive effect of Dicer and Drosha downregulation may in part be related to the augmentation of the angiogenesis inhibitor TSP1. Since a variety of miRNAs are highly expressed and dysregulated by Drosha and/or Dicer siRNA and each miRNA has multiple pro- and anti-angiogenic targets, further studies are required to dissect the complex process of posttranscriptional regulation of gene expression during angiogenesis.

4.2 Regulation and function of miR-92a

4.2.1 The miR-17-92 cluster is highly expressed in EC

As shown in the first part of the study, inhibition of miRNA processing by genetic knockdown of Dicer and Drosha expression impairs endothelial cell functions and angiogenesis (Giraldez et al., 2005; Suarez et al., 2007; Yang et al., 2005) suggesting an important role of miRNAs for endothelial cell biology. Recently, a few miRNAs have been identified to stimulate (let-7f, miR-27b, miR-130 (Chen and Gorski, 2008)) or inhibit (miR-221 and miR-222 (Poliseno et al., 2006)) endothelial sprout formation *in vitro*. Additionally, two recent studies demonstrated the *in vivo* contribution of miR-126, which is highly expressed in endothelial cells, to angiogenic signaling and vascular integrity (Fish et al., 2008; Wang et al., 2008).

In this regard, we mainly focused in the second part of the study on one specific miRNA, miR-92a, and its involvement in endothelial cell function. MiR-92a is a member of the conserved miR-17~92 cluster consisting of miR-17, miR-18a, miR-19a, miR-20a, miR-19b-1 and miR-92a (Ventura et al., 2008), which was shown to be upregulated in tumors (Cerny and Quesenberry, 2004; He et al., 2005; Venturini et al., 2007). Its overexpression in tumor cells promotes tumor angiogenesis (Dews et al., 2006). The oncogenic and pro-angiogenic functions of the miRNAs encoded by the cluster have been attributed to miR-18 and miR-19, which inhibit apoptosis of tumor cells (Ventura et al., 2008; Wang et al., 2008) and promote tumor angiogenesis by suppressing the release of soluble anti-angiogenic factors by tumor cells, thereby affecting endothelial cells in a paracrine manner (Dews et al., 2006).

We selected miR-92a because of the high expression shown in the expression profile, the previously proposed role of the miR-17~92 cluster in tumor angiogenesis, and the several predicted miR-92a targets involved in angiogenic signaling such as Integrin $\alpha 5$, Integrin αv and SIRT1.

4.2.2 miR-92a inhibits angiogenesis *in vitro* and *in vivo*

In contrast to the paracrine pro-angiogenic effects of miR-18 and miR-19 (Dews et al., 2006), two other members of the miR-17-92 cluster, overexpression of the miR-92a using miR-92a precursor (termed pre92) in HUVEC unexpectedly blocks sprout formation in a three-dimensional model of *in vitro* angiogenesis and inhibits vascular network formation in matrigel assays. The development of tubular structures in a spheroid model and matrigel network forming assay depends on several cellular processes, especially migration, proliferation and apoptosis. Indeed, overexpression of miR-92a reduces basal and VEGF-induced EC migration and impairs adhesion to fibronectin. Cytotoxic effects of the pre92 transfection could be excluded by measuring viability and cell proliferation under basal conditions and serum depletion. However, cellular assays reflect only inadequately the complexity of angiogenic processes *in vivo*. In order to reflect the *in vivo* situation, we implanted pre92-transfected HUVEC in matrigel plugs in nude mice. MiR-92a overexpression efficiently blocks the number of invading cells and formation of capillary-like structures observed in matrigel plugs containing control-transfected HUVEC. Additionally, *in vivo* perfused lectin-positive vessels and the hemoglobin content (as a surrogate marker of perfusion) were significantly reduced in the explanted matrigel plugs. These results indicate that overexpression of miR-92a blocks angiogenesis *in vitro* and *in vivo*. Consistent with our findings that overexpression of miR-92a inhibits angiogenesis *in vitro*, downregulation of endothelial miR-92a by 2'-O-methyl antisense oligonucleotides increases sprout formation *in vitro* indicating that inhibition of miR-92a may represent a novel therapeutic strategy to enhance angiogenesis.

4.2.3 MiR-92a is upregulated under ischemic conditions and is efficiently suppressed by antagomir-92a treatment *in vivo*

To block miR-92a expression *in vivo*, we used so-called antagomirs, which are chemically modified antisense oligoribonucleotides developed for inhibition of miRNA expression *in vivo* (Krutzfeldt et al., 2005). Krutzfeldt et al. achieved an almost complete knockdown of miR-122 in all tissues except the brain using an antagomir directed against miR-122 at the concentration of 80 mg/kg bw. Since we were interested in targeting mainly the vasculature, the primary organ taking up substances from the blood, we tested different antagomir concentrations, below the already published concentration of 80 mg/kg, ranging from 1 to 40 mg/kg bw. Injection of 8 mg/kg bw antagomir-92a sufficiently blocks miR-92a expression in heart, spleen, liver and muscle. Moreover, Cy3-labelled antagomir-92a at a concentration of 8 mg/kg mainly targets the vasculature as shown in histological sections. Hence, we choose a concentration of 8 mg/kg for all further *in vivo* studies.

Consistent with the hypothesis that inhibition of miR-92a augments angiogenesis, systemic application of antagomir-92a enhances the number of invading cells and *in vivo* perfused lectin-positive vessels in implanted matrigel plugs. Additionally, it significantly increases perfusion measured by hemoglobin content in matrigel plugs. Extracellular single-stranded RNA can cause increased vascular permeability by mobilizing/stabilizing VEGF and inducing VEGF signaling via the VEGF receptor 2 (Fischer et al., 2007). In order to exclude off-target effects of antagomir-92a treatment, we used two different control antagomirs, both of which having no effect on plug vascularization. Based on the fact that one single miRNA potentially targets several hundred mRNAs in the cell, subsequently dysregulating a global network of genes, we addressed the question, if miR-92a downregulation by antagomir-92a might cause toxic effects in healthy mice. However, no obvious side effects were determined after 8 mg/kg antagomir-92a infusion for two weeks (data not shown). Furthermore, Dr. Olsons group recently presented data showing no toxicity of systemic antagomir treatment up to a concentration of 300 mg/kg in mice (MicroRNA symposium, Cologne, Germany, 6. March 2008), and previous studies have shown that systemic treatment with 3-10 mg/kg LNA-locked anti-miRs are well tolerated in non-human primates (Elmen et al., 2008).

We evaluated the specificity of antagomir-92a treatment by analyzing the expression of various other miRNAs including members of the miR-17~92 cluster and closely related miRNAs such as miR-92b in the hind limb muscle. Antagomir-92a treatment significantly reduces the expression of miR-92a, while not affecting other members of the cluster (miR-18a, miR-19a). Furthermore, it slightly, but non-significantly impairs the expression of the very closely related miR-92b, which only differs from miR-92a by 2 nucleotides. Moreover, miR-24 and miR-93 are not regulated by antagomir-92a. These data demonstrate that antagomir-92a treatment specifically reduces the expression of miR-92a *in vivo* without affecting the expression of other related and non-related miRNAs, thereby increasing vascularization.

We further characterized the physiological role of miR-92a for angiogenic processes by analysing its time-dependent expression in response to ischemia. Given the anti-angiogenic role of miR-92a *in vitro*, it is very astonishing that miR-92a is dramatically upregulated in the ischemic limb at day 1 and 2 after induction of hind limb ischemia. Moreover, miR-18a expressed by the same cluster and thus controlled by the same promoter is upregulated to a lower extent at day 2 and shows another time kinetic of regulation in comparison to miR-92a. This phenomenon might be well explained by the existence of RNA-binding proteins, e.g. hnRNP A1, which expression is required for proper miR-18a processing. HnRNP A1 specifically binds the stem loop of miR-18a in the primary miR-17-92 transcript, therefore enhancing its processing by Drosha (Guil and Caceres, 2007). Furthermore, there is increasing evidence that single proteins can bind to the microprocessor complex, thereby stabilizing/increasing the cropping of pri-miRNA into pre-miRNA without changing the pri-miRNA content (Davis et al., 2008). It is conceivable that proteins, upregulated by hypoxia in ischemic tissue, specifically enhance pri-miR-92a processing while other members of the cluster are not affected. A potential candidate could be HIF-1 α or one of its downstream targets (Wang et al., 1995). However, further experiments need to be performed in order to clarify this issue. Interestingly, ischemia-induced upregulation of miR-92a is completely abrogated 4 days after induction of hind limb ischemia suggesting that factors, highly expressed between day 3 and 4 after induction of ischemia, might downregulate miR-92a. Since it is well-known that VEGF is one of the major pro-angiogenic factors upregulated by ischemia, we investigated the regulation of miR-92a expression by VEGF and another pro-angiogenic factor

bFGF in further detail (data not shown). Surprisingly, low concentrations of VEGF induce a biphasic expression pattern compared to control, upregulate expression of miR-92a at 24 hours, and downregulate miR-92a expression at 48 hours. By contrast high concentrations of VEGF downregulates the expression of miR-92a at both time points (data not shown). In addition and in contrast to VEGF, bFGF increases miR-92a expression at high concentrations indicating that the regulation of miR-92a expression by angiogenic factors is more complex than initially anticipated. As the regulation may not only involve the transcriptional regulation of the miR-17~92 cluster, but also may be influenced by putative effects of growth factor signaling on miR-92a stability, further studies are necessary to evaluate the specific role of growth factor-mediated regulation of miR-92a expression.

4.2.4 Inhibition of miR-92a promotes angiogenesis and functional recovery after ischemia *in vivo*

Based on our findings that miR-92a, which exhibits anti-angiogenic characteristics as shown *in vitro* and *in vivo*, is highly upregulated in the early stage of ischemia, we tested the effect of miR-92a inhibition by antagomir-92a treatment in a model of hind limb ischemia. The intravenous infusion of antagomir-92a immediately after induction of hind limb ischemia leads to a significant reduction in toe necrosis compared to PBS and antagomir-Co treated mice. Consistent with the idea that these effects are due to improved neovascularization of ischemic limbs, the recovery of blood flow is increased by antagomir-92a compared to PBS or control antagomirs. Likewise, the number of capillaries and the number of smooth muscle actin-positive arterioles is increased after antagomir-92a treatment indicating that antagomir-92a improves perfusion and the functional recovery of ischemic limbs. Since we confirmed that antagomir-92a treatment induces a 1.7-fold increase in arterioles after hind limb ischemia, a rescue of necrosis is well conceivable in the context of various published results by others. For instance, eNOS overexpression in mice was shown to increase capillary density to about 1.5-fold at 2 weeks after limb ischemia (Brevetti et al., 2003). Moreover, improvement of angiogenesis by pro-angiogenic growth factors has previously been shown to improve the functional recovery of limbs after ischemia (Li et al., 2005; Lu et al., 2007a). An anti-apoptotic effect by administration of antagomir-

92a might be another reason for the profound functional improvement after ischemia. Although we demonstrate that miR-92a overexpression has no influence on apoptosis or proliferation of EC *in vitro*, it is still unclear to what extent miR-92a affects apoptosis of other cells, particularly myocytes. It is feasible that EC, depleted from miR-92a, exert paracrine factors on surrounding cells, thereby preventing apoptosis. However, further studies are needed, to analyse a potential effect of antagomir-92a treatment on other cell types in more detail.

Neovascularization induced by administration of pro-angiogenic factors has been presented to be a key factor to enhance functional recovery after myocardial infarction (Losordo et al., 1998). To determine the effect of antagomir-92a treatment on functional recovery after acute myocardial infarction, the left coronary artery was occluded and left ventricular (LV) function was determined by Millar catheterization after 14 days. Antagomir-92a treatment improves LV systolic and diastolic function, and significantly reduces enddiastolic pressure and tau (a parameter for the isovolumetric relaxation time) compared to vehicle controls and control antagomir treatment. Furthermore, antagomir-92a treatment reduces the infarct size and significantly augments the number of *in vivo* perfused lectin-positive vessels particularly in the remote and border zone. The increased neovascularization in the border and remote myocardium might additionally prevent negative ventricular remodelling and improve contractile recovery. Antagomir-92a treatment also increased the number of smooth muscle actin positive vessels. Moreover, we determined the number of TUNEL-positive cardiomyocytes at 4 days after induction of myocardial infarction. Cardiomyocyte apoptosis in the infarct and border zone is significantly reduced by antagomir-92a treatment. Considering the notion that we could not detect a direct effect of antagomir-92a on cardiomyocyte apoptosis *in vitro*, the inhibition of cardiomyocyte apoptosis likely reflects an improved neovascularization in part rescuing ischemic tissue in the border zone.

Because miRNAs have multiple targets, and since various cells can be differentially affected depending on their expressed targets, we addressed the question, if the observed improvement in the ischemic models by antagomir-92a is (partially) due to cardiac remodeling, repair and regeneration via affecting non-endothelial cells, such as muscle, interstitial cells and fibroblasts. To study whether antagomir-92a treatment might have direct effects on non-endothelial cell types, we determined the expression

of miR-92a in ischemic hearts by *in situ* hybridization. Interestingly, miR-92a is predominantly expressed in cardiac endothelial cells, whereas only minor expression can be detected in cardiomyocytes. The specificity of the miR-92a probe was evidenced by the reduction of the endothelial miR-92a staining by antagomir-92a treatment. In addition, labelled antagomir-92a was preferentially detected in vessels but not in cardiomyocytes and antagomir-92a treatment does not affect cardiomyocyte apoptosis *in vitro*. These data suggest that the vascular endothelium is likely a key target tissue for the biological actions of antagomir-92a, by neutralizing the anti-angiogenic properties of miR-92a. Though we cannot formally exclude the possibility that antagomir-92a treatment affects alternative cell types during cardiac repair and regeneration, the improved neovascularization and apparent lack of direct effects on cardiomyocytes strongly suggests that enhanced neovascularization, at least in part, explains the cardioprotective properties of antagomir-92a treatment. Therefore, we aim to generate endothelial-restricted miR-92a knockout mice, which will help us to elucidate the function of miR-92a specifically for vascular homeostasis.

4.2.5 MiR-92a effects the expression of a variety of pro-angiogenic genes

Our data raised the question, which downstream targets of miR-92a might be responsible for the observed effects. During the last years, several online available databases based on different algorithms have been developed for reliable prediction of potential miRNA targets (Maziere and Enright, 2007).

Two of the commonly used databases are TargetScan (Grimson et al., 2007) and PicTar (Krek et al., 2005) based on sequence-complementarity of miRNA and target mRNA. The miR-92a targets predicted *in silico* include several regulators of endothelial cell functions and vessel growth, such as the Integrin subunits $\alpha 5$ (Fig. 4.1) and αv , which mediate cell-matrix interactions, anti-apoptotic signaling and cell migration (Francis et al., 2002; Urbich et al., 2002; Yang and Korsmeyer, 1996). Furthermore, other predicted pro-angiogenic targets include the histone deacetylase SIRT1 (Imai et al., 2000; Potente et al., 2007), the small GTP-binding protein RAP1, an angiogenesis-mediating protein involved in Integrin signaling (Chrzanowska-

Wodnicka et al., 2008), the sphingosin-1-phosphate receptor 1 (S1P₁) (Paik et al., 2001), and the mitogen activated kinase kinase 4 (MKK4).

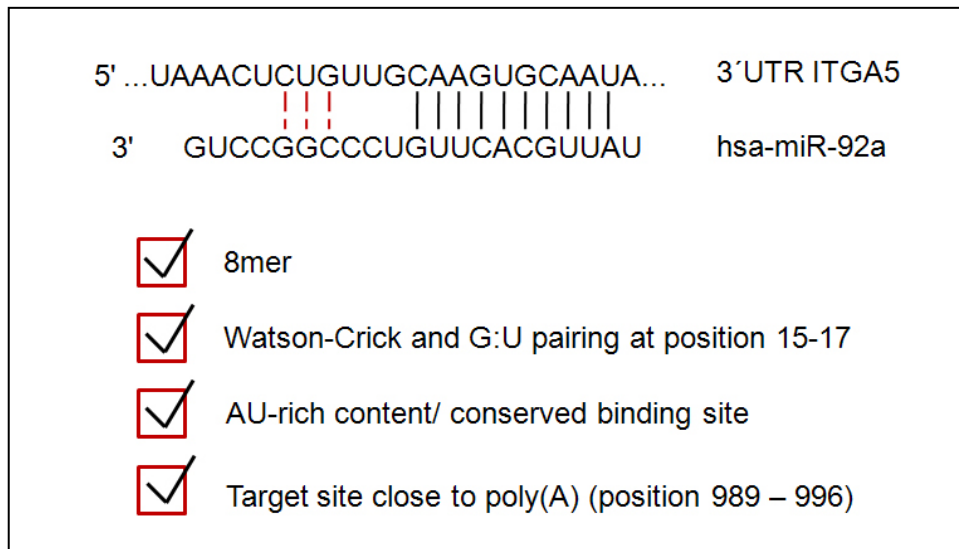


Figure 4.1 Integrin $\alpha 5$ is a predicted target of miR-92a

TargetScan, an online available database, predicts targets based on a specific algorithm. The most important criteria are the sequence complementarity, conservation of binding sites, location within the 3'UTR and target accessibility. Integrin $\alpha 5$ meets all criteria to be a target of miR-92a.

Overexpression of miR-92a in EC causes dysregulation of ~ 7000 genes after 48 h as presented in a microarray expression profile. An explanation for the huge number of dysregulated genes might be the relatively high number of directly regulated miR-92a targets, each in turn involved in different signaling cascades (Fig. 4.2).

Preliminary data suggest that a microarray profiling 24 h after overexpression of miR-92a is more suitable to detect direct miR-92a targets. Integrin $\alpha 5$, belonging to the group of predicted miR-92a target genes, is highly reduced on mRNA level after 24 and 48 h. Moreover, the predicted targets Integrin αv , S1P₁ as well as MKK4 are reduced by overexpression of miR-92a. Accordingly, miR-92a overexpression causes a significant reduction of Integrin $\alpha 5$ protein level. Having shown that antagomir-92a treatment improves neovascularization after ischemia we further investigated, if this effect might be due to increased Integrin $\alpha 5$ expression *in vivo*. Indeed, mRNA and

protein expression of Integrin $\alpha 5$ in muscle is upregulated by administration of antagomir-92a.

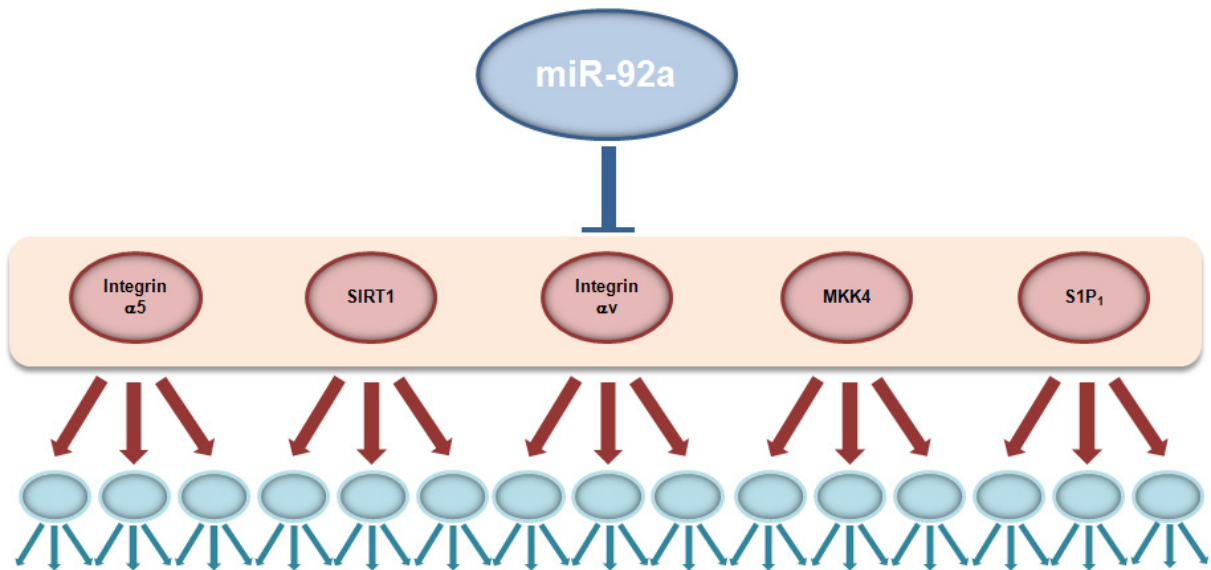


Figure 4.2. miR-92a regulates a whole network of genes

Genes containing one or more miR-92a binding sites in their 3'UTR (potential target genes) are in red. Genes regulated by potential target genes in blue.

In order to clarify, which genes are secondarily regulated in response to Integrin $\alpha 5$ reduction, we performed a second microarray profile after treatment of EC with siRNA targeting Integrin $\alpha 5$. As predicted, several putative direct miR-92a targets such as MKK4 or S1P₁ are not affected by Integrin $\alpha 5$ siRNA. However, a second group of genes, which are downregulated by miR-92a despite the lack of target sequences in their 3'UTR, are also reduced by siRNA against Integrin $\alpha 5$. Hence, these genes might be secondarily regulated as a consequence of Integrin $\alpha 5$ downregulation. The most prominent example is the regulation of endothelial NO-synthase (eNOS), which controls vascular tone and is essential for postnatal neovascularization (Murohara et al., 1998; Palmer et al., 1987). eNOS is downregulated by miR-92a overexpression and Integrin $\alpha 5$ siRNA indicating that eNOS downregulation in response to miR-92a overexpression may occur as a consequence of Integrin $\alpha 5$ mRNA degradation.

However, we are aware that the analysis of mRNA expression gives only limited information about the regulation of potential target genes. Although it has been shown that animal miRNAs can affect mRNA levels either by sharing almost

complete complementarity (Yekta et al., 2004) or also partial base-pairing (Lim et al., 2005) with their target site, they exert their effects largely via post-transcriptional inhibition of protein synthesis (Pillai et al., 2007). Thus, a technique is needed to measure directly genome-wide changes in protein synthesis shortly after changes in miRNA expression. Recently, a new method has been developed to overcome this problem, the stable isotope labeling with amino acids in cell culture (SILAC). Using the SILAC technology, proteins are metabolically labelled by cultivating cells in growth medium containing heavy isotope versions of essential amino acids and subsequently analysed by mass spectrometry (Selbach et al., 2008; Vinther et al., 2006). First data suggest that a miRNA can, either by direct or indirect effects, tune protein synthesis from thousands of genes (Selbach et al., 2008).

On the basis of the crucial role of Integrin $\alpha 5$ in vascular development and angiogenesis (Francis et al., 2002; Yang et al., 1993), we further investigated the direct regulation of Integrin $\alpha 5$ by miR-92a. Cloning of miR-92a seed sequence of the Integrin $\alpha 5$ 3'UTR in a Luciferase reporter construct followed by overexpression of miR-92a demonstrates a direct regulation of Integrin $\alpha 5$ by miR-92a. The specificity of mRNA-miRNA binding was proved using mutated seed sequences.

Demonstrating that Integrin $\alpha 5$ is a direct miR-92a target, we addressed the relevant question, if Integrin $\alpha 5$ contributes to miR-92a-mediated impairment of angiogenesis. Remarkably, inhibition of miR-92a stimulates sprouting of EC *in vitro* only in the presence but not in the absence of Integrin $\alpha 5$, demonstrating that Integrin $\alpha 5$ is a functionally relevant down-stream target of miR-92a in endothelial cells.

5 Conclusion

Dicer and Drosha are the major enzymes involved in microRNA processing. Using siRNA targeting Dicer and Drosha, thereby downregulating a substantial number of microRNAs in EC, we demonstrate a crucial role of both enzymes in angiogenic processes. Interestingly, Dicer inhibition exerts more profound effects on processes like migration and viability of EC in comparison to Drosha inhibition. Moreover, Dicer effects *in vivo* angiogenesis, a process which is unaffected by Drosha. This discrepancy might be partially due to the involvement of Dicer in other cellular processes like heterochromatin formation and to the fact that Dicer and Drosha target mainly different subsets of microRNAs.

In addition, we identified miR-92a as a novel endogenous repressor of the angiogenic program in EC, which impairs their angiogenic functions *in vitro* and *in vivo*. Consistent with these data, blocking miR-92a by systemic infusion of antagomirs enhances neovascularization and functional recovery after ischemia *in vivo*. At first sight, the anti-angiogenic function of miR-92a in EC appears to contradict the previously identified anti-apoptotic and pro-angiogenic activities of the miR-17~92 cluster in tumor cells. However, this apparent discrepancy might be well rationalized by a predominant function of miR-18a and miR-19a in tumor cells, which are responsible for the tumorigenic and non-cell autonomous pro-angiogenic functions of the miR-17~92 cluster (Dews et al., 2006). Instead, miR-92a expression is specifically upregulated in ischemic tissues and appears to cell-autonomously repress the angiogenic potential of EC. Among the various targets and verified regulated genes identified by microarray, we confirmed the downregulation of Integrin $\alpha 5$ *in vitro* and *in vivo*. The relevance of this miR-92a target is evidenced by severe vascular defects in the absence of Integrin $\alpha 5$ (Francis et al., 2002; Yang et al., 1993). In addition, endothelial miR-92a interferes with the expression pattern of genes controlling key EC functions at various levels, some of which, e.g. eNOS, might be secondarily affected by directly targeted genes.

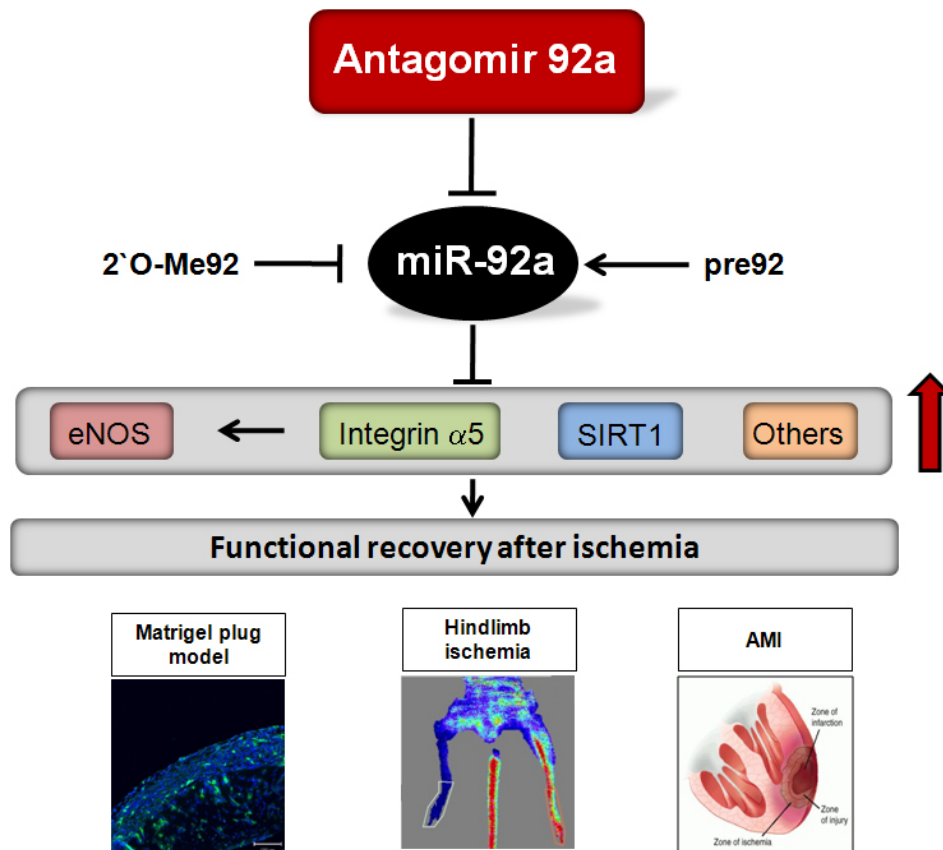


Figure 4.3. Antagomir-92a improves functional recovery after ischemia

Obviously, our data do not formally exclude effects of antagomir-92a on perivascular and other cell types, but surely include effects on EC. Regardless of this, the capacity of miR-92a to target various downstream effectors might be an advantage of miRNA-based therapeutic strategies and may overcome the limited therapeutic capacity of single growth factor or single gene therapies in ischemic diseases, since the highly organized process of vessel growth, maturation and functional maintenance is well known to require the fine-tuned regulation of a set of genes (Fig. 4.3).

6 Zusammenfassung

Angiogenese, die Bildung von Kapillaren aus bereits existierenden Gefäßen, ist ein wichtiger physiologischer Prozess zur Wundheilung und Wiederherstellung des Blutflusses nach Verletzung. Das Ziel der vorliegenden Arbeit war die genaue Untersuchung der Rolle von microRNAs in angiogenen Prozessen.

MicroRNAs sind kleine, einzelsträngige RNA Moleküle, welche die Genexpression durch Bindung an die messenger RNA (mRNA) von Zielgenen und darauffolgenden Degradierung der mRNA oder Repression der Translation regulieren. Die Inhibition der microRNA-prozessierenden Enzyme Dicer und Drosha in Endothelzellen führt zu einer Dysregulation der microRNA Expression und zu einer signifikanten Reduktion der Angiogenese *in vitro*. Im Gegensatz zu Drosha, dessen Inhibition keinen Effekt auf die *in vivo* Angiogenese zeigt, führt die Inhibition von Dicer auch in einem *in vivo* Angiogenese-Modell zu einer deutliche reduzierten Einsprossung von Gefäßen. Zusammenfassend sprechen diese Daten für eine wichtige Rolle von microRNAs in der Endothelzellbiologie.

Der zweite Teil der vorliegenden Arbeit beschränkte sich auf die Untersuchung einer, in Endothelzellen hoch exprimierten microRNA, miR-92a. MiR-92a ist ein Mitglied des miR-17-92 Clusters, für den bereits eine Rolle in der Tumorangioenese beschrieben ist. Die Überexpression der miR-92a in Endothelzellen führt zu einer signifikanten Hemmung der Angiogenese, sowie reduzierter Adhäsion und Migration auf Fibronectin. Zudem wird die Einsprossung von Gefäßen in Matrigel Plugs deutlich gehemmt. In Übereinstimmung hierzu führt die systemische Hemmung der miR-92a mit Hilfe von modifizierten antisense Oligoribonukleotiden (Antagomir-92a) im Mausmodell zu einer Stimulation der Einsprossung von Gefäßen in Matrigel Plugs. In klinisch relevanten Modellen, wie dem Hinterlaufischämie-Modell und dem akuten Myokardinfarkt-Modell, führt die Behandlung mit Antagomir-92a zu einer funktionelle Verbesserung. Immunohistologische Analysen ergaben, dass in den Antagomir-92a behandelten Tieren sowohl die Anzahl der Kapillaren als auch der größeren Gefäße deutlich erhöht ist. Obwohl wir einen direkten Effekt der Antagomir-92a Behandlung auf die Myozyten zum jetzigen Zeitpunkt nicht ausschließen können, weisen unsere Daten definitiv auf eine Stimulation der Angiogenese hin.

Nachdem wir sowohl *in vitro* als auch *in vivo* zeigen konnten, dass miR-92a maßgeblich an angiogenen Prozessen beteiligt ist, stellten wir uns die Frage nach den zugrunde liegenden Zielgenen. Es zeigte sich, dass miR-92a neben einer größeren Anzahl pro-angiogener Faktoren die Integrin Untereinheit $\alpha 5$ sowohl *in vitro* als auch *in vivo* reguliert. Desweiteren konnten wir mit Hilfe eines Luciferase Assays die direkte Regulation von Integrin $\alpha 5$ durch miR-92a zeigen.

Zusammenfassend deuten diese Daten daraufhin, dass Integrin $\alpha 5$ ein Schlüsselregulator der Antagomir-92a-vermittelten Angiogenese ist und somit unmittelbar an der Verbesserung nach Hinterlaufischämie und akutem Myokardinfarkt beteiligt ist.

7 Abbreviations

bFGF	Basic fibroblast growth factor
bp	Base pairs
BrdU	Bromodeoxyuridine
BSA	Bovine serum albumin
bw	body weight
CAD	Coronary artery disease
CAM	Cell adhesion molecules
cDNA	complementary DNA
Co	Control
CTGF	Connective tissue growth factor
CM-Dil	Chloromethylbenzamido derivative of Dil
Cy3	Carbocyanine
DAPI	4',6-diamidino-2-phenylindole
DIG	Digoxigenin
DTT	Dithiothreitol
DNA	Desoxyribonucleic acid
eNOS	endothelial NO synthase
EC	Endothelial cells
EBM	Endothelial basal medium
FACS	Fluorescence-activated cell sorting
FCS	Fetal calf serum
FITC	Fluorescein isothiocyanate
FLT1	VEGF receptor 1
g	grams or g force
GAPDH	Glyceraldehyde-3-phosphate dehydrogenase
H&E stain	hematoxylin and eosin stain
HAF	Human aortic adventitial fibroblasts
HCl	Hydrochloric acid
HCM	Human cardiac myocytes
HEK293	Human embryonal kidney epithelial cells
HMVEC	Human microvascular endothelial cells

HUVEC	Human umbilical vein endothelial cells
<i>i.v.</i>	intra venous
Kb	Kilobase
kDa	Kilodalton
KDR	VEGF receptor 2
LNA	Locked nucleic acids
LV	Left ventricular
miR	microRNA
MKK4	Mitogen-activated kinase kinase 4
mRNA	messenger RNA
n	Number of experiments
n.s.	Not significant
NO	Nitric oxide
OD	Optical density
PBS	Phosphate buffered saline
PMSF	Phenylmethylsulfonylfluorid
RISC	RNA-induced silencing complex
RNA	Ribonucleic acid
RT	Room temperature or reverse transcription
SDS	Sodium dodecyl sulfate
SEM	Standard error of the mean
siRNA	Small interfering RNA
SIRT1	Sirtuin 1
SMC	Human aortic smooth muscle cells
TIE1	Tyrosine kinase receptor 1
TNF	Tumor necrosis factor
TSP1	Thrombospondin 1
TUNEL	Terminal deoxynucleotidyl transferase-mediated uridine 5'-triphosphate-biotin nick end-labeling
UTR	Untranslated region
VEGF	Vascular endothelial growth factor
vWF	von-Willbrand factor
Wt	Wildtype

8 Bibliography

Amaral, P.P., Dinger, M.E., Mercer, T.R., and Mattick, J.S. (2008). The eukaryotic genome as an RNA machine. *Science* **319**, 1787-1789.

Bartel, D.P. (2004). MicroRNAs: genomics, biogenesis, mechanism, and function. *Cell* **116**, 281-297.

Bernstein, E., Caudy, A.A., Hammond, S.M., and Hannon, G.J. (2001). Role for a bidentate ribonuclease in the initiation step of RNA interference. *Nature* **409**, 363-366.

Bhattacharyya, S.N., Habermacher, R., Martine, U., Closs, E.I., and Filipowicz, W. (2006). Relief of microRNA-mediated translational repression in human cells subjected to stress. *Cell* **125**, 1111-1124.

Brevetti, L.S., Chang, D.S., Tang, G.L., Sarkar, R., and Messina, L.M. (2003). Overexpression of endothelial nitric oxide synthase increases skeletal muscle blood flow and oxygenation in severe rat hind limb ischemia. *J Vasc Surg* **38**, 820-826.

Buhler, M., and Moazed, D. (2007). Transcription and RNAi in heterochromatic gene silencing. *Nat Struct Mol Biol* **14**, 1041-1048.

Care, A., Catalucci, D., Felicetti, F., Bonci, D., Addario, A., Gallo, P., Bang, M.L., Segnalini, P., Gu, Y., Dalton, N.D., *et al.* (2007). MicroRNA-133 controls cardiac hypertrophy. *Nat Med* **13**, 613-618.

Carmeliet, P. (2000). Mechanisms of angiogenesis and arteriogenesis. *Nat Med* **6**, 389-395.

Carmeliet, P. (2005). Angiogenesis in life, disease and medicine. *Nature* **438**, 932-936.

Cerny, J., and Quesenberry, P.J. (2004). Chromatin remodeling and stem cell theory of relativity. *J Cell Physiol* **201**, 1-16.

Chen, C.Z., Li, L., Lodish, H.F., and Bartel, D.P. (2004). MicroRNAs modulate hematopoietic lineage differentiation. *Science* **303**, 83-86.

Chen, J.F., Mandel, E.M., Thomson, J.M., Wu, Q., Callis, T.E., Hammond, S.M., Conlon, F.L., and Wang, D.Z. (2006). The role of microRNA-1 and microRNA-133 in skeletal muscle proliferation and differentiation. *Nat Genet* **38**, 228-233.

Chen, J.F., Murchison, E.P., Tang, R., Callis, T.E., Tatsuguchi, M., Deng, Z., Rojas, M., Hammond, S.M., Schneider, M.D., Selzman, C.H., *et al.* (2008). Targeted deletion of Dicer in the heart leads to dilated cardiomyopathy and heart failure. *Proc Natl Acad Sci U S A* **105**, 2111-2116.

Chen, Y., and Gorski, D.H. (2008). Regulation of angiogenesis through a microRNA (miR-130a) that down-regulates antiangiogenic homeobox genes GAX and HOXA5. *Blood* **111**, 1217-1226.

Chrzanowska-Wodnicka, M., Kraus, A.E., Gale, D., White, G.C., 2nd, and Vansluys, J. (2008). Defective angiogenesis, endothelial migration, proliferation, and MAPK signaling in Rap1b-deficient mice. *Blood* **111**, 2647-2656.

Cimmino, A., Calin, G.A., Fabbri, M., Iorio, M.V., Ferracin, M., Shimizu, M., Wojcik, S.E., Aqeilan, R.I., Zupo, S., Dono, M., *et al.* (2005). miR-15 and miR-16 induce apoptosis by targeting BCL2. *Proc Natl Acad Sci U S A* **102**, 13944-13949.

Cobb, B.S., Hertweck, A., Smith, J., O'Connor, E., Graf, D., Cook, T., Smale, S.T., Sakaguchi, S., Livesey, F.J., Fisher, A.G., *et al.* (2006). A role for Dicer in immune regulation. *J Exp Med* **203**, 2519-2527.

Cullen, B.R. (2006). Viruses and microRNAs. *Nat Genet* **38 Suppl**, S25-30.

Cummins, J.M., He, Y., Leary, R.J., Pagliarini, R., Diaz, L.A., Jr., Sjoblom, T., Barad, O., Bentwich, Z., Szafranska, A.E., Labourier, E., *et al.* (2006). The colorectal microRNAome. *Proc Natl Acad Sci U S A* **103**, 3687-3692.

Davis, B.N., Hilyard, A.C., Lagna, G., and Hata, A. (2008). SMAD proteins control DROSHA-mediated microRNA maturation. *Nature* 454, 56-61.

Dews, M., Homayouni, A., Yu, D., Murphy, D., Sevignani, C., Wentzel, E., Furth, E.E., Lee, W.M., Enders, G.H., Mendell, J.T., *et al.* (2006). Augmentation of tumor angiogenesis by a Myc-activated microRNA cluster. *Nat Genet* 38, 1060-1065.

Dhanabal, M., Wu, F., Alvarez, E., McQueeney, K.D., Jeffers, M., MacDougall, J., Boldog, F.L., Hackett, C., Shenoy, S., Khramtsov, N., *et al.* (2005). Recombinant semaphorin 6A-1 ectodomain inhibits in vivo growth factor and tumor cell line-induced angiogenesis. *Cancer Biol Ther* 4, 659-668.

Diehl, F., Rossig, L., Zeiher, A.M., Dimmeler, S., and Urbich, C. (2006). The histone methyltransferase MLL is an upstream regulator of endothelial cell sprout formation. *Blood*.

Dimmeler, S., and Zeiher, A.M. (2000). Akt takes center stage in angiogenesis signaling. *Circ Res* 86, 4-5.

Elmen, J., Lindow, M., Schutz, S., Lawrence, M., Petri, A., Obad, S., Lindholm, M., Hedtjarn, M., Hansen, H.F., Berger, U., *et al.* (2008). LNA-mediated microRNA silencing in non-human primates. *Nature* 452, 896-899.

Esquela-Kerscher, A., and Slack, F.J. (2006). Oncomirs - microRNAs with a role in cancer. *Nat Rev Cancer* 6, 259-269.

Eulalio, A., Huntzinger, E., and Izaurralde, E. (2008). Getting to the root of miRNA-mediated gene silencing. *Cell* 132, 9-14.

Felli, N., Fontana, L., Pelosi, E., Botta, R., Bonci, D., Facchiano, F., Liuzzi, F., Lulli, V., Morsilli, O., Santoro, S., *et al.* (2005). MicroRNAs 221 and 222 inhibit normal erythropoiesis and erythroleukemic cell growth via kit receptor down-modulation. *Proc Natl Acad Sci U S A* 102, 18081-18086.

Ferrara, N., and Davis-Smyth, T. (1997). The biology of vascular endothelial growth factor. *Endocr Rev* 18, 4-25.

Fischer, S., Gerriets, T., Wessels, C., Walberer, M., Kostin, S., Stolz, E., Zheleva, K., Hocke, A., Hippenstiel, S., and Preissner, K.T. (2007). Extracellular RNA mediates endothelial-cell permeability via vascular endothelial growth factor. *Blood* 110, 2457-2465.

Fish, J.E., Santoro, M.M., Morton, S.U., Yu, S., Yeh, R.F., Wythe, J.D., Ivey, K.N., Bruneau, B.G., Stainier, D.Y., and Srivastava, D. (2008). miR-126 regulates angiogenic signaling and vascular integrity. *Dev Cell* 15, 272-284.

Francis, S.E., Goh, K.L., Hodivala-Dilke, K., Bader, B.L., Stark, M., Davidson, D., and Hynes, R.O. (2002). Central roles of alpha5beta1 integrin and fibronectin in vascular development in mouse embryos and embryoid bodies. *Arterioscler Thromb Vasc Biol* 22, 927-933.

Fukumura, D., Kashiwagi, S., and Jain, R.K. (2006). The role of nitric oxide in tumour progression. *Nat Rev Cancer* 6, 521-534.

Fukumura, D., Xavier, R., Sugiura, T., Chen, Y., Park, E.C., Lu, N., Selig, M., Nielsen, G., Taksir, T., Jain, R.K., *et al.* (1998). Tumor induction of VEGF promoter activity in stromal cells. *Cell* 94, 715-725.

Gale, N.W., and Yancopoulos, G.D. (1999). Growth factors acting via endothelial cell-specific receptor tyrosine kinases: VEGFs, angiopoietins, and ephrins in vascular development. *Genes Dev* 13, 1055-1066.

Giraldez, A.J., Cinalli, R.M., Glasner, M.E., Enright, A.J., Thomson, J.M., Baskerville, S., Hammond, S.M., Bartel, D.P., and Schier, A.F. (2005). MicroRNAs regulate brain morphogenesis in zebrafish. *Science* 308, 833-838.

Grimson, A., Farh, K.K., Johnston, W.K., Garrett-Engele, P., Lim, L.P., and Bartel, D.P. (2007). MicroRNA targeting specificity in mammals: determinants beyond seed pairing. *Mol Cell* 27, 91-105.

Grishok, A., Pasquinelli, A.E., Conte, D., Li, N., Parrish, S., Ha, I., Baillie, D.L., Fire, A., Ruvkun, G., and Mello, C.C. (2001). Genes and mechanisms related to RNA interference regulate expression of the small temporal RNAs that control *C. elegans* developmental timing. *Cell* 106, 23-34.

Guil, S., and Caceres, J.F. (2007). The multifunctional RNA-binding protein hnRNP A1 is required for processing of miR-18a. *Nat Struct Mol Biol* 14, 591-596.

Hammond, S.M., Boettcher, S., Caudy, A.A., Kobayashi, R., and Hannon, G.J. (2001). Argonaute2, a link between genetic and biochemical analyses of RNAi. *Science* 293, 1146-1150.

Harris, T.A., Yamakuchi, M., Ferlito, M., Mendell, J.T., and Lowenstein, C.J. (2008). MicroRNA-126 regulates endothelial expression of vascular cell adhesion molecule 1. *Proc Natl Acad Sci U S A* 105, 1516-1521.

He, L., Thomson, J.M., Hemann, M.T., Hernando-Monge, E., Mu, D., Goodson, S., Powers, S., Cordon-Cardo, C., Lowe, S.W., Hannon, G.J., *et al.* (2005). A microRNA polycistron as a potential human oncogene. *Nature* 435, 828-833.

Hebert, S.S., Horre, K., Nicolai, L., Papadopoulou, A.S., Mandemakers, W., Silahdaroglu, A.N., Kauppinen, S., Delacourte, A., and De Strooper, B. (2008). Loss of microRNA cluster miR-29a/b-1 in sporadic Alzheimer's disease correlates with increased BACE1/beta-secretase expression. *Proc Natl Acad Sci U S A* 105, 6415-6420.

Hirata, Y., Yoshimi, H., Takata, S., Watanabe, T.X., Kumagai, S., Nakajima, K., and Sakakibara, S. (1988). Cellular mechanism of action by a novel vasoconstrictor endothelin in cultured rat vascular smooth muscle cells. *Biochem Biophys Res Commun* 154, 868-875.

Hua, Z., Lv, Q., Ye, W., Wong, C.K., Cai, G., Gu, D., Ji, Y., Zhao, C., Wang, J., Yang, B.B., *et al.* (2006). MiRNA-directed regulation of VEGF and other angiogenic factors under hypoxia. *PLoS ONE* 1, e116.

Ignarro, L.J., Buga, G.M., Wood, K.S., Byrns, R.E., and Chaudhuri, G. (1987). Endothelium-derived relaxing factor produced and released from artery and vein is nitric oxide. *Proc Natl Acad Sci U S A* 84, 9265-9269.

Li, M., Takenaka, H., Asai, J., Ibusuki, K., Mizukami, Y., Maruyama, K., Yoon, Y.S., Wecker, A., Luedemann, C., Eaton, E., *et al.* (2006). Endothelial progenitor thrombospondin-1 mediates diabetes-induced delay in reendothelialization following arterial injury. *Circ Res* 98, 697-704.

Imai, S., Armstrong, C.M., Kaeberlein, M., and Guarente, L. (2000). Transcriptional silencing and longevity protein Sir2 is an NAD-dependent histone deacetylase. *Nature* 403, 795-800.

Iruela-Arispe, M.L., Bornstein, P., and Sage, H. (1991). Thrombospondin exerts an antiangiogenic effect on cord formation by endothelial cells in vitro. *Proc Natl Acad Sci U S A* 88, 5026-5030.

Jain, R.K. (2003). Molecular regulation of vessel maturation. *Nat Med* 9, 685-693.

Kamei, M., Saunders, W.B., Bayless, K.J., Dye, L., Davis, G.E., and Weinstein, B.M. (2006). Endothelial tubes assemble from intracellular vacuoles in vivo. *Nature* 442, 453-456.

Kawahara, Y., Zinshteyn, B., Sethupathy, P., Iizasa, H., Hatzigeorgiou, A.G., and Nishikura, K. (2007). Redirection of silencing targets by adenosine-to-inosine editing of miRNAs. *Science* 315, 1137-1140.

Kim, J., Inoue, K., Ishii, J., Vanti, W.B., Voronov, S.V., Murchison, E., Hannon, G., and Abeliovich, A. (2007). A MicroRNA feedback circuit in midbrain dopamine neurons. *Science* 317, 1220-1224.

Kim, K.J., Li, B., Winer, J., Armanini, M., Gillett, N., Phillips, H.S., and Ferrara, N. (1993). Inhibition of vascular endothelial growth factor-induced angiogenesis suppresses tumour growth in vivo. *Nature* 362, 841-844.

Knight, S.W., and Bass, B.L. (2002). The role of RNA editing by ADARs in RNAi. *Mol Cell* 10, 809-817.

Kobayashi, T., Lu, J., Cobb, B.S., Rodda, S.J., McMahon, A.P., Schipani, E., Merckenschlager, M., and Kronenberg, H.M. (2008). Dicer-dependent pathways regulate chondrocyte proliferation and differentiation. *Proc Natl Acad Sci U S A* 105, 1949-1954.

Komuro, I., Kurihara, H., Sugiyama, T., Yoshizumi, M., Takaku, F., and Yazaki, Y. (1988). Endothelin stimulates c-fos and c-myc expression and proliferation of vascular smooth muscle cells. *FEBS Lett* 238, 249-252.

Korff, T., and Augustin, H.G. (1998). Integration of endothelial cells in multicellular spheroids prevents apoptosis and induces differentiation. *J Cell Biol* 143, 1341-1352.

Krek, A., Grun, D., Poy, M.N., Wolf, R., Rosenberg, L., Epstein, E.J., MacMenamin, P., da Piedade, I., Gunsalus, K.C., Stoffel, M., *et al.* (2005). Combinatorial microRNA target predictions. *Nat Genet* 37, 495-500.

Krutzfeldt, J., Rajewsky, N., Braich, R., Rajeev, K.G., Tuschl, T., Manoharan, M., and Stoffel, M. (2005). Silencing of microRNAs in vivo with 'antagomirs'. *Nature* 438, 685-689.

Kuwabara, T., Hsieh, J., Nakashima, K., Taira, K., and Gage, F.H. (2004). A small modulatory dsRNA specifies the fate of adult neural stem cells. *Cell* 116, 779-793.

Lagos-Quintana, M., Rauhut, R., Lendeckel, W., and Tuschl, T. (2001). Identification of novel genes coding for small expressed RNAs. *Science* 294, 853-858.

Lau, N.C., Lim, L.P., Weinstein, E.G., and Bartel, D.P. (2001). An abundant class of tiny RNAs with probable regulatory roles in *Caenorhabditis elegans*. *Science* 294, 858-862.

le Sage, C., Nagel, R., Egan, D.A., Schrier, M., Mesman, E., Mangiola, A., Anile, C., Maira, G., Mercatelli, N., Ciafre, S.A., *et al.* (2007). Regulation of the p27(Kip1) tumor

suppressor by miR-221 and miR-222 promotes cancer cell proliferation. *Embo J* 26, 3699-3708.

Lee, R.C., and Ambros, V. (2001). An extensive class of small RNAs in *Caenorhabditis elegans*. *Science* 294, 862-864.

Lee, R.C., Feinbaum, R.L., and Ambros, V. (1993). The *C. elegans* heterochronic gene *lin-4* encodes small RNAs with antisense complementarity to *lin-14*. *Cell* 75, 843-854.

Lee, Y., Ahn, C., Han, J., Choi, H., Kim, J., Yim, J., Lee, J., Provost, P., Radmark, O., Kim, S., *et al.* (2003). The nuclear RNase III Drosha initiates microRNA processing. *Nature* 425, 415-419.

Lehmann, U., Hasemeier, B., Christgen, M., Muller, M., Romermann, D., Langer, F., and Kreipe, H. (2008). Epigenetic inactivation of microRNA gene *hsa-mir-9-1* in human breast cancer. *J Pathol* 214, 17-24.

Li, X., Tjwa, M., Moons, L., Fons, P., Noel, A., Ny, A., Zhou, J.M., Lennartsson, J., Li, H., Lutun, A., *et al.* (2005). Revascularization of ischemic tissues by PDGF-CC via effects on endothelial cells and their progenitors. *J Clin Invest* 115, 118-127.

Lim, L.P., Lau, N.C., Garrett-Engele, P., Grimson, A., Schelter, J.M., Castle, J., Bartel, D.P., Linsley, P.S., and Johnson, J.M. (2005). Microarray analysis shows that some microRNAs downregulate large numbers of target mRNAs. *Nature* 433, 769-773.

Linsley, P.S., Schelter, J., Burchard, J., Kibukawa, M., Martin, M.M., Bartz, S.R., Johnson, J.M., Cummins, J.M., Raymond, C.K., Dai, H., *et al.* (2007). Transcripts targeted by the microRNA-16 family cooperatively regulate cell cycle progression. *Mol Cell Biol* 27, 2240-2252.

Losordo, D.W., Vale, P.R., Symes, J.F., Dunnington, C.H., Esakof, D.D., Maysky, M., Ashare, A.B., Lathi, K., and Isner, J.M. (1998). Gene therapy for myocardial

angiogenesis: initial clinical results with direct myocardial injection of phVEGF165 as sole therapy for myocardial ischemia. *Circulation* 98, 2800-2804.

Lu, H., Xu, X., Zhang, M., Cao, R., Brakenhielm, E., Li, C., Lin, H., Yao, G., Sun, H., Qi, L., *et al.* (2007a). Combinatorial protein therapy of angiogenic and arteriogenic factors remarkably improves collateralogenesis and cardiac function in pigs. *Proc Natl Acad Sci U S A* 104, 12140-12145.

Lu, Y., Thomson, J.M., Wong, H.Y., Hammond, S.M., and Hogan, B.L. (2007b). Transgenic over-expression of the microRNA miR-17-92 cluster promotes proliferation and inhibits differentiation of lung epithelial progenitor cells. *Dev Biol* 310, 442-453.

Lund, E., Guttinger, S., Calado, A., Dahlberg, J.E., and Kutay, U. (2004). Nuclear export of microRNA precursors. *Science* 303, 95-98.

Maziere, P., and Enright, A.J. (2007). Prediction of microRNA targets. *Drug Discov Today* 12, 452-458.

Murohara, T., Asahara, T., Silver, M., Bauters, C., Masuda, H., Kalka, C., Kearney, M., Chen, D., Symes, J.F., Fishman, M.C., *et al.* (1998). Nitric oxide synthase modulates angiogenesis in response to tissue ischemia. *J Clin Invest* 101, 2567-2578.

Obernosterer, G., Martinez, J., and Alenius, M. (2007). Locked nucleic acid-based in situ detection of microRNAs in mouse tissue sections. *Nat Protoc* 2, 1508-1514.

Okamura, K., Hagen, J.W., Duan, H., Tyler, D.M., and Lai, E.C. (2007). The Mirtron Pathway Generates microRNA-Class Regulatory RNAs in *Drosophila*. *Cell* 130, 89-100.

Paik, J.H., Chae, S., Lee, M.J., Thangada, S., and Hla, T. (2001). Sphingosine 1-phosphate-induced endothelial cell migration requires the expression of EDG-1 and EDG-3 receptors and Rho-dependent activation of alpha vbeta3- and beta1-containing integrins. *J Biol Chem* 276, 11830-11837.

Palmer, R.M., Ferrige, A.G., and Moncada, S. (1987). Nitric oxide release accounts for the biological activity of endothelium-derived relaxing factor. *Nature* 327, 524-526.

Patarroyo, M., and Makgoba, M.W. (1989). Leucocyte adhesion to cells in immune and inflammatory responses. *Lancet* 2, 1139-1142.

Patten, R.D., Aronovitz, M.J., Deras-Mejia, L., Pandian, N.G., Hanak, G.G., Smith, J.J., Mendelsohn, M.E., and Konstam, M.A. (1998). Ventricular remodeling in a mouse model of myocardial infarction. *Am J Physiol* 274, H1812-1820.

Pillai, R.S., Bhattacharyya, S.N., and Filipowicz, W. (2007). Repression of protein synthesis by miRNAs: how many mechanisms? *Trends Cell Biol* 17, 118-126.

Place, R.F., Li, L.C., Pookot, D., Noonan, E.J., and Dahiya, R. (2008). MicroRNA-373 induces expression of genes with complementary promoter sequences. *Proc Natl Acad Sci U S A* 105, 1608-1613.

Poliseno, L., Tuccoli, A., Mariani, L., Evangelista, M., Citti, L., Woods, K., Mercatanti, A., Hammond, S., and Rainaldi, G. (2006). MicroRNAs modulate the angiogenic properties of HUVECs. *Blood* 108, 3068-3071.

Potente, M., Ghaeni, L., Baldessari, D., Mostoslavsky, R., Rossig, L., Dequiedt, F., Haendeler, J., Mione, M., Dejana, E., Alt, F.W., *et al.* (2007). SIRT1 controls endothelial angiogenic functions during vascular growth. *Genes Dev* 21, 2644-2658.

Potente, M., Urbich, C., Sasaki, K., Hofmann, W.K., Heeschen, C., Aicher, A., Kollipara, R., DePinho, R.A., Zeiher, A.M., and Dimmeler, S. (2005). Involvement of FoxO transcription factors in angiogenesis and postnatal neovascularization. *J Clin Invest* *in press*.

Rinn, J.L., Kertesz, M., Wang, J.K., Squazzo, S.L., Xu, X., Brugmann, S.A., Goodnough, L.H., Helms, J.A., Farnham, P.J., Segal, E., *et al.* (2007). Functional demarcation of active and silent chromatin domains in human HOX loci by noncoding RNAs. *Cell* 129, 1311-1323.

Ruby, J.G., Jan, C.H., and Bartel, D.P. (2007). Intronic microRNA precursors that bypass Drosha processing. *Nature* 448, 83-86.

Saito, Y., Liang, G., Egger, G., Friedman, J.M., Chuang, J.C., Coetzee, G.A., and Jones, P.A. (2006). Specific activation of microRNA-127 with downregulation of the proto-oncogene BCL6 by chromatin-modifying drugs in human cancer cells. *Cancer Cell* 9, 435-443.

Salven, P., Ruotsalainen, T., Mattson, K., and Joensuu, H. (1998). High pre-treatment serum level of vascular endothelial growth factor (VEGF) is associated with poor outcome in small-cell lung cancer. *Int J Cancer* 79, 144-146.

Sato, Y. (2001). Current understanding of the biology of vascular endothelium. *Cell Struct Funct* 26, 9-10.

Schaefer, A., O'Carroll, D., Tan, C.L., Hillman, D., Sugimori, M., Llinas, R., and Greengard, P. (2007). Cerebellar neurodegeneration in the absence of microRNAs. *J Exp Med* 204, 1553-1558.

Selbach, M., Schwanhausser, B., Thierfelder, N., Fang, Z., Khanin, R., and Rajewsky, N. (2008). Widespread changes in protein synthesis induced by microRNAs. *Nature* 455, 58-63.

Sempere, L.F., Freemantle, S., Pitha-Rowe, I., Moss, E., Dmitrovsky, E., and Ambros, V. (2004). Expression profiling of mammalian microRNAs uncovers a subset of brain-expressed microRNAs with possible roles in murine and human neuronal differentiation. *Genome Biol* 5, R13.

Silvestre, J.S., Mallat, Z., Tedgui, A., and Levy, B.I. (2008). Post-ischaemic neovascularization and inflammation. *Cardiovasc Res* 78, 242-249.

Simons, M. (2005). Angiogenesis: where do we stand now? *Circulation* 111, 1556-1566.

Suarez, Y., Fernandez-Hernando, C., Pober, J.S., and Sessa, W.C. (2007). Dicer dependent microRNAs regulate gene expression and functions in human endothelial cells. *Circ Res* 100, 1164-1173.

Thomson, J.M., Parker, J., Perou, C.M., and Hammond, S.M. (2004). A custom microarray platform for analysis of microRNA gene expression. *Nat Methods* 1, 47-53.

Urbich, C., Dernbach, E., Reissner, A., Vasa, M., Zeiher, A.M., and Dimmeler, S. (2002). Shear stress-induced endothelial cell migration involves integrin signaling via the fibronectin receptor subunits alpha(5) and beta(1). *Arterioscler Thromb Vasc Biol* 22, 69-75.

van Rooij, E., Sutherland, L.B., Liu, N., Williams, A.H., McAnally, J., Gerard, R.D., Richardson, J.A., and Olson, E.N. (2006). A signature pattern of stress-responsive microRNAs that can evoke cardiac hypertrophy and heart failure. *Proc Natl Acad Sci U S A* 103, 18255-18260.

van Rooij, E., Sutherland, L.B., Qi, X., Richardson, J.A., Hill, J., and Olson, E.N. (2007). Control of stress-dependent cardiac growth and gene expression by a microRNA. *Science* 316, 575-579.

Varkonyi-Gasic, E., Wu, R., Wood, M., Walton, E.F., and Hellens, R.P. (2007). Protocol: a highly sensitive RT-PCR method for detection and quantification of microRNAs. *Plant Methods* 3, 12.

Ventura, A., Young, A.G., Winslow, M.M., Lintault, L., Meissner, A., Erkeland, S.J., Newman, J., Bronson, R.T., Crowley, D., Stone, J.R., *et al.* (2008). Targeted deletion reveals essential and overlapping functions of the miR-17 through 92 family of miRNA clusters. *Cell* 132, 875-886.

Venturini, L., Battmer, K., Castoldi, M., Schultheis, B., Hochhaus, A., Muckenthaler, M.U., Ganser, A., Eder, M., and Scherr, M. (2007). Expression of the miR-17-92 polycistron in chronic myeloid leukemia (CML) CD34+ cells. *Blood* 109, 4399-4405.

- Vinther, J., Hedegaard, M.M., Gardner, P.P., Andersen, J.S., and Arctander, P. (2006). Identification of miRNA targets with stable isotope labeling by amino acids in cell culture. *Nucleic Acids Res* 34, e107.
- Viswanathan, S.R., Daley, G.Q., and Gregory, R.I. (2008). Selective blockade of microRNA processing by Lin28. *Science* 320, 97-100.
- Volpe, T.A., Kidner, C., Hall, I.M., Teng, G., Grewal, S.I., and Martienssen, R.A. (2002). Regulation of heterochromatic silencing and histone H3 lysine-9 methylation by RNAi. *Science* 297, 1833-1837.
- Wang, G.L., Jiang, B.H., Rue, E.A., and Semenza, G.L. (1995). Hypoxia-inducible factor 1 is a basic-helix-loop-helix-PAS heterodimer regulated by cellular O₂ tension. *Proc Natl Acad Sci U S A* 92, 5510-5514.
- Wang, Q.L., and Li, Z.H. (2007). The functions of microRNAs in plants. *Front Biosci* 12, 3975-3982.
- Wang, S., Aurora, A.B., Johnson, B.A., Qi, X., McAnally, J., Hill, J.A., Richardson, J.A., Bassel-Duby, R., and Olson, E.N. (2008). The endothelial-specific microRNA miR-126 governs vascular integrity and angiogenesis. *Dev Cell* 15, 261-271.
- Weber, B., Stresmann, C., Brueckner, B., and Lyko, F. (2007). Methylation of human microRNA genes in normal and neoplastic cells. *Cell Cycle* 6, 1001-1005.
- Wienholds, E., Kloosterman, W.P., Miska, E., Alvarez-Saavedra, E., Berezikov, E., de Bruijn, E., Horvitz, H.R., Kauppinen, S., and Plasterk, R.H. (2005). MicroRNA expression in zebrafish embryonic development. *Science* 309, 310-311.
- Wightman, B., Burglin, T.R., Gatto, J., Arasu, P., and Ruvkun, G. (1991). Negative regulatory sequences in the lin-14 3'-untranslated region are necessary to generate a temporal switch during *Caenorhabditis elegans* development. *Genes Dev* 5, 1813-1824.

Wightman, B., Ha, I., and Ruvkun, G. (1993). Posttranscriptional regulation of the heterochronic gene *lin-14* by *lin-4* mediates temporal pattern formation in *C. elegans*. *Cell* 75, 855-862.

Xiao, C., Srinivasan, L., Calado, D.P., Patterson, H.C., Zhang, B., Wang, J., Henderson, J.M., Kutok, J.L., and Rajewsky, K. (2008). Lymphoproliferative disease and autoimmunity in mice with increased miR-17-92 expression in lymphocytes. *Nat Immunol* 9, 405-414.

Yanagisawa, M., Kurihara, H., Kimura, S., Tomobe, Y., Kobayashi, M., Mitsui, Y., Yazaki, Y., Goto, K., and Masaki, T. (1988). A novel potent vasoconstrictor peptide produced by vascular endothelial cells. *Nature* 332, 411-415.

Yang, E., and Korsmeyer, S.J. (1996). Molecular thanatopsis: a discourse on the Bcl-2 family and cell death. *Blood* 88, 386-401.

Yang, J.T., Rayburn, H., and Hynes, R.O. (1993). Embryonic mesodermal defects in alpha 5 integrin-deficient mice. *Development* 119, 1093-1105.

Yang, W.J., Yang, D.D., Na, S., Sandusky, G.E., Zhang, Q., and Zhao, G. (2005). Dicer is required for embryonic angiogenesis during mouse development. *J Biol Chem* 280, 9330-9335.

Yekta, S., Shih, I.H., and Bartel, D.P. (2004). MicroRNA-directed cleavage of HOXB8 mRNA. *Science* 304, 594-596.

Yi, R., O'Carroll, D., Pasolli, H.A., Zhang, Z., Dietrich, F.S., Tarakhovskiy, A., and Fuchs, E. (2006). Morphogenesis in skin is governed by discrete sets of differentially expressed microRNAs. *Nat Genet* 38, 356-362.

Yin, H., and Lin, H. (2007). An epigenetic activation role of Piwi and a Piwi-associated piRNA in *Drosophila melanogaster*. *Nature* 450, 304-308.

Zhao, Y., Ransom, J.F., Li, A., Vedantham, V., von Drehle, M., Muth, A.N., Tsuchihashi, T., McManus, M.T., Schwartz, R.J., and Srivastava, D. (2007).

Dysregulation of cardiogenesis, cardiac conduction, and cell cycle in mice lacking miRNA-1-2. *Cell* 129, 303-317.

Zhao, Y., Samal, E., and Srivastava, D. (2005). Serum response factor regulates a muscle-specific microRNA that targets Hand2 during cardiogenesis. *Nature* 436, 214-220.

Zhong, T.P., Rosenberg, M., Mohideen, M.A., Weinstein, B., and Fishman, M.C. (2000). gridlock, an HLH gene required for assembly of the aorta in zebrafish. *Science* 287, 1820-1824.

Lebenslauf

Angelika Bonauer, geb. Kühbacher

Baumweg 27
60316 Frankfurt
Tel. 069 / 43057028
Email: bonauer@med.uni-frankfurt.de

geboren am 21. September 1977
in Hilden im Rheinland

verheiratet

Hochschulstudium

seit September 2005

Promotion an der Universität Frankfurt

Thema:
Die Bedeutung von microRNAs für die Funktion von
Endothelzellen
am Institut für Kardiovaskuläre Regeneration, Zentrum
für Molekulare Medizin, Prof. S. Dimmeler

Nov 1999 – Sep 2004

Biologie an der Universität Regensburg
Abschluss: **Diplom-Biologin**, Note: sehr gut (1.4)

Diplomarbeit:
Identification of plasma membrane proteins in
subdomains (rafts) by immunoprecipitation
am Institut für Zellbiologie und Pflanzenphysiologie,
Lst. Prof. W. Tanner
Note Vordiplom: befriedigend (2.8)

Schulbildung

1988 – 1997

Gymnasium in Düsseldorf
Abschluss:
Allgemeine Hochschulreife, Note: befriedigend (3.0)

1984 – 1988

Grundschule in Erkrath

Vorträge und Posterpräsentationen

seit September 2005

Vorträge bei Fachkongressen und Tagungen

Foundation Leducq Transatlantic Network for Cardiac
Regeneration Meeting 2008, London, „Regulation and
function of microRNAs in ischemic diseases“

74. Jahrestagung der deutschen kardiologischen Gesellschaft 2008, Mannheim, „microRNA-92a: ein zentraler Regulator der postnatalen Gefäßneubildung“

Kongress der American Heart Association 2007, Orlando, „Identification of pro- and anti-angiogenic microRNAs“

73. Jahrestagung der deutschen kardiologischen Gesellschaft 2007, Mannheim, „Role of microRNA-regulating enzymes Dicer and Drosha for endothelial cell biology“

30. Jahrestagung der deutschen Gesellschaft für Zellbiologie 2007, Frankfurt, „Role of microRNA-regulating enzymes Dicer and Drosha for endothelial cell biology“

Kongress der American Heart Association 2006, Chicago, „Role of microRNA-regulating enzymes Dicer and Drosha for endothelial cell biology“

seit September 2005

Poster bei Fachkongressen und Tagungen

Leopoldina Seminar on Remodeling and Reverse Remodeling in the Cardiopulmonary System 2008, Bad Nauheim, „MicroRNA-92a controls vessel growth and functional recovery in response to ischemia“

ATVB Early Career Session 2007, Orlando, „Identification of pro- and anti-angiogenic microRNAs“

Keystone Symposia 2007, Keystone, „Role of Dicer and Drosha for endothelial microRNA expression and angiogenesis“

30. Jahrestagung der deutschen Gesellschaft für Zellbiologie 2007, Frankfurt, „Role of microRNA-regulating enzymes Dicer and Drosha for endothelial cell biology“

Summerschool des Transregio 23, Rietzlern, 2006, „Role of microRNA-regulating enzymes Dicer and Drosha for endothelial cell biology“

Auszeichnungen

2008

Rudi Busse-Young Investigator Award für Experimentelle Kardiologie, 74. Jahrestagung der deutschen kardiologischen Gesellschaft 2008, Mannheim

Publikationen

Angelika Bonauer, Guillaume Carmona, Masayoshi Iwasaki, Masamichi Koyanagi, Ariane Fischer, Jana Burchfield, Henrik Fox, Carmen Doebele, Emmanouil Chavakis, Michael Potente, Marc Tjwa, Carmen Urbich, Andreas M. Zeiher, Stefanie Dimmeler
MicroRNA-92a controls vessel growth and functional recovery in response to ischemia
Manuscript submitted

Urbich C, Kuehbacher A, Dimmeler S
Role of microRNAs in vascular diseases, inflammation and angiogenesis
Cardiovasc Res. 2008, Sep 1;79(4):581-8

Kuehbacher A, Urbich C, Dimmeler S
Targeting microRNA expression to regulate angiogenesis
Trend Pharmacol Sci. 2008 Jan;29(1):12-5

Kuehbacher A, Urbich C, Zeiher AM, Dimmeler S
Role of Dicer and Drosha for endothelial microRNA expression and angiogenesis
Circ Res. 2007, Jul 6;101(1):59-68

Eidesstattliche Erklärung

Ich versichere an Eides statt, daß ich die vorliegenden Arbeit eigenständig ausgeführt und keine anderen als die angegebenen Hilfsmittel verwendet habe.

Alle Stellen, die im Wortlaut oder Sinn entsprechend aus anderen Arbeiten übernommen wurden, habe ich mit Quellenangaben als Zitat kenntlich gemacht.

Diese Arbeit wurde in dieser oder veränderter Form keiner anderen Prüfungsbehörde vorgelegt.

Frankfurt am Main, den 29.10.2008

Angelika Bonauer